SHEARON HARRIS NUCLEAR POWER PLANT, UNIT NO. 1
DOCKET NO. 50-400/RENEWED LICENSE NO. NPF-63
LICENSE AMENDMENT REQUEST FOR REVISION TO TECHNICAL SPECIFICATION
CORE OPERATING LIMITS REPORT (COLR) REFERENCES
FOR REALISTIC LARGE BREAK LOCA ANALYSIS

ENCLOSURE 4
AREVA REPORT ANP-3011 (NP), REVISION 1 (NON-PROPRIETARY)
(162 Pages)

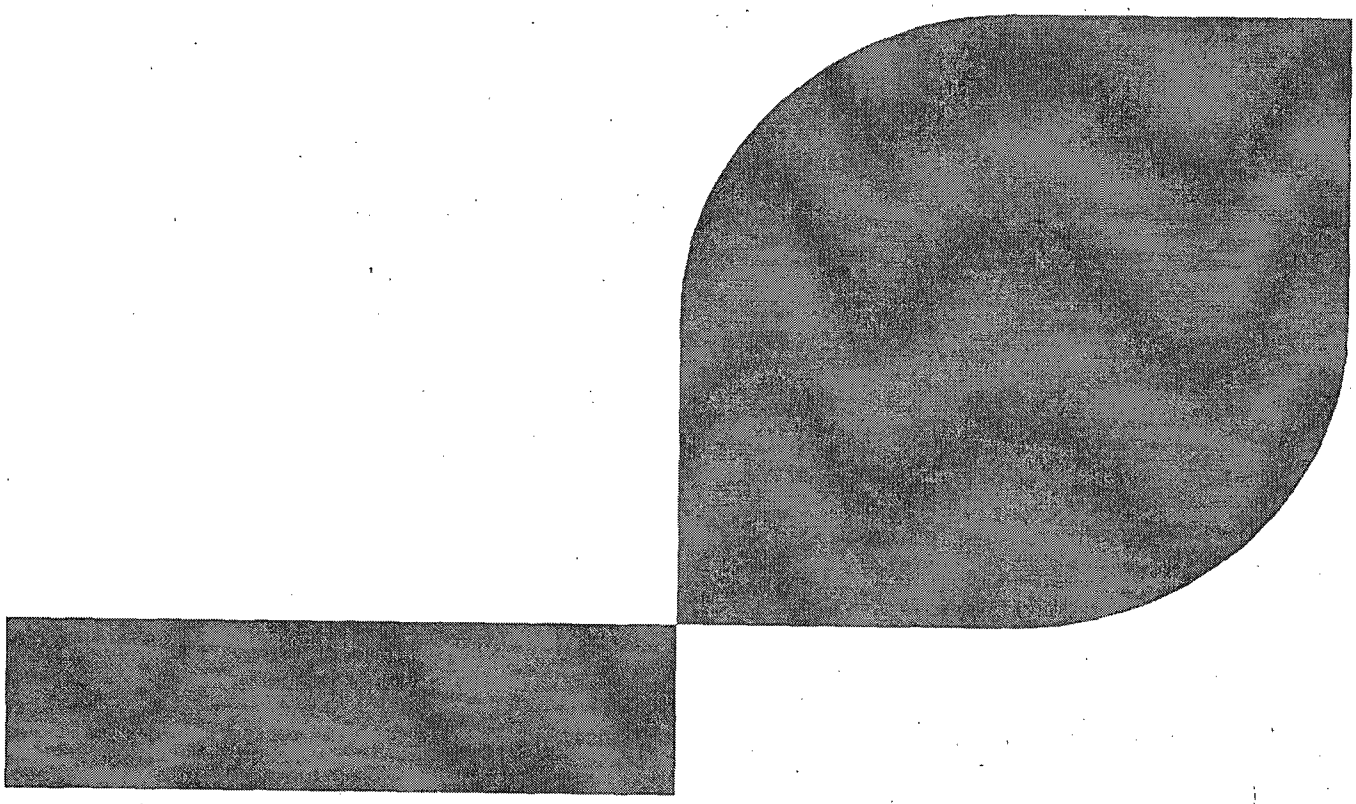

ANP-3011(NP)
Revision 001

Harris Nuclear Plant Unit 1 Realistic Large Break LOCA Analysis

August 2011

AREVA NP Inc.

AREVA

Nature of Changes

Item	Page	Description and Justification
1.	All	This is a new document.
2.	Page 59 and 60	Data was corrected to include cycle specific values.

Table of Contents

Table of Contents
(continued)

This document contains a total of 162 pages.

List of Tables

Page

List of Figures

Page

List of Figures
(continued)

Page

List of Figures
(continued)

Page

Nomenclature

AFD	Axial Flux Difference
ASI	Axial Shape Index
BLEU	Blended Low Enriched Uranium
BWR	Boiling Water Reactor
CCTF	Cylindrical Core Test Facility
CFR	Code of Federal Regulations
CPHS	Containment Pressure High Signal
CSAU	Code Scaling, Applicability, and Uncertainty
DC	Downcomer
DEGB	Double-Ended Guillotine Break
DFSS	Design For Six Sigma
DNB	Departure from Nucleate Boiling
ECCS	Emergency Core Cooling System
EFPH	Effective Full Power Hours
EM	Evaluation Model
FA	Fuel Assembly
FLECHT-SEASET	Full-Length Emergency Core Heat Transfer Separate Effects and Systems Effects Tests
F_Q	Total Peaking Factor
$F_{\Delta H}$	Nuclear Enthalpy Rise Factor
HHSI	High Head Safety Injection
HFP	Hot Full Power
HNP	Harris Nuclear Plant
LANL	Los Alamos National Laboratory
LEFM	Leading Edge Flow Meter
LHGR	Linear Heat Generation Rate
LHSI	Low Head Safety Injection
LOCA	Loss of Coolant Accident
LOFT	Loss of Fluid Test
LOOP	Loss of Offsite Power
MSIV	Main Steam Isolation Valve
NRC	U. S. Nuclear Regulatory Commission
NSSS	Nuclear Steam Supply System

Nomenclature (Continued)

PCT	Peak Clad Temperature
PIRT	Phenomena Identification and Ranking Table
PLHGR	Planar Linear Heat Generation Rate
PPLS	Pressurizer Pressure Low Signal
PWR	Pressurized Water Reactor
RAI	Request for Additional Information
RAS	Recirculation Actuation Signal
RCP	Reactor Coolant Pump
RCS	Reactor Coolant System
RLBLOCA	Realistic Large Break Loss of Coolant Accident
RV	Reactor Vessel
RWST	Refueling Water Storage Tank
SGLS	Steam Generator Low (pressure) Signal
SIAS	Safety Injection Activation Signal
SI	Safety Injection
SER	Safety Evaluation Report
THTF	Thermal Hydraulic Test Facility
UHI	Upper Head Injection
w/o	Weight Percent

1.0 INTRODUCTION

This report describes and provides results from a RLBLOCA analysis for the Harris Nuclear Plant (HNP) Unit 1. The plant is a Westinghouse 3-loop design with a rated thermal power of 2948 MWt and dry atmospheric containment. The loops contain three RCPs, three U-tube steam generators and a pressurizer.

The analysis supports operation for Cycle 18 and beyond with AREVA NP's 17x17 HTP fuel design using standard UO_2 fuel with 2%, 4%, 6%, and 8% Gd_2O_3 and M5 or Zircaloy-4 cladding. Studies presented in this report are applicable unless changes in the Technical Specifications, Core Operating Limits Report, core design, fuel design, plant hardware, or plant operation invalidate the results presented herein. The analysis was performed in compliance with the NRC-approved RLBLOCA EM (Reference 1) with exceptions noted below. Analysis results confirm the 10CFR50.46 (b) acceptance criteria presented in Section 3.0 are met and serve as the basis for operation of the HNP Unit 1 with AREVA NP fuel.

The non-parametric statistical methods inherent in the AREVA NP RLBLOCA methodology provide for the consideration of a full spectrum of break sizes, break configuration (guillotine or split break), axial shapes, and plant operational parameters. A conservative single-failure assumption is applied in which the loss of one train of the pumped ECCS injection is simulated. Regardless of the single-failure assumption, all containment pressure-reducing systems are assumed fully functional. The effects of Gadolinia-bearing fuel rods and peak fuel rod exposures are considered.

The following are deviations from the approved RLBLOCA EM (Reference 1) that were requested by the NRC.

The assumed reactor core power for the Harris realistic large break loss-of-coolant accident is 2958 MWt. This analyzed power bounds both current operation at a core power of 2900 MWt with 2% (58 MWt) power uncertainty and proposed MUR operation at a core power of 2948 MWt with 0.34% (10 MWt) power uncertainty. The power was not sampled in the analysis. This is not expected to have an adverse effect on the PCT results.

The RLBLOCA analysis was performed with a version of S-RELAP5 that requires both the void fraction to be less than 0.95 and the clad temperature to be less than 900 °F before the rod is allowed to quench. This may result in a slight increase in PCT results when compared to an analysis not subject to these constraints.

The RLBLOCA analysis was performed with a version of S-RELAP5 that limits the contribution of the Forslund-Rohsenow model to no more than 15 percent of the total heat transfer at and above a void fraction of 0.9. This may result in a slight increase in PCT results when compared to previous analyses for similar plants.

The split versus double-ended break type is no longer related to break area. In concurrence with Regulatory Guide 1.157, both the split and the double-ended break will range in area between the

minimum break area (A_{min}) and an area of twice the size of the broken pipe. The determination of break configuration, split versus double-ended, will be made after the break area is selected based on a uniform probability for each occurrence. A_{min} was calculated to be 26 percent of the DEGB area (see Section 5.6 for further discussion). This is not expected to have an effect on PCT results.

In concurrence with the NRC's interpretation of GDC 35, a set of 59 cases was run with a LOOP assumption and a second set with a No-LOOP assumption. The set of 59 cases that predicted the highest PCT is reported in Section 2 and Section 3, herein. The results from both case sets are shown in Figure 3-23. The effect on PCT results is expected to be minor.

During recent RLBLOCA EM modeling studies, it was noted that cold leg condensation efficiency may be under-predicted. Water entering the DC post-accumulator injection remained sufficiently subcooled to absorb DC wall heat release without significant boiling. However, tests (Reference 7) indicate that the steam and water entering the DC from the cold leg, subsequent to the end of accumulator injection, reach near saturation resulting from the condensation efficiency ranging between 80 to 100 percent. To assure that cold leg condensation would not be under-predicted, a RLBLOCA EM update was made. Noting that saturated fluid entering the DC is the most conservative modeling scheme, steam and liquid multipliers were developed so as to approximately saturate the cold leg fluid before it enters the DC. The multipliers were developed through scoping studies using a number of plant configurations—Westinghouse-designed 3- and 4-loop plants, and CE-designed plants. The results of the scoping study indicated that multipliers of 10 and 150 for liquid and steam, respectively, were appropriate to produce saturated fluid entering the DC. The RLBLOCA EM departure was discussed with the NRC and the NRC agreed that the approach described immediately above was satisfactory in the interim. The modification is implemented post-accumulation injection, 10 seconds after the vapor void fraction in the bottom of the accumulator becomes greater than 90 percent. Thus, the accumulators have injected all their water into the cold legs, and the nitrogen cover gas has entered the system and been mostly discharged through the break before the condensation efficiency is increased by the factors of 10 and 150, for liquid and vapor respectively. Providing saturated fluid conditions at the DC entrance conservatively reduces both the DC driving head and the core flooding rate. Recall that test results indicate that fluid conditions entering the DC range from saturated to slightly subcooled. Hence, it is conservative to force an approximation of saturated conditions for fluid entering the DC.

AREVA Inc. has acknowledged an issue concerning fuel thermal conductivity degradation as a function of burnup as raised by the NRC. In order to manage this issue, AREVA Inc. is modifying the way RODEX3A temperatures are compensated in the RLBLOCA Revision 0/Transition methodology. In the current process, the RLBLOCA computes PCTs at many different times during an operating cycle. For each specific time in cycle, the fuel conditions are computed using RODEX3A prior to starting the S-RELAP5 portion of the analysis. A steady state condition for the given time in cycle using S-RELAP5 is established. A base fuel centerline temperature is established in this process. Then two-transformation adjustments to the base fuel temperature are computed. The first transformation is a linear adjustment for an exposure of 10 MWd/MTU or higher. In the new process, a polynomial transformation is used in the first transformation instead of a linear transformation. The rest of the RLBLOCA process for initializing the S-RELAP5 fuel rod temperature should not be altered and the rest of LOCA transient should also continue in the original fashion. Section 6 will provide additional

information on the adjustment and adding once-burned fuel to the analysis. Note that these changes are also deviations required by the NRC that are departures from the approved evaluation model.

Through review of several recent submittals, NRC staff has identified some issues related to AREVA methodologies, some of which were employed in the development of the HNP Unit 1 RLBLOCA analysis. These issues, and the proposed remedies, were discussed with the NRC in a meeting on March 1, 2011. The purpose of Section 6 is to support NRC review of the HNP Unit 1 RLBLOCA analysis by providing information related to methodology changes implemented as a result of the NRC's concerns. Included in Section 6 is a discussion of the effects of swelling, rupture, and the subsequent potential for fuel relocation.

This plant specific methodology (and the deviations from EMF-2103 (P)(A), Revision 0 contained herein) will be replaced at the discretion of Progress Energy by the use EMF-2103, Revision 2 or higher upon approval of the specific revision by the NRC. Notification to the NRC of such a change will be the update of the COLR and/or submittal of an administrative change to the HNP TS COLR references to replace ANP-3011 with EMF-2103.

2.0 SUMMARY

The limiting PCT analysis is based on the parameter specification given in Table 2-1 for the limiting case. The limiting PCT is 1919 °F occurring on a fresh UO_2 rod in a case with offsite power available (NO-LOOP) conditions. Gadolinia-bearing rods of 2, 4, 6, and 8 w/o Gd_2O_3 were also analyzed, but were not limiting. This RLBLOCA result is based on a case set of 59 individual transient cases for LOOP and 59 individual transient cases for No-LOOP conditions. The core is composed only of AREVA NP 17x17 thermal hydraulically compatible fuel designs; hence, there is no mixed core consideration.

The analysis assumes full core power operation at 2958 MWt (including uncertainties), a steam generator tube plugging level of 3 percent in all steam generators, a total peaking factor (F_Q) up to a value of 2.52 (including uncertainties, but no axial dependency), and a nuclear enthalpy rise factor ($F_{\Delta H}$) up to a value of 1.73 (including uncertainty). This analysis also addresses typical operational ranges or technical specification limits (whichever is applicable) with regard to pressurizer pressure and level; accumulator pressure, temperature (based on containment temperature), and level; core average temperature; core flow; containment pressure and temperature; and RWST temperature.

The AREVA RLBLOCA Transition Package methodology (on a forward fit basis) explicitly analyzes fresh and once-burned fuel assemblies to respond to recent NRC issues. The second-burned fuel assemblies have minimal power and are typically located on the periphery; therefore would not be limiting in regards to PCT for a RLBLOCA analysis. The AREVA core management design process ensures that the twice-burnt reinsert fuel does not have the limiting $F_{\Delta H}$. The analysis demonstrates that the 10 CFR 50.46(b) criteria listed in Section 3.0 are satisfied.

Table 2-1: Summary of Major Parameters for Limiting Transient

	Fresh UO_2	Once-Burned UO_2
Core Average Burnup (EFPH)	8302[1]	8302[2]
Core Power (MWt)	2958	2958
Total Peaking (F_Q)	2.242	2.242
Radial Peak ($F_{\Delta H}$)	1.730	1.645[3]
Axial Offset	0.1006	0.1006
Break Type	Guillotine	Guillotine
Break Size (ft^2/side)	3.6922	3.6922
Offsite Power Availability	Available	Available
Decay Heat Multiplier	1.000	1.000

[1] This is ~ 18.8 GWd/MTU in burnup for the fresh fuel.
[2] This is ~ 39.7 GWd/MTU in burnup for the once-burnt fuel.
[3] Calculated using Fresh Fuel F_r x K(Burnup) multiplier (0.9509 at 8302 EFPH) from Figure 6-4.

3.0 ANALYSIS

The purpose of the analysis is to verify typical technical specification peaking factor limits and the adequacy of the ECCS by demonstrating that the following 10CFR 50.46(b) criteria are met:

- The calculated maximum fuel element cladding temperature shall not exceed 2200 °F.
- The calculated total oxidation of the cladding shall nowhere exceed 0.17 times the total cladding thickness before oxidation.
- The calculated total amount of hydrogen generated from the chemical reaction of the cladding with water or steam shall not exceed 0.01 times the hypothetical amount that would be generated if all of the metal in the cladding cylinders surrounding the fuel excluding the cladding surrounding the plenum volume were to react.
- The calculated changes in core geometry shall be such that the core remains amenable to cooling.
- Long-term cooling is established and maintained after the LOCA.

The analysis did not evaluate the 10CFR 50.46(b) long-term cooling criterion, as this is handled in a separate analysis.

The RLBLOCA analysis conservatively considers blockage effects due to clad swelling and rupture in the prediction of the hot fuel rod PCT. The effects of combined loads (LOCA) on the fuel assembly components have been evaluated by AREVA and the resulting loads are below the allowable stress limit for all the components. The combination of compliance with Criterion 1 (< 2200°F) and the LOCA loads evaluation ensures no permanent deformation to the fuel assemblies; thereby demonstrating compliance with Criterion (4).

Section 3.1 of this report describes the postulated LBLOCA event. Section 3.2 describes the models used in the analysis. Section 3.3 describes the 3-loop PWR plant and summarizes the system parameters used in the analysis. Compliance to the SER is addressed in Section 3.4. Section 3.5 summarizes the results of the RLBLOCA analysis. Section 4 provides the conclusions and Section 5 discusses the additional information provided under the "Transition Package" on EMF-2103. Section 6 addresses recent NRC issues on RLBLOCA submittals and Section 7 contains the reference list.

3.1 Description of the LBLOCA Event

A LBLOCA is initiated by a postulated rupture of the RCS primary piping. Based on deterministic studies, the worst break location is in the cold leg piping between the reactor coolant pump and the reactor vessel for the RCS loop containing the pressurizer. The break initiates a rapid depressurization of the RCS. A reactor trip signal is initiated when the low pressurizer pressure trip setpoint is reached; however, reactor trip is conservatively neglected in the analysis. The reactor is shut down by coolant voiding in the core.

The plant is assumed to be operating normally at full power prior to the accident. The cold leg break is assumed to open instantaneously. For this break, a rapid depressurization occurs, along with a core flow stagnation and reversal. This causes the fuel rods to experience DNB. Subsequently, the limiting fuel rods are cooled by film boiling and convection to steam. The coolant voiding creates a strong negative reactivity effect and core fission ends. As heat transfer from the fuel rods is reduced, the cladding temperature rises.

Coolant in all regions of the RCS begins to flash. At the break plane, the loss of subcooling in the coolant results in substantially reduced break flow. This reduces the depressurization rate, and leads to a period of positive core flow or reduced downflow as the reactor coolant pumps in the intact loops continue to supply water to the vessel (in No-LOOP conditions). Cladding temperatures may be reduced and some portions of the core may rewet during this period. The positive core flow or reduced downflow period ends as two-phase conditions occur in the reactor coolant pumps, reducing their effectiveness. Once again, the core flow reverses as most of the vessel fluid mass flows out through the broken cold leg.

Mitigation of the LBLOCA begins when the SIAS is tripped. This signal is initiated by either high containment pressure or low pressurizer pressure. Regulations require that a worst single-failure be considered. This single-failure has been determined to be the loss of one ECCS pumped injection train. The AREVA RLBLOCA methodology conservatively assumes an on-time start and normal lineups of the containment spray to conservatively reduce containment pressure and increase break flow. Hence, the analysis assumes that one charging pump, one HHSI pump, one LHSI pump and two containment spray pumps are operating.

When the RCS pressure falls below the accumulator pressure, fluid from the accumulators is injected into the cold legs. In the early delivery of accumulator water, high pressure and high break flow will drive some of this fluid to bypass the core. During this bypass period, core heat transfer remains poor and fuel rod cladding temperatures increase. As RCS and containment pressures equilibrate, ECCS water begins to fill the lower plenum and eventually the lower portions of the core; thus, core heat transfer improves and cladding temperatures decrease.

Eventually, the relatively large volume of accumulator water is exhausted and core recovery must rely on pumped ECCS coolant delivery alone. As the accumulators empty, the nitrogen gas used to pressurize the accumulators exits through the break. This gas release may result in a short period of improved core heat transfer as the nitrogen gas displaces water in the downcomer. After the nitrogen

gas has been expelled, the ECCS temporarily may not be able to sustain full core cooling because of the core decay heat and the higher steam temperatures created by quenching in the lower portions of the core. Peak fuel rod cladding temperatures may increase for a short period until more energy is removed from the core by the charging, SI and LHSI while the decay heat continues to fall. Steam generated from fuel rod rewet will entrain liquid and pass through the core, vessel upper plenum, the hot legs, the steam generator, and the reactor coolant pump before it is vented out the break. Some steam may flow to the upper head and pass through the spray nozzles, which provide a vent path to the break. The resistance of this flow path to the steam flow is balanced by the driving force of water filling the downcomer. This resistance may act to retard the progression of the core reflood and postpone core wide cooling. Eventually (within a few minutes of the accident), the core reflood will progress sufficiently to ensure core wide cooling. Full core quench occurs within a few minutes after core wide cooling. Long-term cooling is then sustained with the LHSI system.

3.2 Description of Analytical Models

The RLBLOCA methodology is documented in EMF-2103 *Realistic Large Break LOCA Methodology* (Reference 1). The methodology follows the Code Scaling, Applicability, and Uncertainty (CSAU) evaluation methodology (Reference 2). This method outlines an approach for defining and qualifying a best-estimate thermal-hydraulic code and quantifies the uncertainties in a LOCA analysis.

The RLBLOCA methodology consists of the following computer codes:

- RODEX3A for computation of the initial fuel stored energy, fission gas release, and fuel-cladding gap conductance.
- S-RELAP5 for the system calculation (includes ICECON for containment response).
- AUTORLBLOCA for generation of ranged parameter values, transient input, transient runs, and general output documentation.

The governing two-fluid (plus non-condensibles) model with conservation equations for mass, energy, and momentum transfer is used. The reactor core is modeled in S-RELAP5 with heat generation rates determined from reactor kinetics equations (point kinetics) with reactivity feedback, and with actinide and decay heating.

The two-fluid formulation uses a separate set of conservation equations and constitutive relations for each phase. The effects of one phase on the other are accounted for by interfacial friction, and heat and mass transfer interaction terms in the equations. The conservation equations have the same form for each phase; only the constitutive relations and physical properties differ.

The modeling of plant components is performed by following guidelines developed to ensure accurate accounting for physical dimensions and that the dominant phenomena expected during the LBLOCA event are captured. The basic building blocks for modeling are hydraulic volumes for fluid paths and heat structures for heat transfer. In addition, special purpose components exist to represent specific

components such as the RCPs or the steam generator separators. All geometries are modeled at the resolution necessary to best resolve the flow field and the phenomena being modeled within practical computational limitations.

System nodalization details are shown in Figures 3-1 through 3-5. A point of clarification: in Figure 3-1, break modeling uses two junctions regardless of break type—split or guillotine; for guillotine breaks, Junction 151 is deleted, it is retained fully open for split breaks. Hence, total break area is the sum of the areas of both break junctions.

A typical calculation using S-RELAP5 begins with the establishment of a steady-state initial condition with all loops intact. The input parameters and initial conditions for this steady-state calculation are chosen to reflect plant technical specifications or to match measured data. Additionally, the RODEX3A code provides initial conditions for the S-RELAP5 fuel models. Specific parameters are discussed in Section 3.3.

Following the establishment of an acceptable steady-state condition, the transient calculation is initiated by introducing a break into one of the loops (specifically, the loop with the pressurizer). The evolution of the transient through blowdown, refill and reflood is computed continuously using S-RELAP5. Containment pressure is also calculated by S-RELAP5 using containment models derived from ICECON (Reference 4), which is based on the CONTEMPT-LT code (Reference 3).

The methods used in the application of S-RELAP5 to the LBLOCA are described in Reference 1. A detailed assessment of this computer code was made through comparisons to experimental data, many benchmarks with cladding temperatures ranging from 1,700 °F (or less) to above 2,200 °F. These assessments were used to develop quantitative estimates of the ability of the code to predict key physical phenomena in a PWR LBLOCA. Various models—for example, the core heat transfer, the decay heat model and the fuel cladding oxidation correlation—are defined based on code-to-data comparisons and are, hence, plant independent.

The RV internals are modeled in detail (Figures 3-3 through 3-5) based on specific inputs supplied by Progress Energy. Nodes and connectivity, flow areas, resistances and heat structures are all accurately modeled. The location of the hot assembly/hot pin(s) is unrestricted; however, the channel is always modeled to restrict appreciable upper plenum liquid fallback.

The final step of the best-estimate methodology is to combine all the uncertainties related to the code and plant parameters, and estimate the PCT at a high probability level. The steps taken to derive the PCT uncertainty estimate are summarized below:

1. Base Plant Input File Development

   First, base RODEX3A and S-RELAP5 input files for the plant (including the containment input file) are developed. Code input development guidelines are applied to ensure that model nodalization is consistent with the model nodalization used in the code validation.

2. Sampled Case Development

The non-parametric statistical approach requires that many "sampled" cases be created and processed. For every set of input created, each "key LOCA parameter" is randomly sampled over a range established through code uncertainty assessment or expected operating limits (provided by plant technical specifications or data). Those parameters considered "key LOCA parameters" are listed in Table 3-1. This list includes both parameters related to LOCA phenomena (based on the PIRT provided in Reference 1) and to plant operating parameters.

3. Determination of Adequacy of ECCS

The RLBLOCA methodology uses a non-parametric statistical approach to determine values of PCT at the 95 percent probability level. Total oxidation and total hydrogen are based on the limiting PCT case. The adequacy of the ECCS is demonstrated when these results satisfy the criteria set forth in Section 3.0.

3.3 Plant Description and Summary of Analysis Parameters

The plant analysis presented in this report is for a Westinghouse-designed PWR, which has three loops, each with a hot leg, a U-tube steam generator, and a cold leg with a RCP[4]. The RCS also includes one pressurizer connected to a hot leg. The core contains (157) AREVA 17x17 HTP fuel assemblies with 2%, 4%, 6% and 8% gadolinia pins. The ECCS includes one HHSI, one LHSI and one accumulator injection path per RCS loop. The break is modeled in the same loop as the pressurizer, as directed by the RLBLOCA methodology. The RLBLOCA transients are of sufficiently short duration that the switchover to sump cooling water (i.e., RAS) for ECCS pumped injection need not be considered.

It is important to note that the analyses performed for this report specifically characterizes M5-clad HTP fuel; this material will be initially implemented at Harris as a fresh batch in Cycle 18. Once-burned assemblies are included in the analyses. Actually, burned fuel assemblies in Cycle 18 will be comprised of HTP fuel clad with Zircaloy-4. The fuel assembly mechanical designs are the same, independent of cladding type and the need for evaluation of mixed core effects is unnecessary as a result. Additionally, the once-burned M5 pin analysis results are applicable to the Zircaloy-4 clad with the exception of localized oxidation.

The differences in a 3-loop Westinghouse-designed plant LOCA results for fuels clad with M5 or Zircaloy-4, using the AREVA RLBLOCA EM have been examined closely and reported in Appendix E of the EM (Reference 1). These sensitivity studies indicate that, all things being equal besides the cladding material, there are no significant differences in PCT prediction. In AREVA RLBLOCA EM applications, the initial clad oxidation layer is added to the transient oxide growth to produce the total and compared to the 10CFR50.46 limit for local oxidation. The initial oxide thickness for Zircaloy-4,

[4] The RCPs are Westinghouse 93A type pumps. The homologous pump performance curves for this type of pump were input to the S-RELAP5 plant model.

specific to the burnup used in the limiting case analysis of the once-burned fuel is calculated and the totals associated with Zircaloy-4 local oxidation are reported in the analysis results. All other results for the once-burned fuel are applicable to either clad type. In this specific RLBLOCA analysis for Harris Nuclear Plant Unit 1 the once-burned fuel is not limiting in PCT, regardless of whether M5 or Zircaloy-4 material is used as cladding.

The S-RELAP5 model explicitly describes the RCS, RV, pressurizer, and accumulator lines. The ECCS includes an accumulator path and a LHSI/HHSI path per RCS loop. The HHSI and LHSI feed into a common header that connects to each cold leg pipe downstream of the RCP discharge. The ECCS pumped injection is modeled as a table of flow versus backpressure. This model also describes the secondary-side steam generator that is instantaneously isolated (closed MSIV and feedwater trip) at the time of the break. A symmetric steam generator tube plugging level of 3 percent per steam generator was assumed.

Plant input modeling parameters were provided by Progress Energy specifically for the HNP Unit 1. By procedure, Progress Energy maintains plant documentation current, and directly communicates with AREVA on plant design and operational issues regarding reload cores. Progress Energy and AREVA will continue to interact in that fashion regarding the use of AREVA fuel in the HNP Unit 1. Both entities have ongoing processes that assure the ranges and values of input parameters for the HNP Unit 1 RLBLOCA analysis bound those of the as-operated plant.

As described in the AREVA RLBLOCA methodology, many parameters associated with LBLOCA phenomenological uncertainties and plant operation ranges are sampled. A summary of those parameters is given in Table 3-1. The LBLOCA phenomenological uncertainties are provided in Reference 1. Values for process or operational parameters, including ranges of sampled process parameters, and fuel design parameters used in the analysis are given in Table 3-2. Plant data are analyzed to develop uncertainties for the process parameters sampled in the analysis. Table 3-3 presents a summary of the uncertainties used in the analysis. Two parameters, RWST temperature for SI flows and diesel start time, are set at conservative bounding values for all calculations. Where applicable, the sampled parameter ranges are based on technical specification limits or supporting plant calculations that provide more bounding values.

For the AREVA NP RLBLOCA EM, dominant containment parameters, as well as NSSS parameters, were established via a PIRT process. Other model inputs are generally taken as nominal or conservatively biased. The PIRT outcome yielded two important (relative to PCT) containment parameters—containment pressure and temperature. In many instances, the conservative guidance of CSB 6-2 (Reference 5) was used in setting the remainder of the containment model input parameters. As noted in Table 3-3, containment temperature is a sampled parameter. Containment pressure response is indirectly ranged by sampling the upper containment volume (Table 3-3). The minimum containment value was without any biasing as 2.266E6 ft^3. The maximum value is a simplified value computed as the available volume of 2.61E6 ft^3. This volume was calculated as the volume of the containment building with no water in the sump.

The initial conditions and boundary conditions are given in Table 3-8. The building spray is modeled at maximum heat removal capacity. All spray flow is delivered to the containment. Fan coolers are assumed operating from time zero of the LBLOCA transient.

Passive heat sink parameters are listed in Table 3-9. In accordance with Reference 1, the condensing heat transfer coefficient is intended to be closer to a best-estimate instead of a bounding high value. A [ ][5] Uchida heat transfer coefficient multiplier was specifically validated for use in Harris through application of the process used in the RLBLOCA EM (Reference 1) sample problems.

[5] A conservative Uchida heat transfer coefficient multiplier of [ ] was used for the RLBLOCA analysis. A sensitivity run for the limiting case using a [ ] Uchida heat transfer coefficient multiplier was performed and yielded significantly lower PCT results.

3.4 SER Compliance

A number of requirements on the methodology are stipulated in the conclusions section of the SER for the RLBLOCA methodology (Reference 1). These requirements have all been fulfilled during the application of the methodology as addressed in Table 3-4.

Five non-limiting PCT cases were potential candidates for blowdown quench (SER Item 7) and were closely inspected. For each of the five cases, the peak node clad temperature, fluid saturation temperature at that node, and accumulator injection transient were considered. Since the cladding temperature remained above the saturation temperature, none of the cases showed blowdown quench.

Several measures have been taken to prevent the top-down quench (SER Item 8). The upper plenum nodalization features include:

- the CCFL model is applied on all core exit junctions,
- the reverse form loss at the hot channel and central core exits were increased by a factor of 1000 at the beginning of core reflood.

Cases can exhibit periodic positive integrated flow (indicating flow in an upward direction), constant integrated flow (no flow), or negative integrated flow (flow moving from the top-down). Core flows can reverse at break initiation, during blowdown, and reverse flow can continue until the core begins to be recovered by accumulator and ECCS injection. Top-down quench, then, is judged as a potential problem if the hot channel exit flow reverses after the beginning of core recovery. The direction of movement of the quench front can be determined by a careful inspection of the propagation of the cladding temperatures. For all cases examined, the cladding temperatures show a progressive quenching with bottom nodes quenching earlier and subsequently giving way to the cooling of the higher elevation nodes. No evidence of top-down quench was observed. The modeling precautions taken to prevent top-down quench are sufficient and no evidence of top-down quench was observed.

Therefore, compliance to the SER restriction has been demonstrated.

3.5 Realistic Large Break LOCA Results

Two case sets of 59 transient calculations were performed sampling the parameters listed in Table 3-1. For each case set, PCT was calculated for fresh and once-burned UO_2 and Gadolinia-bearing rods with concentrations of 2, 4, 6 and 8 w/o Gd_2O_3. The limiting case set, which contained the PCT, was the set with offsite power available (No-LOOP). The limiting PCT (1919 °F) occurred in Case 5 for a fresh UO_2 rod. The once-burned rod limiting PCT (1890 °F) occurred in Case 5 for a UO_2 rod. The major parameters for the limiting transient are presented in Table 2-1. Table 3-5 lists the results of the limiting case. The fraction of total hydrogen generated was not directly calculated; however, it is conservatively bounded by the calculated total percent oxidation, which is well below the 1 percent limit. The best-estimate PCT case is Case 27, which corresponded to the median case out of the 59-case set with offsite power available. The nominal PCT was 1536 °F. This result can be used to quantify the relative conservatism in the limiting case result. In this analysis, it was 383 °F.

The case results, event times and analysis plots for the limiting PCT case are shown in Table 3-5, Table 3-6, and in Figures 3-11 through 3-21. Figure 3-6 shows linear scatter plots of the key parameters sampled for the 59 calculations. Parameter labels appear to the left of each individual plot. These figures show the parameter ranges used in the analysis. Figures 3-7 and 3-8 show the time of PCT and break size versus PCT scatter plots for the 59 No-LOOP calculations, respectively. Figures 3-9 and 3-10 show the maximum oxidation and total oxidation versus PCT scatter plots for the 59 No-LOOP calculations, respectively. Figure 3-11 shows the containment volume versus PCT scatter plot for the 59 No-LOOP calculations. Key parameters for the limiting PCT case are shown in Figures 3-12 through 3-22. Figure 3-12 is the plot of PCT independent of elevation; this figure clearly indicates that the transient exhibits a sustained and stable quench. A comparison of PCT results from both case sets is shown in Figure 3-23.

Table 3-1: Sampled LBLOCA Parameters

Phenomenological	
	Time in cycle (peaking factors, axial shape, rod properties, burnup)
	Break type (guillotine versus split)
	Critical flow discharge coefficients (break)
	Decay heat[6]
	Critical flow discharge coefficients (surgeline)
	Initial upper head temperature
	Film boiling heat transfer
	Dispersed film boiling heat transfer
	Critical heat flux
	T_{min} (intersection of film and transition boiling)
	Initial stored energy
	Downcomer hot wall effects
	Steam generator interfacial drag
	Condensation interphase heat transfer
	Metal-water reaction
Plant[7]	
	Offsite power availability[8]
	Break size
	Pressurizer pressure
	Pressurizer liquid level
	Accumulator pressure
	Accumulator liquid level
	Accumulator temperature (based on lower compartment containment temperature)
	Containment temperature
	Containment volume
	Initial RCS flow rate
	Initial operating RCS temperature

6 Not sampled in analysis, multiplier set to 1.0.
7 Uncertainties for plant parameters are based on typical plant-specific data.
8 Not sampled, see Section 5.9.

Table 3-2: Plant Operating Range Supported by the LOCA Analysis

	Event	Operating Range
1.0	**Plant Physical Description**	
	1.1 Fuel	
	a) Cladding outside diameter	0.376 in.
	b) Cladding inside diameter	0.328 in.
	c) Cladding thickness	0.024 in.
	d) Pellet outside diameter	0.3215 in.
	e) Pellet density	95 percent of theoretical
	f) Active fuel length	144 in.
	g) Resinter densification	[ ]
	h) Gd_2O_3 concentrations	2, 4, 6, 8 w/o
	1.2 RCS	
	a) Flow resistance	Analysis
	b) Pressurizer location	Analysis assumes location giving most limiting PCT (broken loop)
	c) Hot assembly location	Anywhere in core
	d) Hot assembly type	17x17
	e) SG tube plugging	≤ 3 percent
2.0	**Plant Initial Operating Conditions**	
	2.1 Reactor Power	
	a) Nominal reactor power	2958 MWt[9]
	b) F_Q	≤ 2.52[10]
	c) $F_{\Delta H}$	≤ 1.73[11]
	2.2 Fluid Conditions	
	a) Loop flow	109.2 Mlbm/hr ≤ M ≤ 115.3 Mlbm/hr
	b) RCS average temperature	582.0°F ≤ T ≤ 594.8°F
	c) Upper head temperature	~Tcold Temperature[12]

9 Consistent with rated core power of 2900 MWt and 2% measurement uncertainty or MUR conditions of 2948 MWt and 0.34% uncertainty.

10 The peaking factor includes measurement and engineering uncertainty.

11 The $F_{\Delta H}$ value is listed in COLR; while the 4% measurement uncertainty is a Technical Specifications limit.

12 Upper head temperature will change based on sampling of RCS temperature

Table 3-2 Plant Operating Range Supported by the LOCA Analysis (Continued)

	d) Pressurizer pressure	2200 psia ≤ P ≤ 2288 psia
	e) Pressurizer level	Gaussian distribution mean of 60% and standard deviation of 7.4%. Distribution on the high side up to 92%.
	f) Accumulator pressure	599.7 psia ≤ P ≤ 679.7 psia
	g) Accumulator liquid volume	994.6 ft^3 ≤ V ≤ 1029.4 ft^3
	h) Accumulator temperature	80°F ≤ T ≤ 130°F (It's coupled with containment temperature)
	i) Accumulator resistance fL/D	As-built piping configuration
	j) Minimum ECCS boron	≥ 2400 ppm
3.0	**Accident Boundary Conditions**	
	a) Break location	Any RCS piping location
	b) Break type	Double-ended guillotine or split
	c) Break size (each side, relative to cold leg pipe area)	0.26 ≤ A ≤ 1.0 full pipe area (split) 0.26 ≤ A ≤ 1.0 full pipe area (guillotine)
	d) Worst single-failure	Loss of Diesel (one train of ECCS)
	e) Offsite power	On or Off
	f) ECCS pumped injection temperature	125°F
	g) HHSI pump delay	17 s (w/ offsite power) 29 s (w/o offsite power)
	h) LHSI pump delay	27 s (w/ offsite power) 37 s (w/o offsite power)
	i) Containment pressure	14.7 psia, nominal value
	j) Containment temperature	80°F ≤ T ≤ 130°F
	k) Containment sprays delay	0 s
	l) Containment spray water temperature	40°F

Table 3-2 Plant Operating Range Supported by the LOCA Analysis (Continued)

m) LHSI Flow

BROKEN_LOOP

RCS pressure	LHSI flow
psia	gpm
0.	1832.0
15.	1832.0
20.	1791.1
30.	1707.6
35.	1664.9
40.	1621.5
50.	1532.5
70.	1318.8
120.	546.2
125.	491.9
125.01	0.0
3000.	0.0

INTACT_LOOP1

RCS pressure	LHSI flow
psia	gpm
0.	916.0
15.	916.0
20.	895.6
30.	853.8
35.	832.4
40.	810.8
50.	766.3
70.	659.3
120.	273.1
125.	246.0
125.01	0.0
3000.	0.0

INTACT_LOOP2

RCS pressure	LHSI flow
psia	gpm
0.	916.0
15.	916.0
20.	895.6
30.	853.8
35.	832.4
40.	810.8
50.	766.3
70.	659.3
120.	273.1
125.	246.0
125.01	0.0
3000.	0.0

Table 3-2 Plant Operating Range Supported by the LOCA Analysis (Continued)

n) HHSI Flow

BROKEN_LOOP

RCS Pressure	HHSI Flow
psia	gpm
10.	206.3
15.	206.3
20.	206.1
30.	205.7
40.	205.3
50.	204.9
70.	204.1
120.	202.1
500.	186.3
1001.	161.9
1150.	154.0
1609.	124.4
1775.	114.5
2037.	91.2
2141.	72.7
2193.	60.8
2246.	35.1
2296.	0.0
3000.	0.0

INTACT_LOOP1

RCS Pressure	HHSI Flow
psia	gpm
10.	129.6
15.	129.6
20.	129.4
30.	129.2
40.	128.9
50.	128.7
70.	128.2
120.	126.9
500.	117.0
1001.	101.7
1150.	96.8
1609.	78.3
1775.	72.4
2037.	58.7
2141.	49.2
2193.	44.6
2246.	28.6
2296.	0.0
3000.	0.0

INTACT_LOOP2

RCS Pressure	HHSI Flow
psia	gpm
10.	129.6
15.	129.6
20.	129.4
30.	129.2
40.	128.9
50.	128.7
70.	128.2
120.	126.9
500.	117.0
1001.	101.7
1150.	96.8
1609.	78.3
1775.	72.4
2037.	58.7
2141.	49.2
2193.	44.6
2246.	28.6
2296.	0.0
3000.	0.0

Table 3-3: Statistical Distributions Used for Process Parameters

Parameter	Operational Uncertainty Distribution	Parameter Range	Measurement Uncertainty Distribution[13]	Standard Deviation
Pressurizer Pressure (psia)	Uniform	2200 – 2288	N/A	N/A
Pressurizer Liquid Level (percent)	Gaussian	60	N/A	7.4%
Accumulator Liquid Volume (ft^3)	Uniform	994.6 – 1029.4	N/A	N/A
Accumulator Pressure (psia)	Uniform	599.7 – 679.7	N/A	N/A
Containment/Accumulator Temperature (°F)	Uniform	80 – 130	N/A	N/A
Containment Volume (ft^3)	Uniform	2,266,000 – 2,610,000	N/A	N/A
Initial RCS Flow Rate (Mlbm/hr)	Uniform	109.2 – 115.3	N/A	N/A
Initial RCS Operating Temperature (Tavg) (°F)	Uniform	582.0 – 594.6	N/A	N/A
RWST Temperature (°F)	Point	125	N/A	N/A
RWST Temperature for Containment Sprays (°F)	Point	40	N/A	N/A
Offsite Power Availability[14]	Binary	0,1	N/A	N/A
Delay for Containment Cooling (s)	Point	0.0	N/A	N/A
HHSI Delay (s)	Point	17 (w/ offsite power) 29 (w/o offsite power)	N/A	N/A
LHSI Delay (s)	Point	27 (w/ offsite power) 37 (w/o offsite power)	N/A	N/A

[13] All measurement uncertainties were incorporated into the operational ranges

[14] This is no longer a sampled parameter. One set of 59 cases is run with LOOP and one set of 59 cases is run with No-LOOP.

Table 3-4: SER Conditions and Limitations

SER Conditions and Limitations	Response
1. A CCFL violation warning will be added to alert the analyst to CCFL violation in the downcomer should such occur.	There was no significant occurrence of CCFL violation in the downcomer for this analysis. Violations of CCFL were noted in a statistically insignificant number of time steps.
2. AREVA NP has agreed that it is not to use nodalization with hot leg to downcomer nozzle gaps.	Hot leg nozzle gaps were not modeled.
3. If AREVA NP applies the RLBLOCA methodology to plants using a higher planar linear heat generation rate (PLHGR) than used in the current analysis, or if the methodology is to be applied to an end-of-life analysis for which the pin pressure is significantly higher, then the need for a blowdown clad rupture model will be reevaluated. The evaluation may be based on relevant engineering experience and should be documented in either the RLBLOCA guideline or plant specific calculation file.	The current HNP calculation set contains 4 cases for which the initial fuel pin rupture occurred more than 2 seconds prior to the beginning of core recovery (BOCREC). Rupture within 2 seconds of BOCREC is considered a reflood rupture. Each of the 4 cases was evaluated with a swelling, rupture, and fuel relocation model and found to be conservatively evaluated by the base, no rupture, evaluation model. A summary of the swelling, rupture, and fuel relocation model and studies is presented in Section 6.9 of this topical.
4. Slot breaks on the top of the pipe have not been evaluated. These breaks could cause the loop seals to refill during late reflood and the core to uncover again. These break locations are an oxidation concern as opposed to a PCT concern since the top of the core can remain uncovered for extended periods of time. Should an analysis be performed for a plant with loop seals with bottom elevations that are below the top elevation of the core, AREVA NP will evaluate the effect of the deep loop seal on the slot breaks. The evaluation may be based on relevant engineering experience and should be documented in either the RLBLOCA guideline or plant-specific calculation file.	The evaluation of slot breaks is documented in the AREVA RLBLOCA analysis guidelines and in response to RAI #25 for EMF-2103(P)(A) Rev. 0.
5. The model applies to 3 and 4 loop Westinghouse- and CE-designed nuclear steam systems.	HNP Unit 1 is a Westinghouse 3-loop plant.
6. The model applies to bottom reflood plants only (cold side injection into the cold legs at the reactor coolant discharge piping).	HNP Unit 1 is a bottom reflood plant.
7. The model is valid as long as blowdown quench does not occur. If blowdown quench occurs, additional justification for the blowdown heat transfer model and uncertainty are needed or the calculation is corrected. A blowdown quench is characterized by a temperature reduction of the peak cladding temperature (PCT) node to saturation temperature during the blowdown period.	No cases displayed evidence of a blowdown quench.

Table 3-4: SER Conditions and Limitations *(Continued)*

SER Conditions and Limitations	Response
8. The reflood model applies to bottom-up quench behavior. If a top-down quench occurs, the model is to be justified or corrected to remove top quench. A top-down quench is characterized by the quench front moving from the top to the bottom of the hot assembly.	Core quench initiated at the bottom of the core and proceeded upward; no cases showed downward flow past beginning of core recovery.
9. The model does not determine whether Criterion 5 of 10 CFR 50.46, long term cooling, has been satisfied. This will be determined by each applicant or licensee as part of its application of this methodology.	Long-term cooling was not evaluated in this analysis.
10. Specific guidelines must be used to develop the plant-specific nodalization. Deviations from the reference plant must be addressed.	The nodalization in the plant model is consistent with the Westinghouse 3-loop sample calculation that was submitted to the NRC for review. Figure 3-1 shows the loop noding used in this analysis. (NOTE only Loop 1 is shown in the figure; Loops 2 and 3 are identical to Loop 1, except that only Loop 1 contains the pressurizer and the break). Figure 3-2 shows the steam generator model. Figure 3-3, 3-4, and 3-5 show reactor vessel nodding diagrams.
11. A table that contains the plant-specific parameters and the range of the values considered for the selected parameter during the topical report approval process must be provided. When plant-specific parameters are outside the range used in demonstrating acceptable code performance, the licensee or applicant will submit sensitivity studies to show the effects of that deviation.	Simulation of clad temperature response is a function of phenomenological correlations that have been derived either analytically or experimentally. The important correlations have been validated for the RLBLOCA methodology and a statement of the range of applicability has been documented. The correlations of interest are the set of heat transfer correlations as described in Reference 1. Table 3-7 presents the summary of the full range of applicability for the important heat transfer correlations, as well as the ranges calculated in the limiting case of this analysis. Calculated values for other parameters of interest are also provided. As is evident, the plant-specific parameters fall within the methodology's range of applicability.
12. The licensee or applicant using the approved methodology must submit the results of the plant-specific analyses, including the calculated worst break size, PCT, and local and total oxidation.	Analysis results are discussed in Section 3.5
13. The licensee or applicant wishing to apply AREVA NP realistic large break loss-of-coolant accident (RLBLOCA) methodology to M5 clad fuel must request an exemption for its use until the planned rulemaking to modify 10 CFR 50.46(a)(i) to include M5 cladding material has been completed.	The Harris plant will have 17x17 HTP fuel bundles with M5 clad. Progress Energy has submitted the exemption request to implement M5 cladding (Reference 20).

Table 3-5: Summary of Results for the Limiting PCT Case

Case #5 (offsite power available)	Fresh UO_2 Rod (M5 Cladding)	Once-Burned UO_2 Rod (M5 Cladding)	Once-Burned UO_2 Rod (Zr-4 Cladding)
PCT			
Temperature	1919 °F	1890 °F	-
Time	103 s	103 s	-
Elevation	10.043 ft	10.043	-
Metal-Water Reaction			
Pre-transient Oxidation (%)	0.9464	1.6825	3.4447
Transient Local Oxidation Maximum (%)	2.9394	2.7016	2.7016
Total Local Oxidation Maximum (%)	3.8858	4.3841	6.1463
Percent Total Whole Core Oxidation	0.0497	N/A	N/A

Table 3-6: Calculated Event Times for the Limiting PCT Case

Event	Time (s)
Break Opened	0.0
RCP Trip	N/A
SIAS Issued	0.4
Start of Broken Loop Accumulator Injection	8.0
Start of Intact Loop Accumulator Injection (Loops 2 and 3 respectively)	11.9 and 11.9
Broken Loop HHSI Delivery Began	17.4
Intact Loop HHSI Delivery Began (Loop 2 and 3 respectively)	17.4 and 17.4
Beginning of Core Recovery (Beginning of Reflood)	26.4
LHSI Available	27.4
Broken Loop LHSI Delivery Began	27.4
Intact Loop LHSI Delivery Began (Loop 2 and 3 respectively)	27.4 and 27.4
Broken Loop Accumulator Emptied	32.6
Intact Loop Accumulators Emptied (Loops 2, and 3 respectively)	34.8 and 34.6
PCT Occurred (1919°F)	103
Transient Calculation Terminated	794.3

Table 3-7: Heat Transfer Parameters for the Limiting Case

Table 3-8: Containment Initial and Boundary Conditions

Containment Net Free Volume	2,266,000 – 2,610,000
Initial Conditions	
Containment Pressure (nominal)	14.7 psia
Containment Temperature	80 °F – 130 °F
RWST Temperature	125 °F
Outside Temperature	40 °F
Humidity	100 percent
Containment Spray	
Number of Pumps operating	2
Quench System Total Spray Flow	5,000 gpm
Minimum Spray Temperature	40°F
Fan Cooler System Start Time	0 seconds

Table 3-9: Passive Heat Sinks in Containment

Heat Sink	Surface Area (ft^2)	Slab Material	Thickness (in)
Containment Dome	26546.0	Paint-2	0.005
		Carbon Steel	0.5
		Concrete	30.0
External Cylinder Wall	63065.0	Paint-2	0.005
		Carbon Steel	0.375
		Concrete	54.0
1 In. Steel Liner Concrete	2280.0	Paint-2	0.005
		Carbon Steel	1.0
		Concrete	54.0
Concrete	82525.0	Concrete	45.0
Stainless Steel Liner Concrete	6756.0	Stainless Steel	0.1872
		Concrete	0.6
Sump	29320.0	Concrete	45.0
Piping	5703.0	Paint-3	0.005
		Carbon Steel	0.1966
Piping	3870.0	Paint-3	0.005
		Carbon Steel	0.4181
Structural Heat Sink	53810.0	Paint-2	0.005
		Carbon Steel	0.312
Electrical	33066.0	Galvanizing (Zinc)	0.0015
		Carbon Steel	0.1745
Embedded Stainless	1030.0	Stainless Steel	0.3902
		Concrete	3.2244
Effective Stainless (Not Embedded, Steel Pipe, Structural Steel, and Strainer Screen)	9143.0	Stainless Steel	0.22397
Structural Heat Sink	30300.0	Paint-2	0.005
		Carbon Steel	1.0
Not Embedded Structural	119467.0	Paint-2	0.005
		Carbon Steel	0.1738
Structural Heat Sink	66753.0	Paint-2	0.005
		Carbon Steel	0.5004
Embedded Structural	3472.0	Paint-2	0.005
		Carbon Steel	0.3405
		Concrete	3.2244
Embedded Structural	13899.0	Paint-2	0.005
		Carbon Steel	1.444
		Concrete	3.2244
Ductwork	5430.0	Paint-4	0.008
		Carbon Steel	0.1248
Ductwork	39672.0	Galvanizing Zinc	0.0015
		Carbon Steel	0.029
Seismic Hangers	84386.0	Paint-2	0.005
		Carbon Steel	0.1876

Table 3-9: Passive Heat Sinks in Containment, *(Continued)*

Material Properties		
Material	**Thermal Conductivity (Btu/hr-ft-°F)**	**Volumetric Heat Capacity (Btu/hr-ft3-°F)**
Carbon Steel	26.0	53.9
Paint-2	0.23	42.6
Paint-3	0.23	147.0
Paint-4	0.23	42.6
Galvanizing (Zinc)	64.0	40.6
Concrete	0.92	22.62
Stainless Steel	9.4	53.9

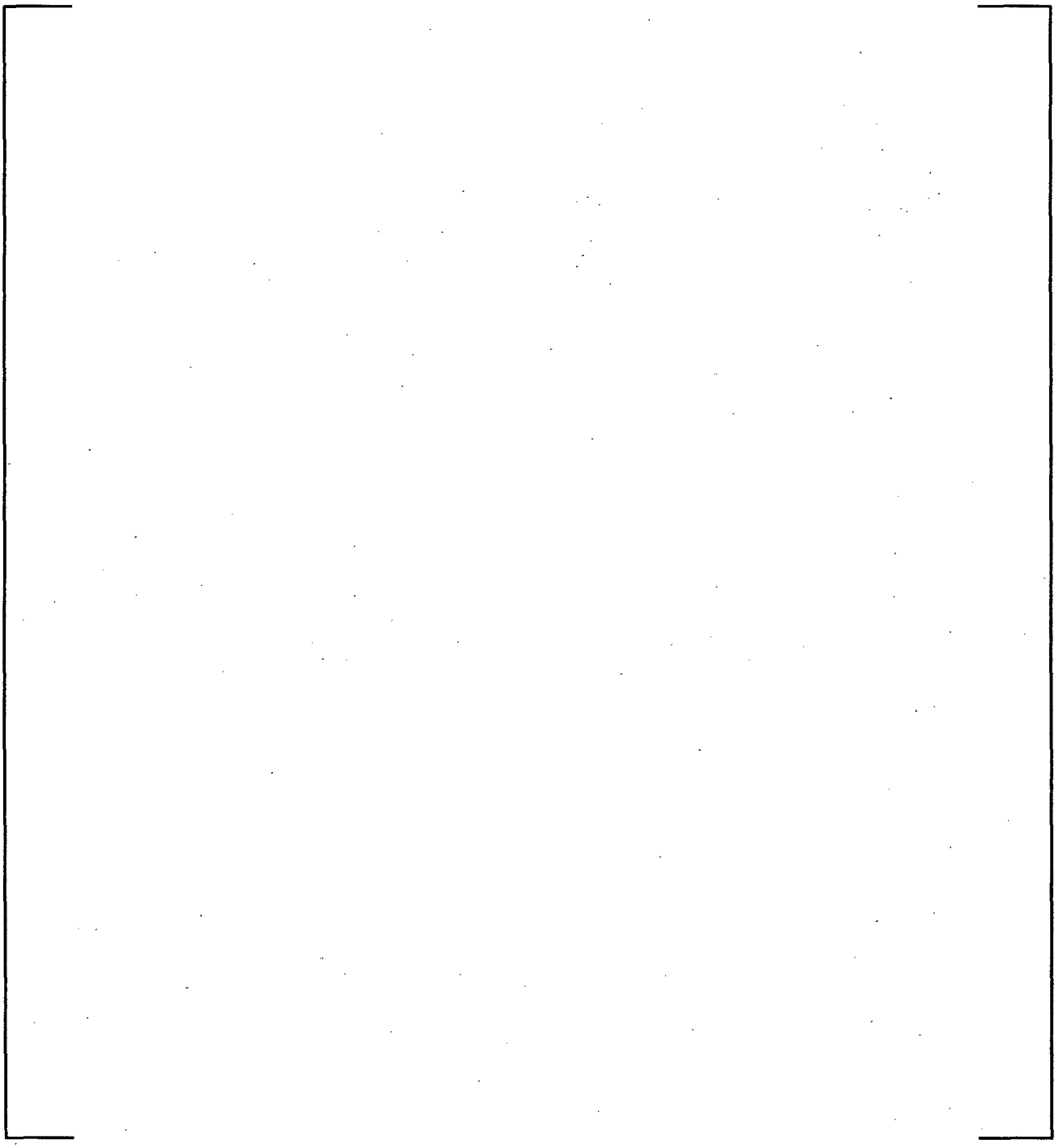

Figure 3-1: Primary System Noding

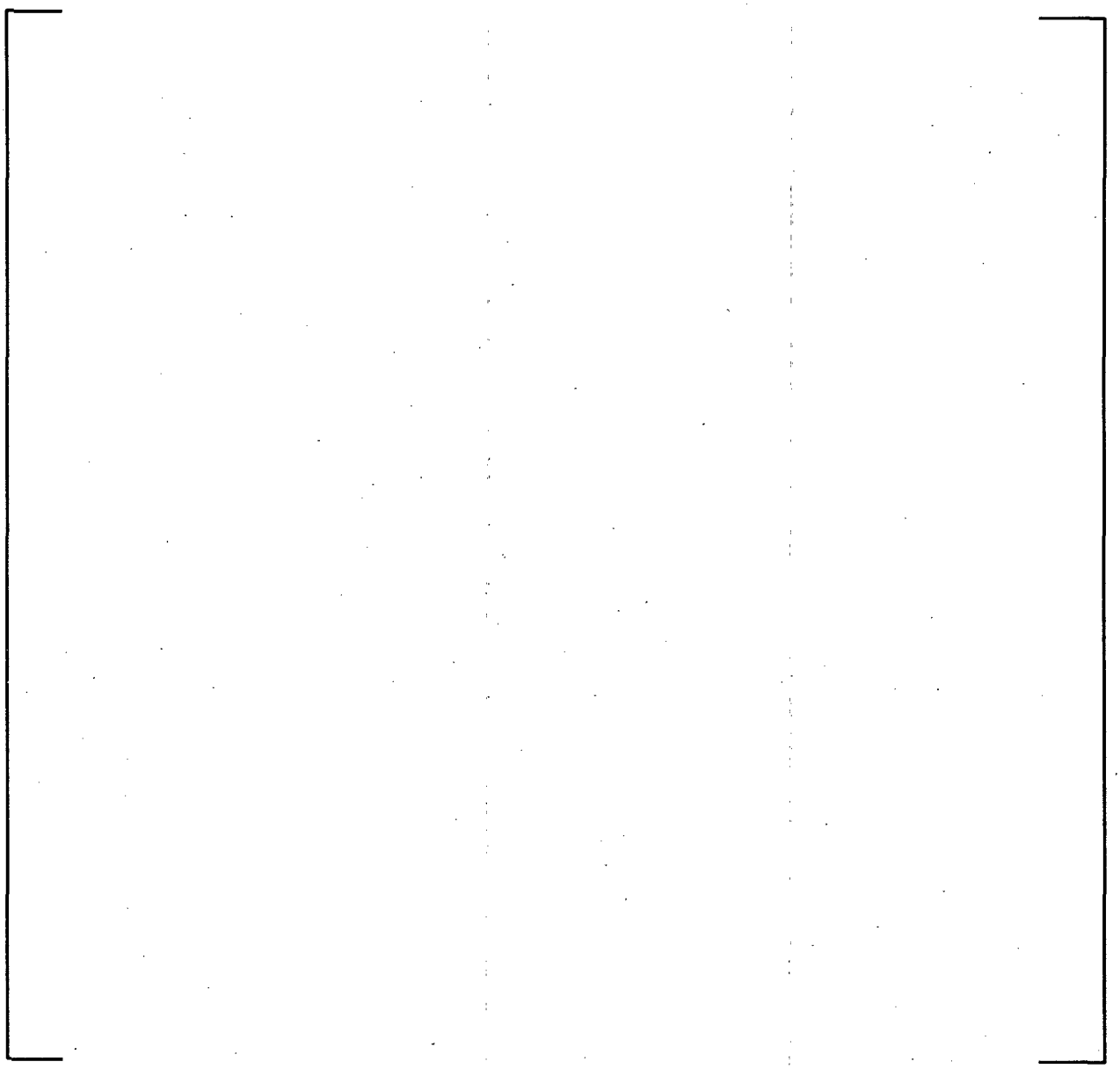

Figure 3-2: Secondary System Noding

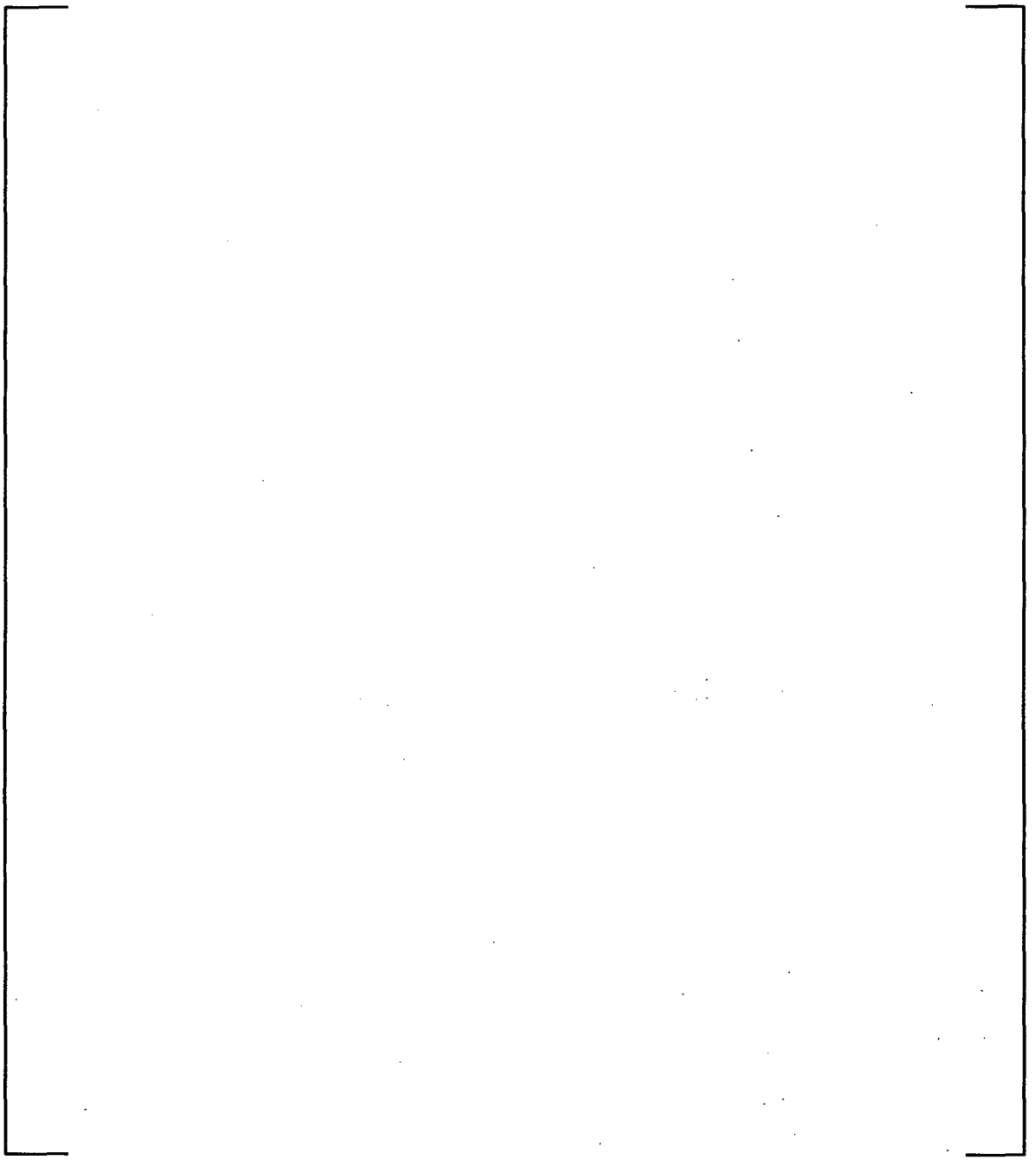

Figure 3-3: Reactor Vessel Noding

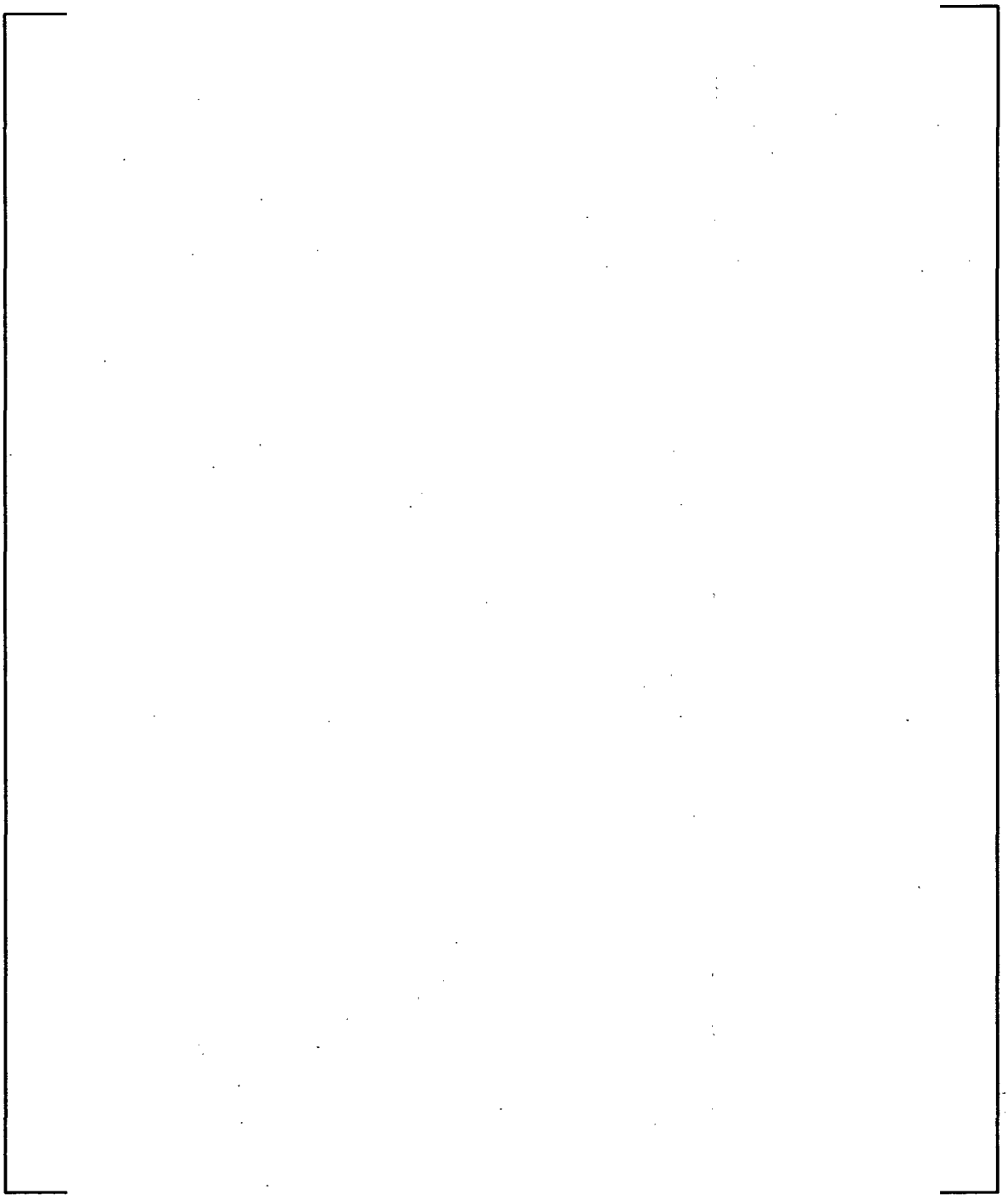

Figure 3-4: Core Noding Detail

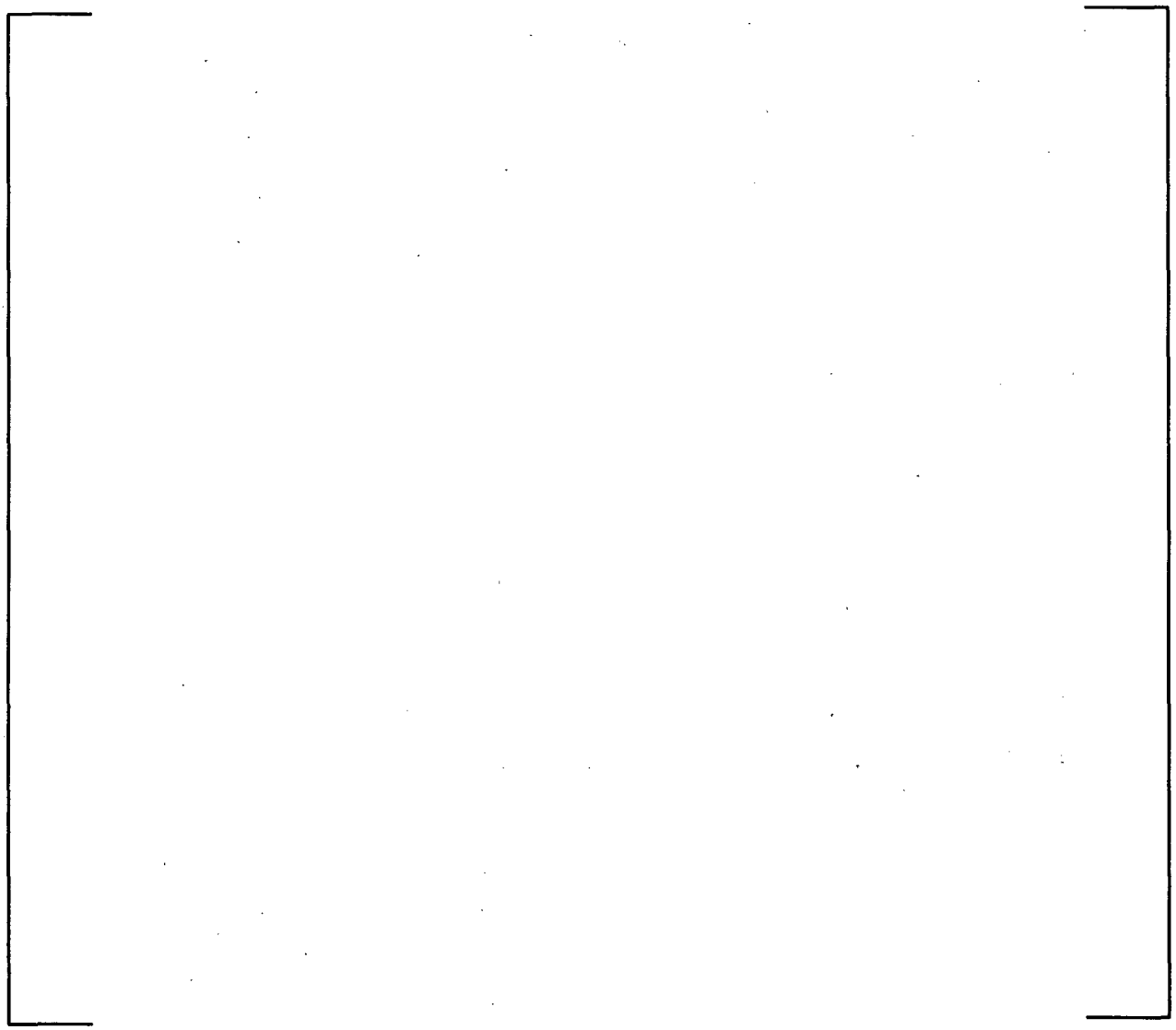

Figure 3-5: Upper Plenum Noding Detail

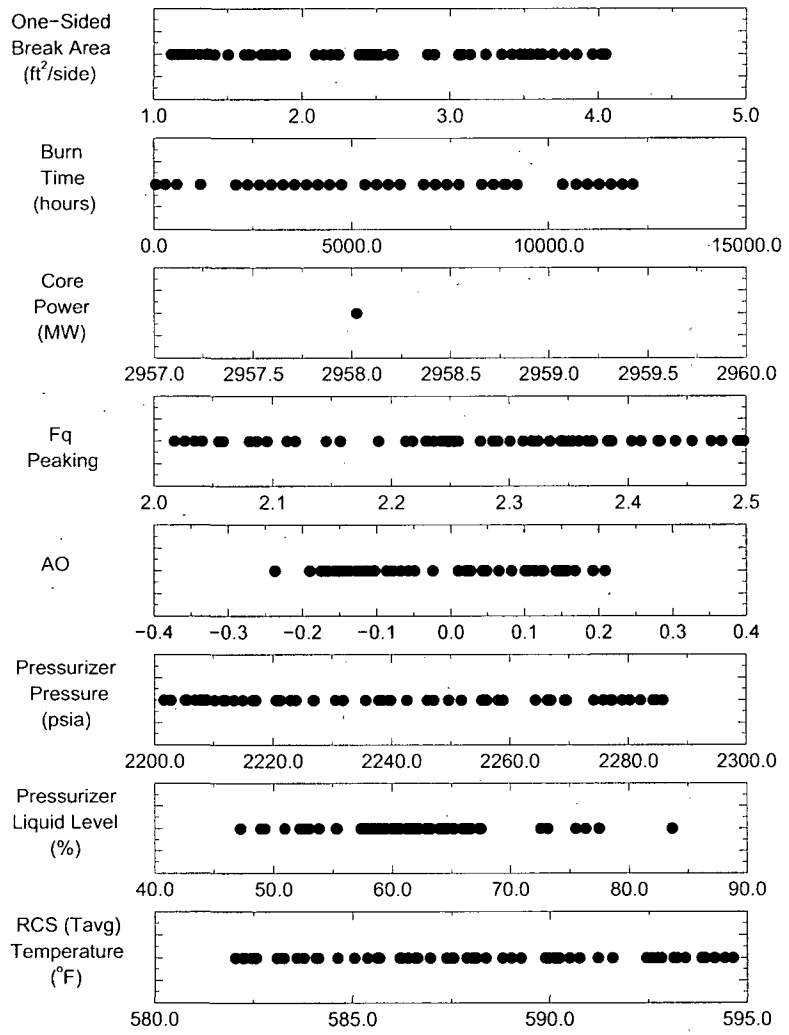

Figure 3-6: Scatter Plot of Operation Parameters

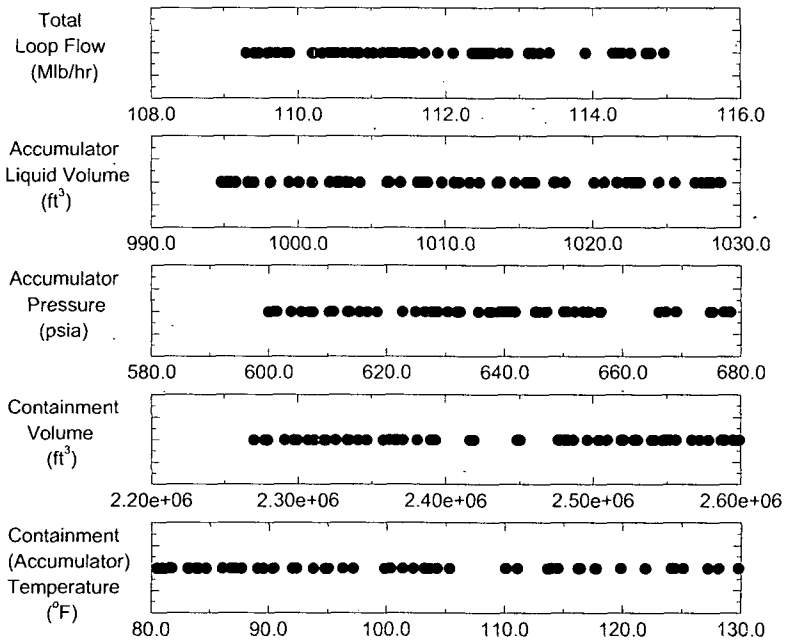

Figure 3-6 Scatter Plot of Operation Parameters (Continued)

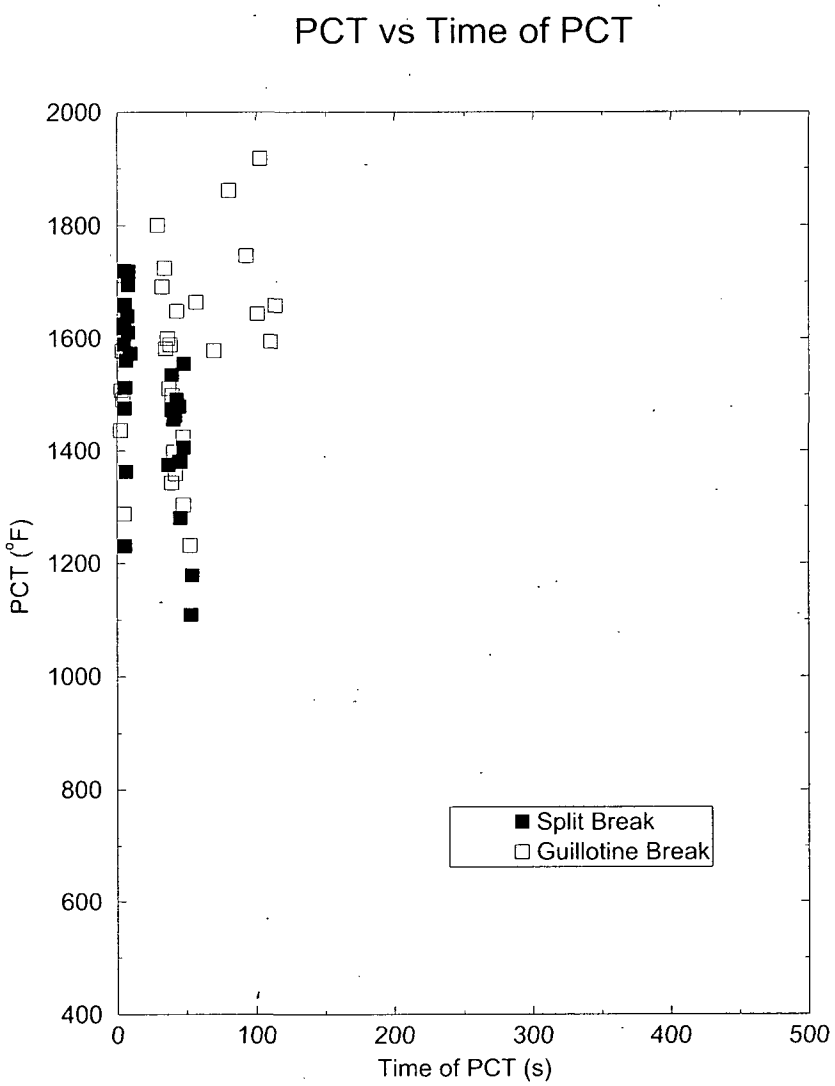

Figure 3-7: PCT versus PCT Time Scatter Plot from 59 No-LOOP Calculations

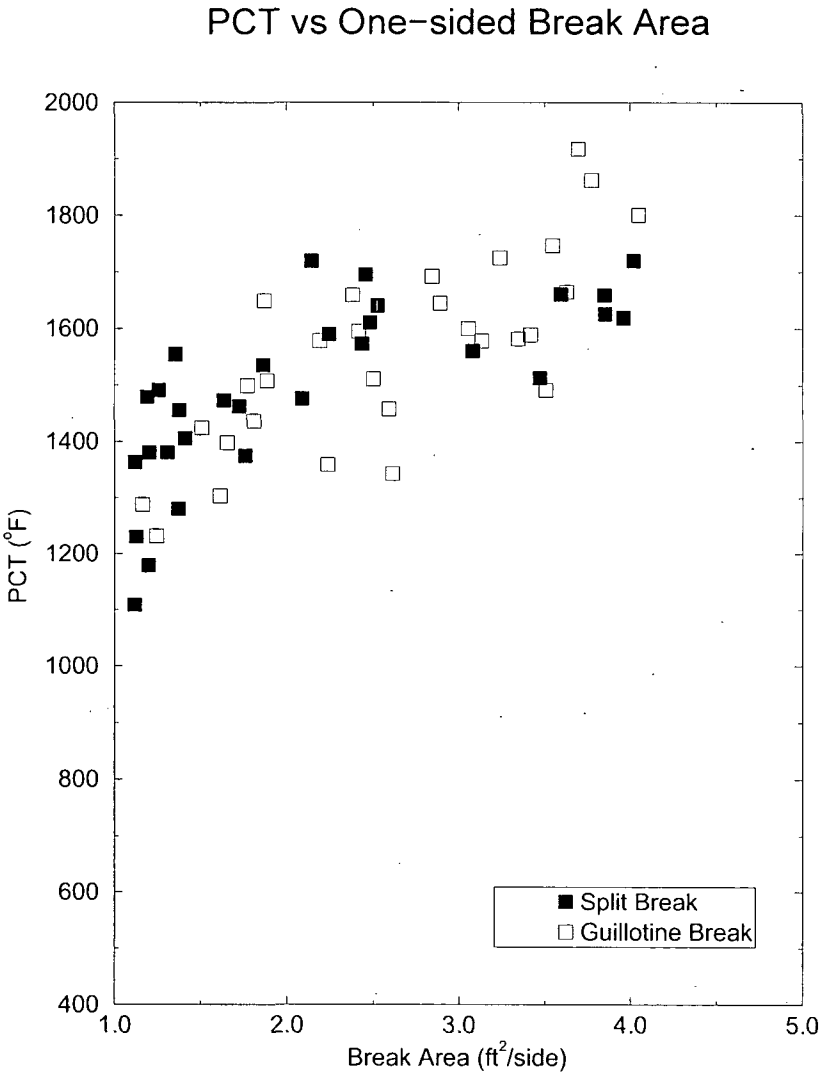

Figure 3-8: PCT versus Break Size Scatter Plot from 59 No-LOOP Calculations

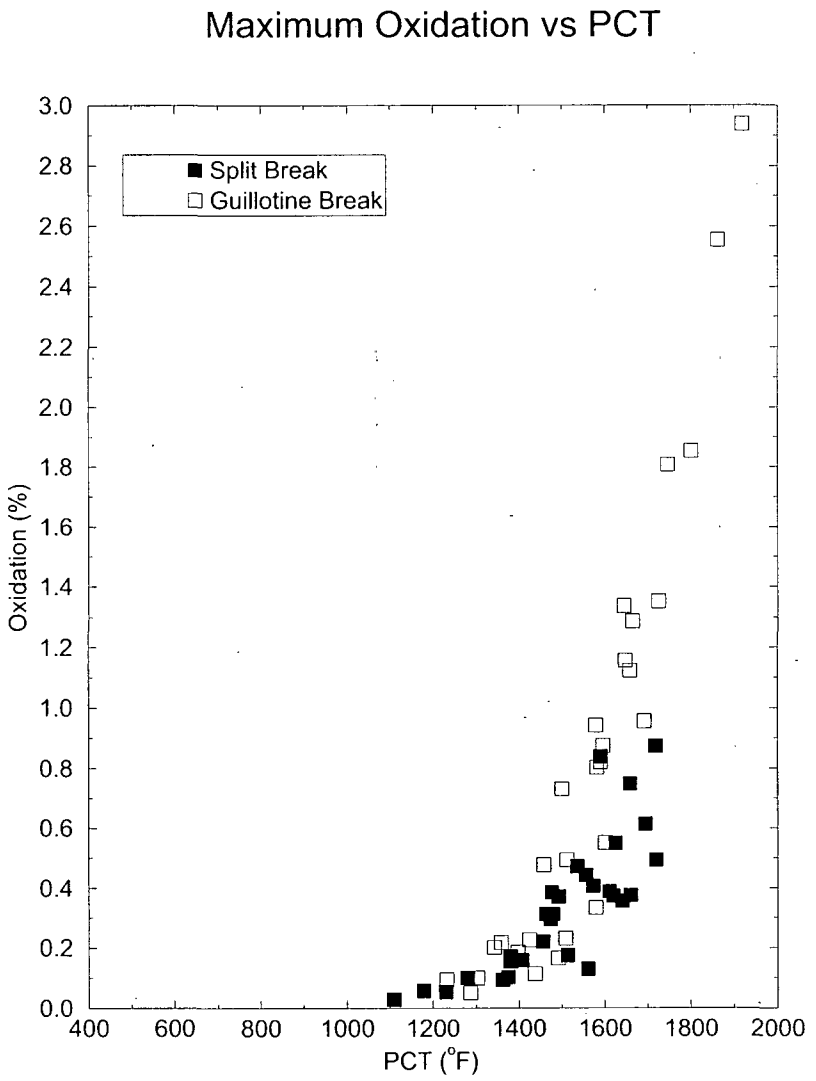

Figure 3-9: Maximum Oxidation versus PCT Scatter Plot from 59 No-LOOP Calculations

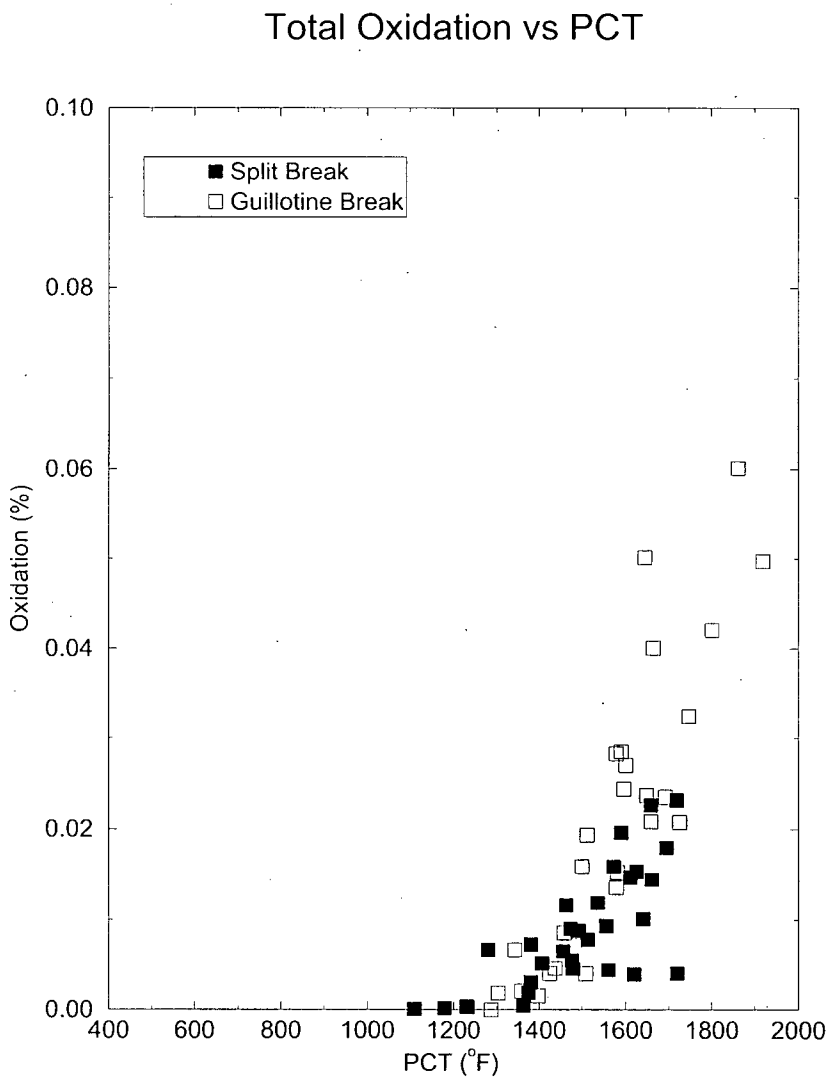

Figure 3-10: Total Oxidation versus PCT Scatter Plot from 59 No-LOOP Calculations

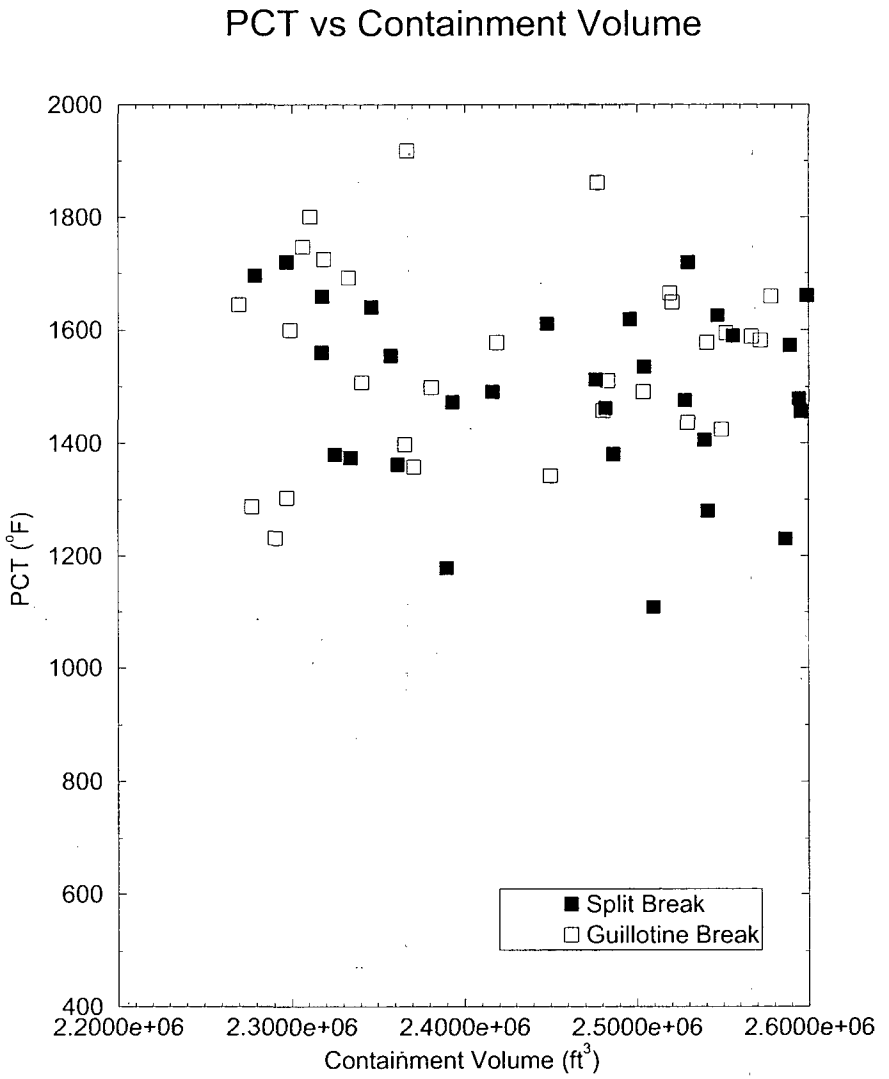

Figure 3-11: Containment Volume versus PCT Scatter Plot from 59 No-LOOP Calculations

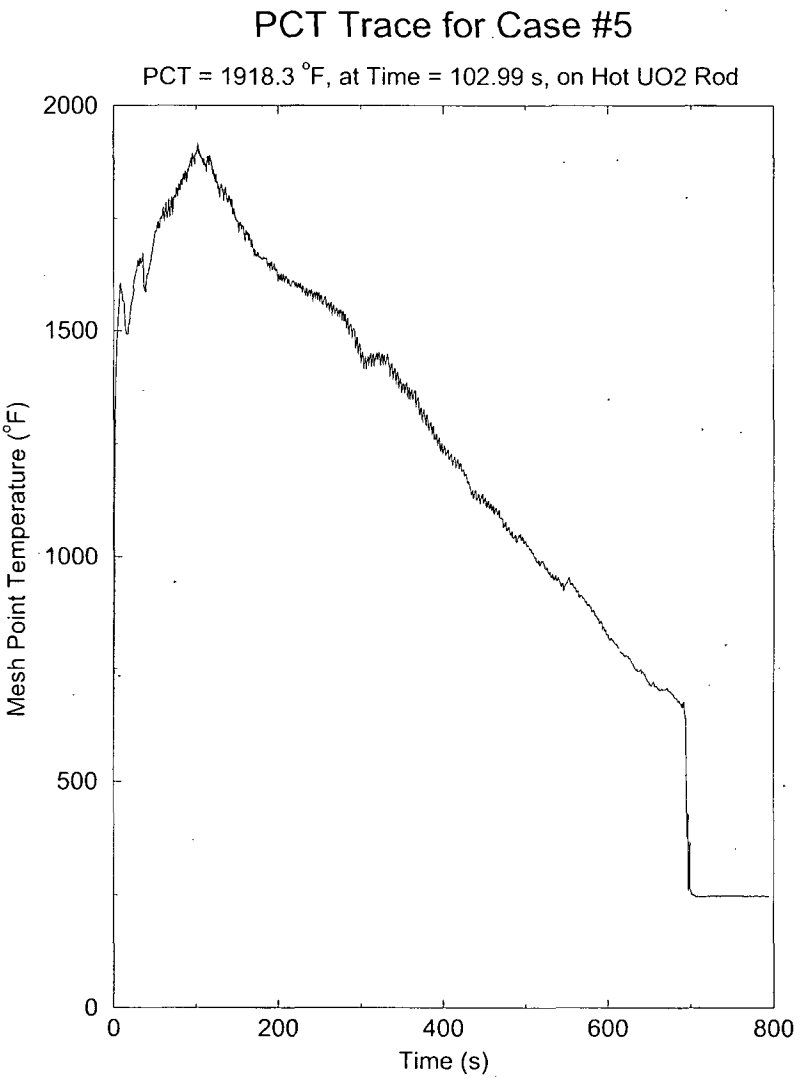

ID:03615 11Jun2011 20:30:52 R5DMX

Figure 3-12: Peak Cladding Temperature (Independent of Elevation) for the Limiting Case

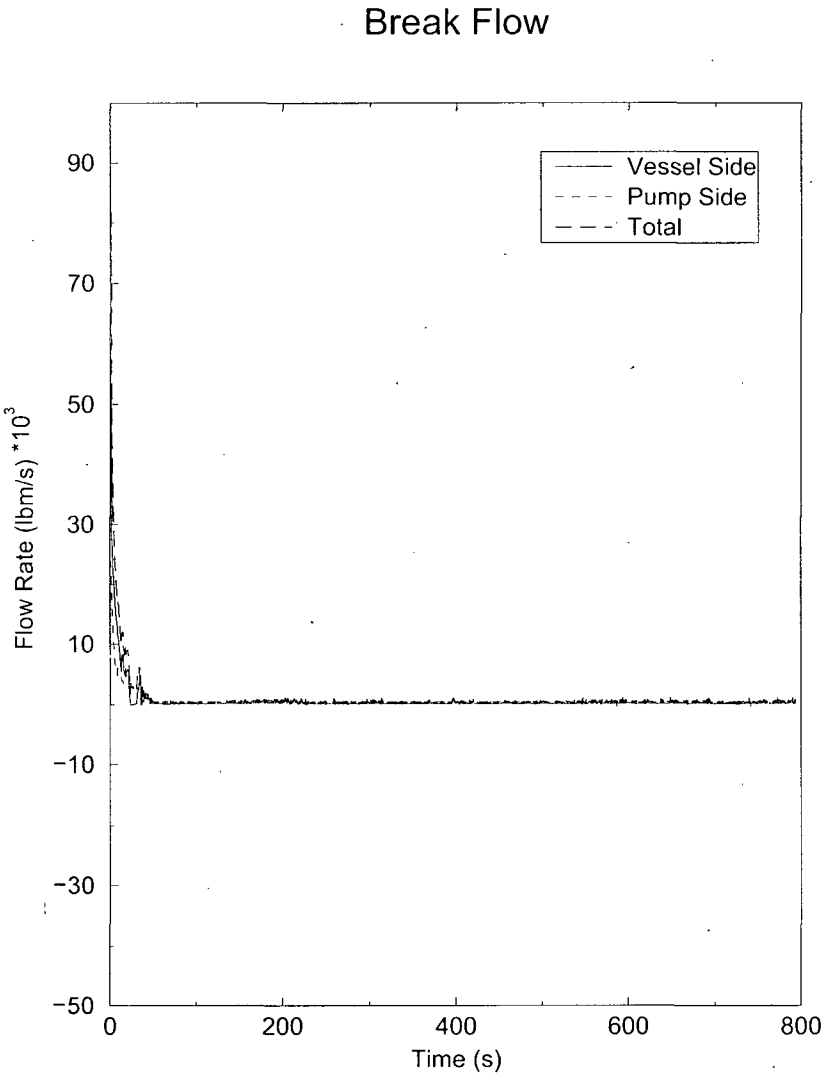

ID:03615 11Jun2011 20:30:52 R5DMX

Figure 3-13: Break Flow for the Limiting Case

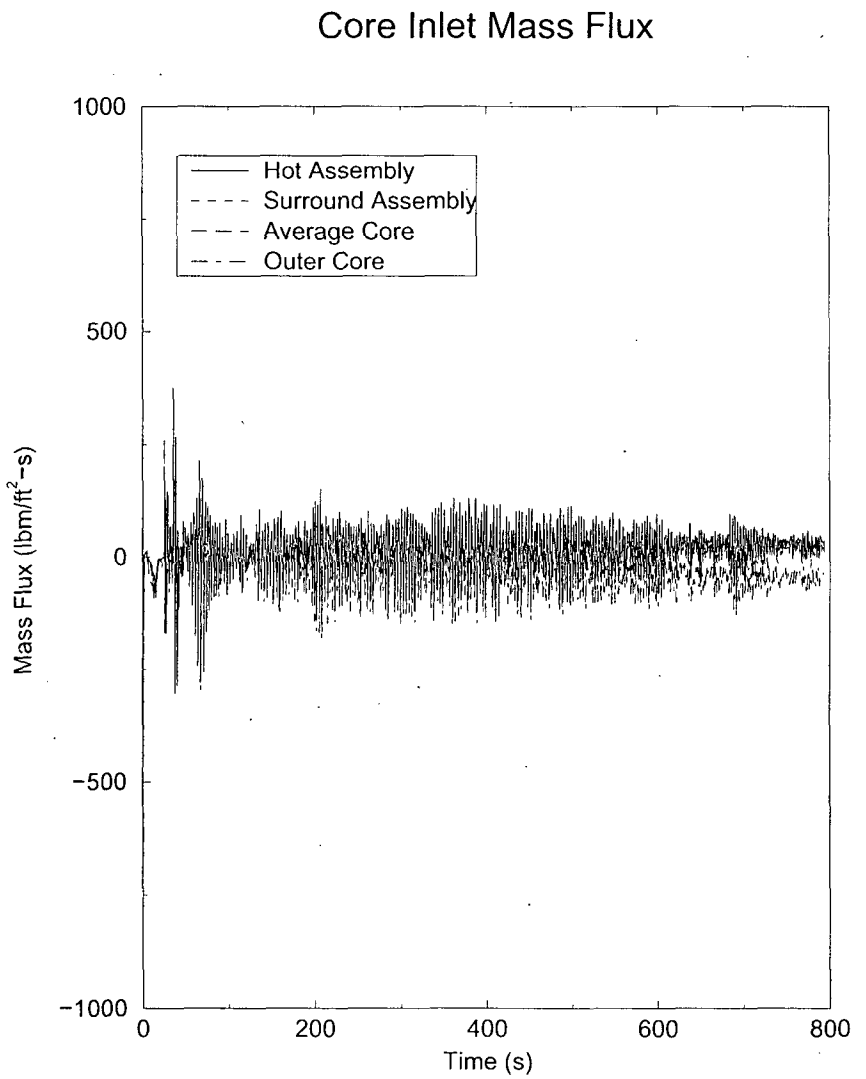

ID:03615 11Jun2011 20:30:52 R5DMX

Figure 3-14: Core Inlet Mass Flux for the Limiting Case

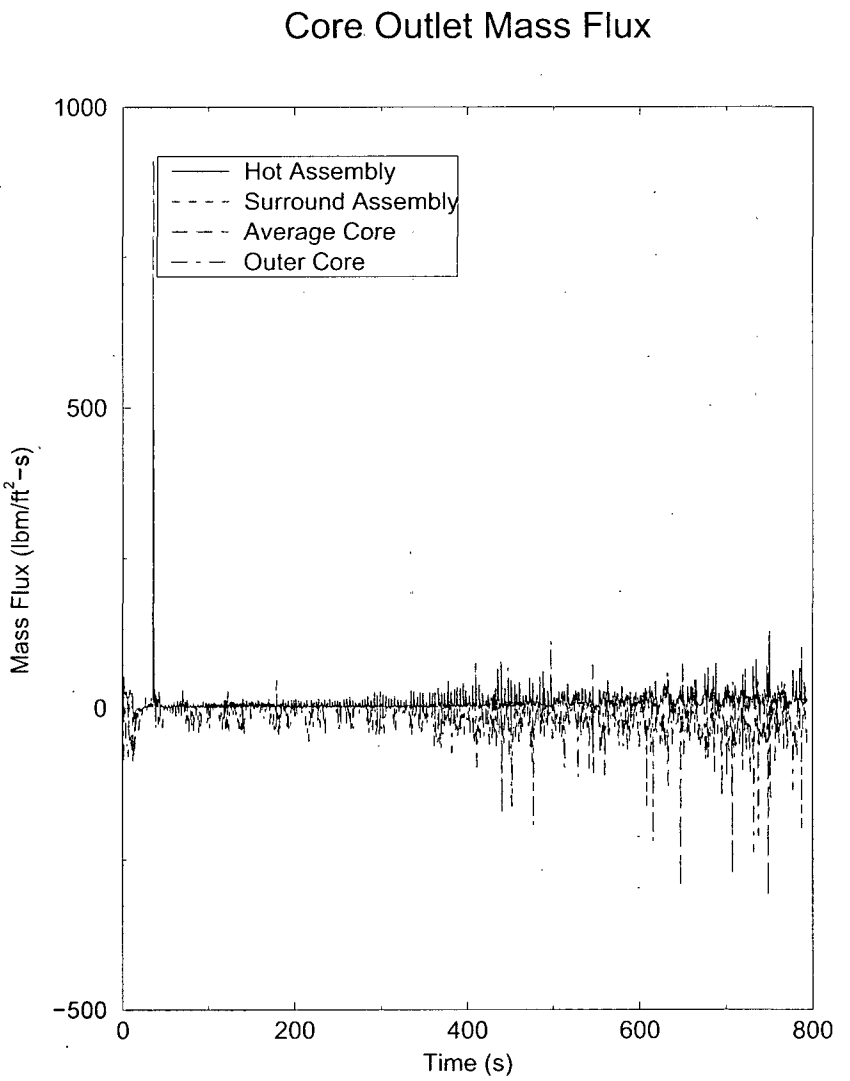

Figure 3-15: Core Outlet Mass Flux for the Limiting Case

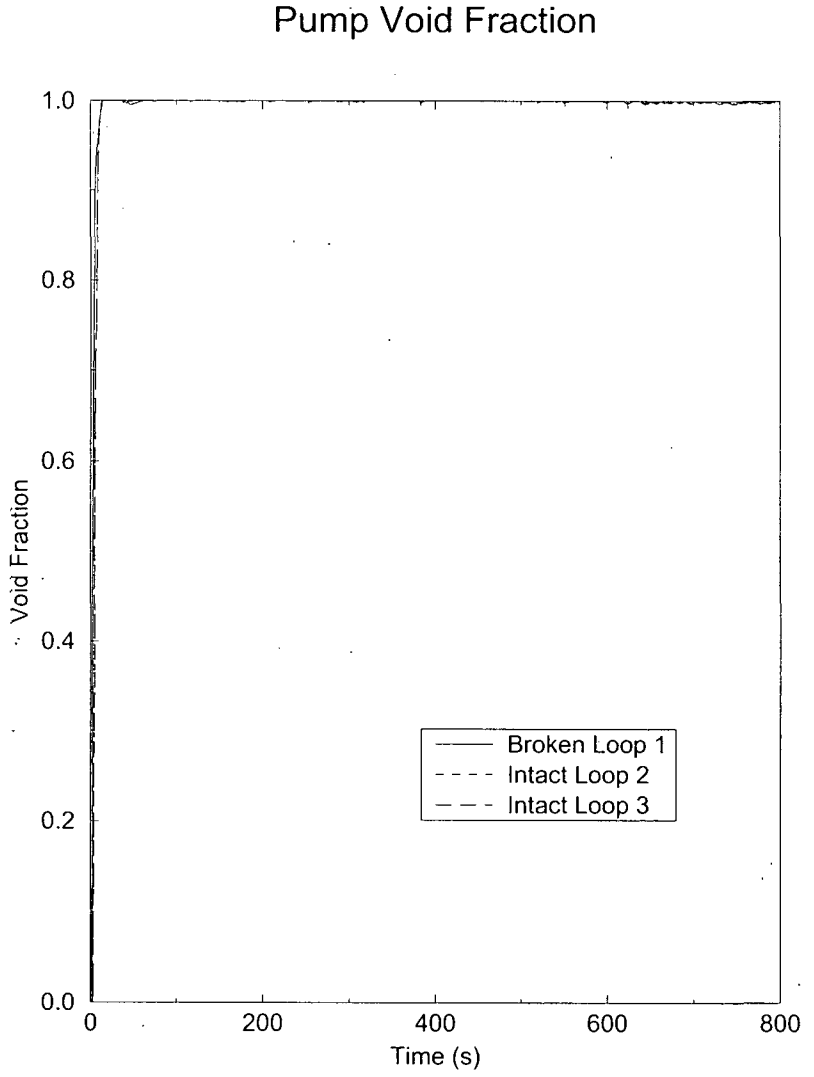

ID:03615 11Jun2011 20:30:52 R5DMX

Figure 3-16: Void Fraction at RCS Pumps for the Limiting Case

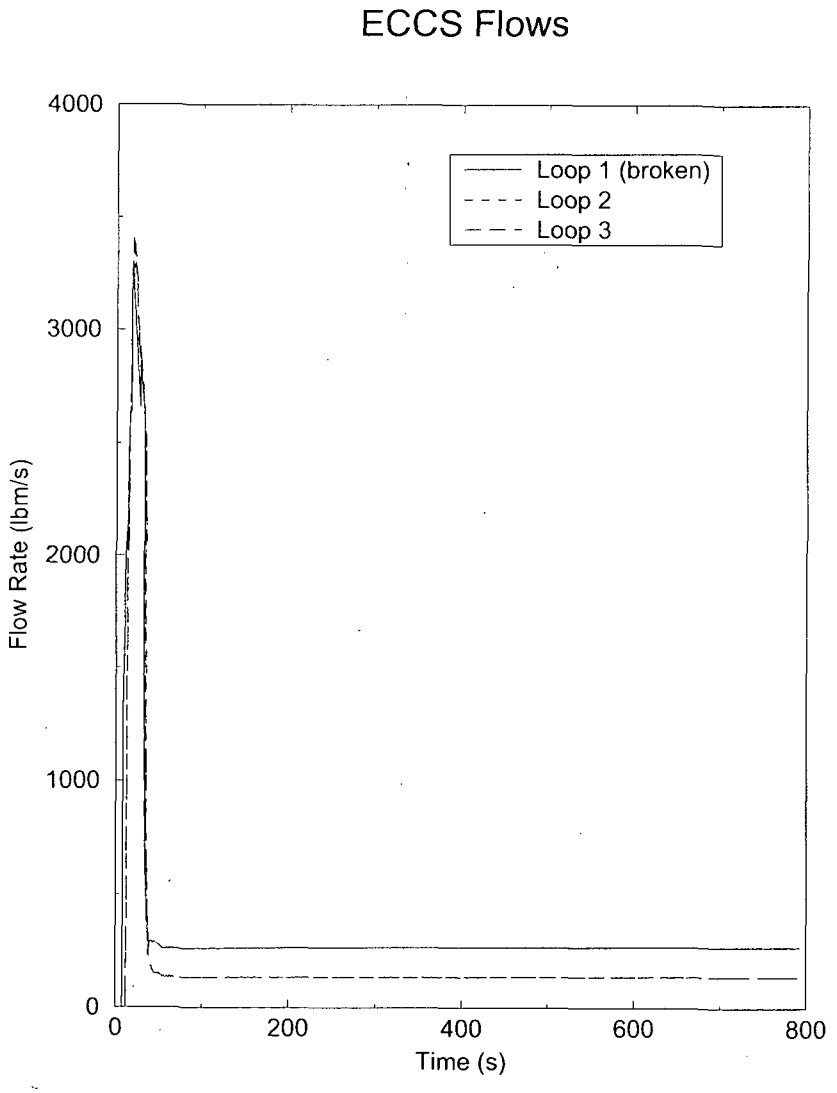

Figure 3-17: ECCS Flows (Includes Accumulator, HHSI and LHSI) for Limiting Case

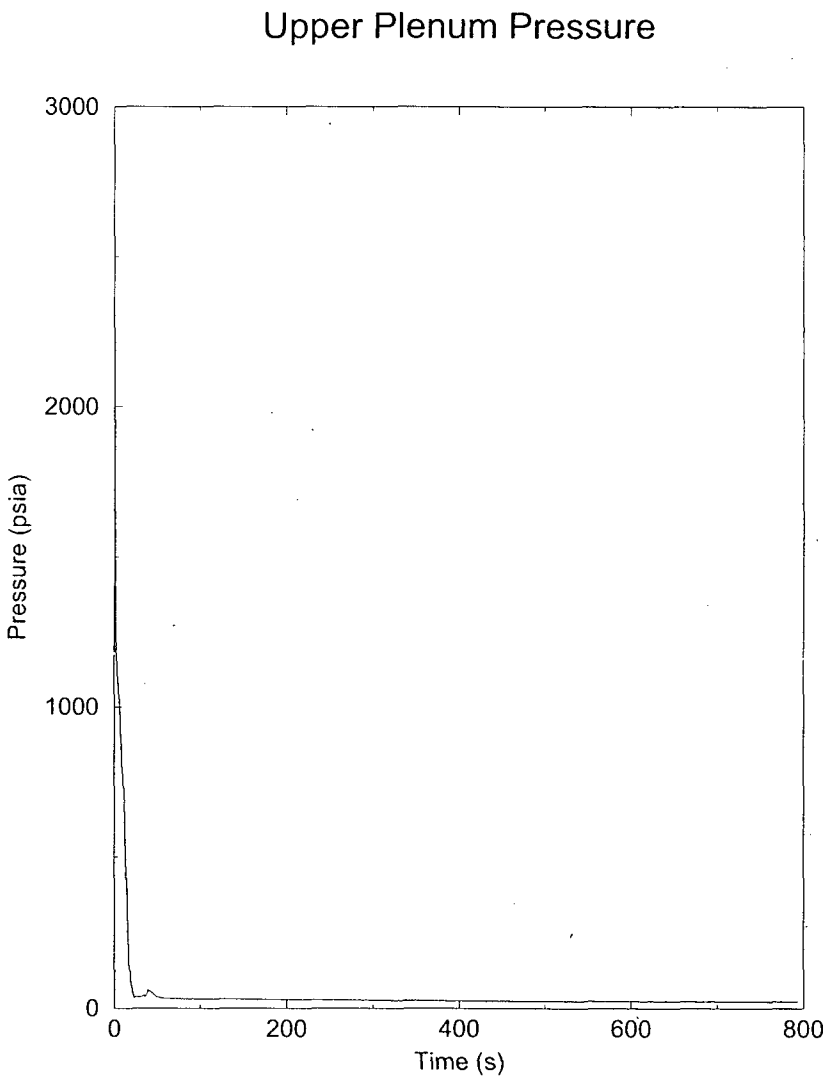

Figure 3-18: Upper Plenum Pressure for the Limiting Case

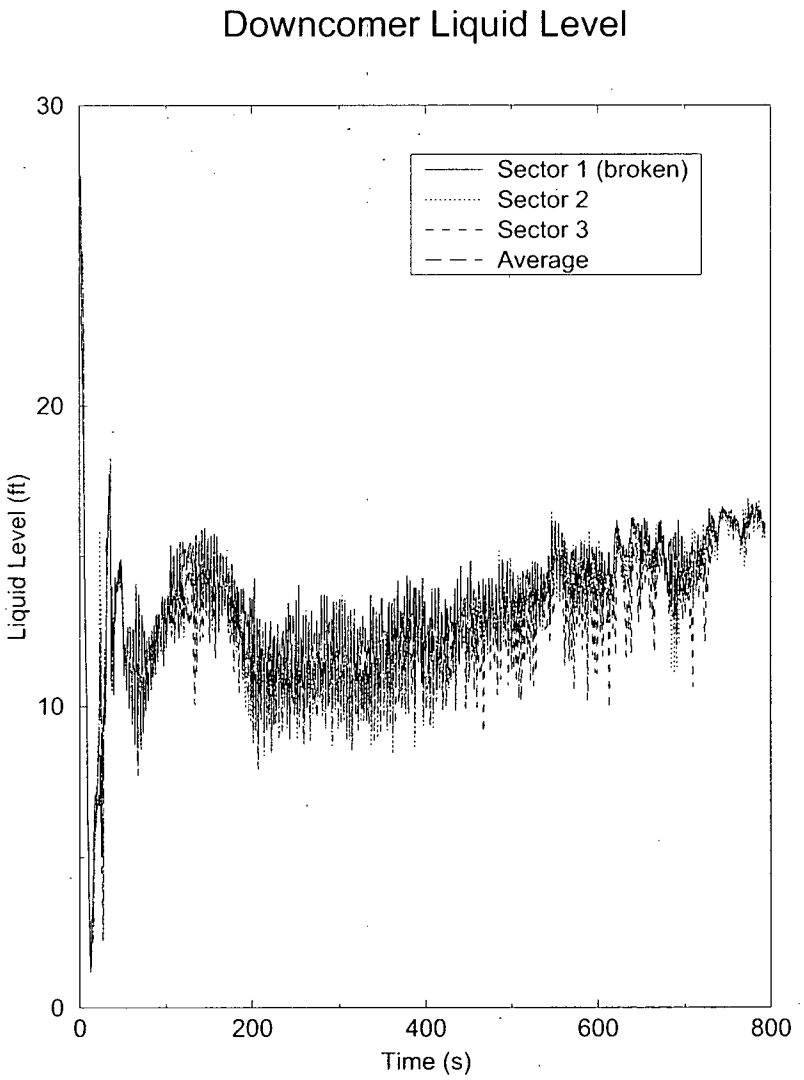

Figure 3-19: Collapsed Liquid Level in the Downcomer for the Limiting Case

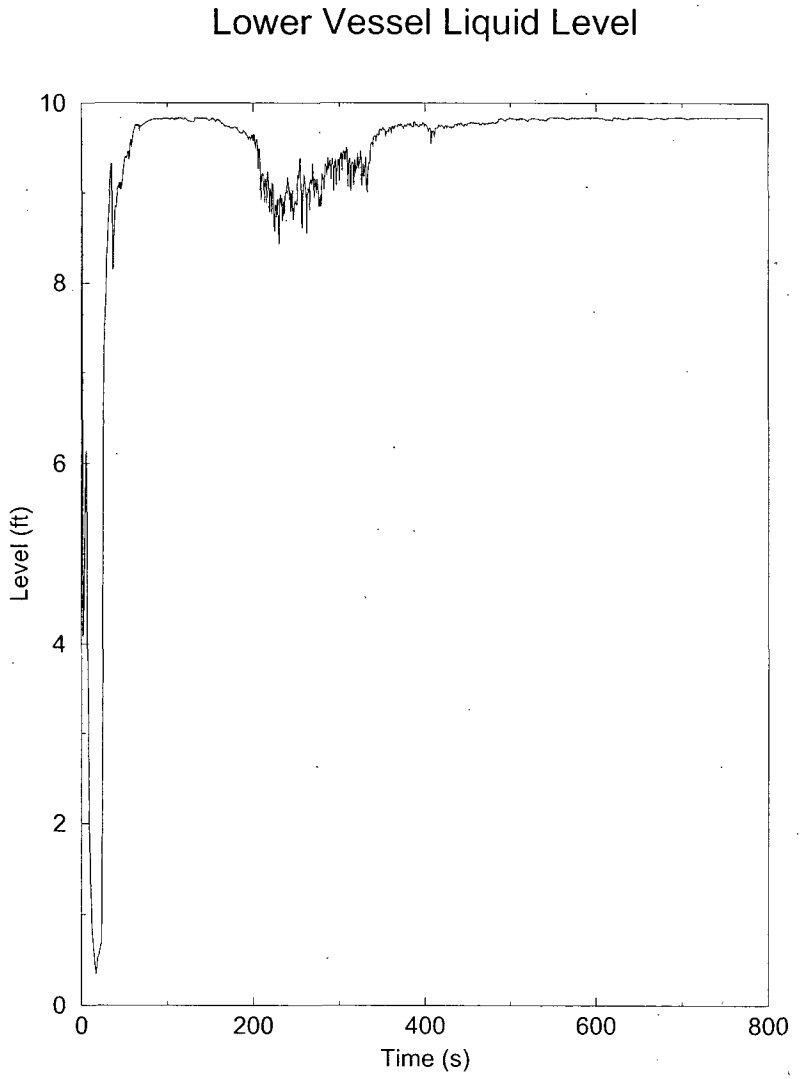

Figure 3-20: Collapsed Liquid Level in the Lower Plenum for the Limiting Case

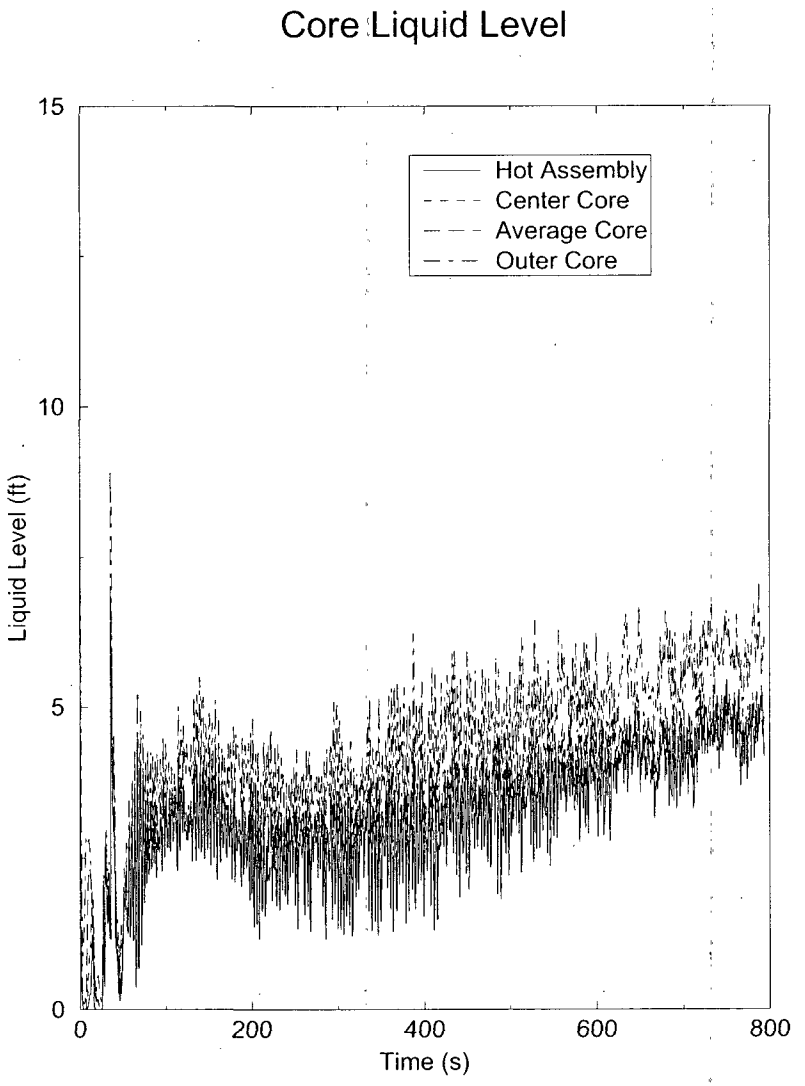

ID:03615 11Jun2011 20:30:52 R5DMX

Figure 3-21: Collapsed Liquid Level in the Core for the Limiting Case

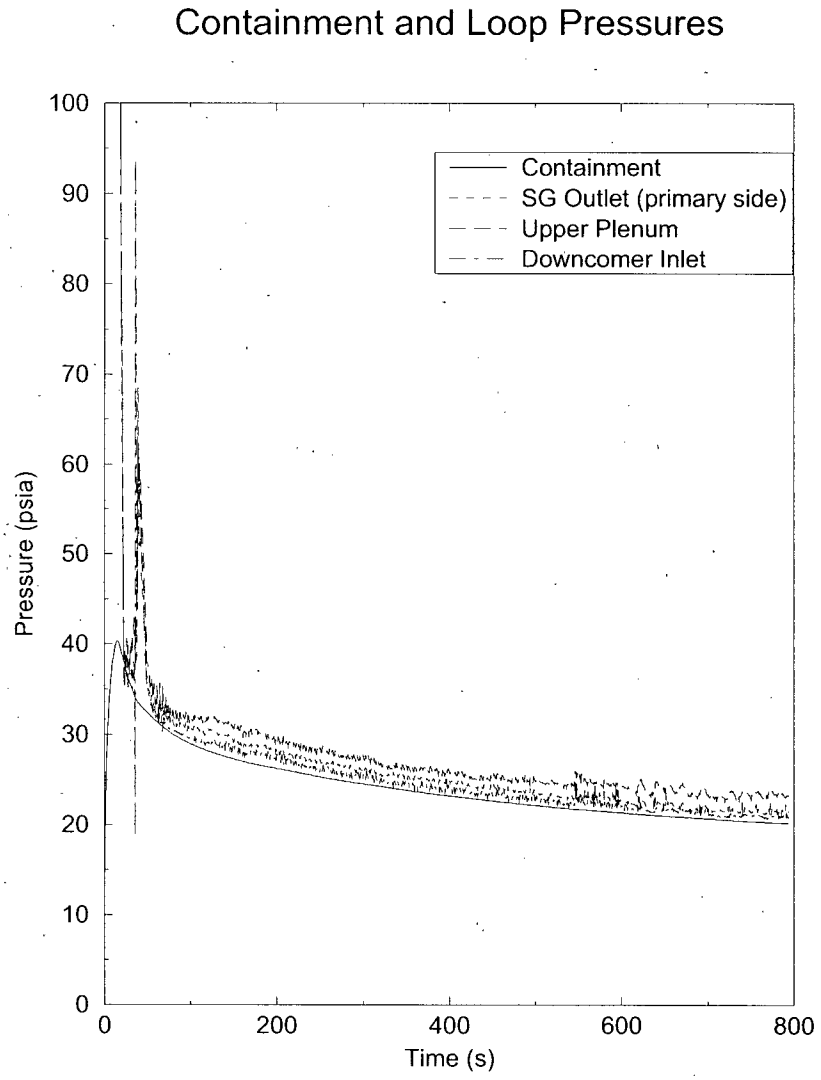

Figure 3-22: Containment and Loop Pressures for the Limiting Case

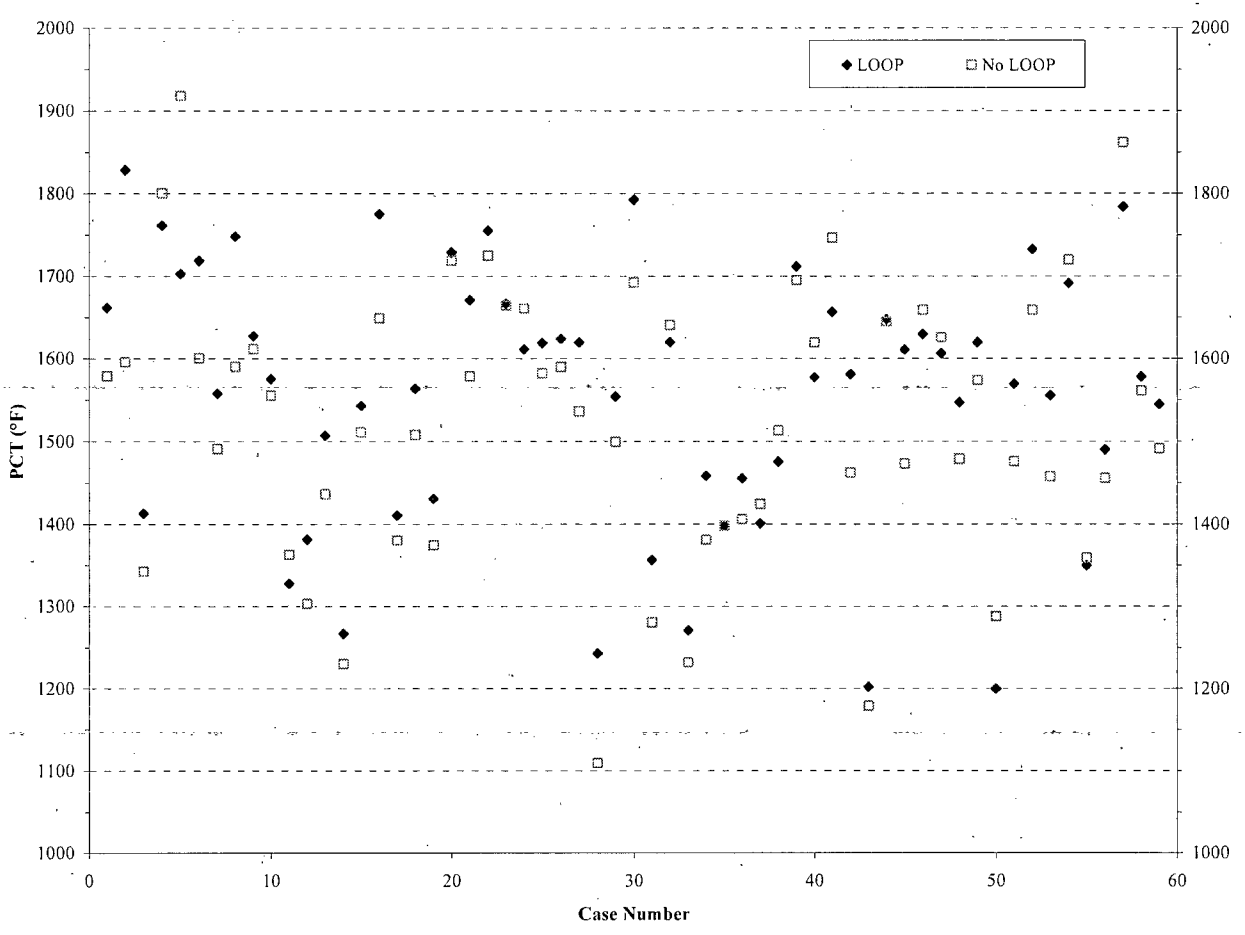

Figure 3-23: GDC 35 LOOP versus No-LOOP Cases

4.0 CONCLUSIONS

The results of the RLBLOCA analysis show that the limiting No LOOP case has a PCT of 1919 °F, and a maximum oxidation thickness and hydrogen generation that fall well within regulatory requirements.

The analysis supports operation at a safety analysis power level of 2958 MWt (nominal core power including uncertainties), a steam generator tube plugging level of up to 3 percent in all steam generators, a total peaking factor (F_Q) of 2.52 (including uncertainty) and a nuclear enthalpy rise factor ($F_{\Delta H}$) of 1.73 (including uncertainty) with no axial or burnup dependent power peaking limit.

5.0 TRANSITION PACKAGE – ADDITIONAL INFORMATION SUPPORTING EMF 2103 REV. 0

Section 5 contains responses to typical RAI questions posed by the NRC on EMF-2103 Revision 0 plant applications. In some instances, these requests cross-referenced documentation provided on dockets other than those for which the request is made. AREVA discussed these and similar questions from the NRC draft SER for Revision 1 of EMF-2103 in a meeting with the NRC on December 12, 2007. AREVA agreed to provide the following additional information within new submittals of a Realistic Large Break LOCA report; this additional information is referred to as the "Transition Package."

5.1 Reactor Power

Question: *Reactor Power - Table 3-2, Item 2.1, and its associated Footnote 1 indicate that the assumed reactor core power "includes uncertainties." The use of a reactor power assumption other than 102 percent, regardless of BE or Appendix K methodology, is permitted by Title 10 of the Code of Federal Regulations (10 CFR), Part 50, Appendix K.I.A, "Required and Acceptable Features of The Evaluation Models, 'Sources of Heat During a LOCA." However, Appendix K.I.A also states: "... An assumed power level lower than the level specified in this paragraph [1.02 times the licensed power level], (but not less than the licensed power level) may be used provided . . ."*

Response: As indicated in Item 2.1 of Table 3-2 herein, the assumed reactor core power for the Harris realistic large break loss-of-coolant accident is 2958 MWt. This value represents a value that bounds both current licensed power level (2900 MWt with an uncertainty of 2%) and proposed operation with a Measurement Uncertainty Recapture (MUR) operation (2948 MWt with 0.34%). The MUR application is under separate review by the NRC.

5.2 Rod Quench

Question: *Does the version of S-RELAP5 used to perform the computer runs assure that the void fraction is less than 95 percent and the fuel cladding temperature is less than 900 °F before it allows rod quench?*

Response: Yes, the version of S-RELAP5 employed for the HNP Unit 1 LAR requires that both the void fraction is less than 0.95 and the clad temperature is less than the minimum temperature for film boiling heat transfer (T_{min}) before the rod is allowed to quench. T_{min} is a sampled parameter in the RLBLOCA methodology with a mean value of 626 K and a standard deviation of 33.6 K, making it very unlikely that Tmin would exceed 755 K (900 °F). For the HNP Unit 1 case set T_{min} was never sampled above 697.3K (795.5 °F). This is a change to the approved RLBLOCA EM (Reference 1). This feature is carried forward into the UAPR09 version of S-RELAP5.

5.3 Rod-to-Rod Thermal Radiation

Question: *Provide justification that the S-RELAP5 rod-to-rod thermal radiation model applies to the Harris core.*

Response: The Realistic LBLOCA methodology, (Reference 1), does not provide modeling of rod-to-rod radiation. The fuel rod surface heat transfer processes included in the solution at high temperatures are: film boiling, convection to steam, rod to liquid radiation and rod to vapor radiation. This heat transfer package was assessed against various experimental data sets involving both moderate (1600 °F – 2000 °F) and high (2000 °F to over 2200 °F) peak cladding temperatures and shown to be conservative when applied nominally. The normal distribution of the experimental data was then determined. During the execution of an RLBLOCA evaluation, the heat transferred from a fuel rod is determined by the application of a multiplier to the nominal heat transfer model. This multiplier is determined by a random sampling of the normal distribution of the experimental data benchmarked. Because the data include the effects of rod-to-rod radiation, it is reasonable to conclude that the modeling implicitly includes an allocation for rod-to-rod radiation effects. As will be demonstrated, the approach is reasonable because the conditions within actual limiting fuel assemblies assure that the actual rod-to-rod radiation is larger than the allocation provided through normalization to the experiments.

The FLECHT-SEASET tests evaluated covered a range of PCTs from 1,651 to 2,239 °F and the THTF tests covered a range of PCTs from 1,000 to 2,200 °F. Since the test bundle in either FLECHT-SEASET or THTF is surrounded by a test vessel, which is relatively cool compared to the heater rods, substantial radiation from the periphery rods to the vessel wall can occur. The rods selected for assessing the RLBLOCA reflood heat transfer package were chosen from the interior of the test assemblies to minimize the impact of radiation heat transfer to the test vessel. The result was that the assessment rods comprise a set which is primarily isolated from cold wall effects by being surrounded by powered rods at reasonably high temperatures.

As a final assessment, three benchmarks independent of THTF and FLECHT-SEASET were performed. These benchmarks were selected from the Cylindrical Core Test Facility (CCTF), LOFT, and the Semiscale facilities. Because these facilities are more integral tests and together cover a wide range of scale, they also serve to show that scale effects are accommodated within the code calculations.

The results of these calculations are provided in Section 5.3.4, Evaluation of Code Biases, page 4-100, of Reference 1. The CCTF results are shown in Figures 4.180 through 4.192, the LOFT results in Figures 4.193 through 4.201, and the Semiscale results in Figures 4.202 through 4.207. As expected, these figures demonstrate that the comparison between the code calculations and data is improved with the application of the derived biases. The CCTF, LOFT, and Semiscale benchmarks further indicate that, whatever consideration of rod-to-rod radiation is implicit in the S-RELAP5 reflood heat transfer modeling, it does not significantly effect code predictions under conditions where radiation is minimized. The measured PCTs in these assessments ranged from approximately 1,000 to 1,540 °F. At these temperatures, there is little rod-to-rod radiation. Given the good agreement between the

biased code calculations and the CCTF, LOFT, and Semiscale data, it can be concluded that there is no significant over prediction of the total heat transfer coefficient.

Notwithstanding any conservatism evidenced by experimental benchmarks, the application of the model to commercial nuclear power plants provides some additional margins due to limitations within the experiments. The benchmarked experiments, FLECHT SEASET and ORNL Thermal Hydraulic Test Facility (THTF), used to assess the S-RELAP5 heat transfer model, Reference 1, incorporated constant rod powers across the experimental assembly. Temperature differences that occurred were the result of guide tube, shroud or local heat transfer effects. In the operation of a pressurized water reactor (PWR) and in the RLBLOCA evaluation, a radial local peaking factor is present, creating power differences that tend to enhance the temperature differences between rods. In turn, these temperature differences lead to increases in net radiation heat transfer from the hotter rods. The expected rod-to-rod radiation will likely exceed that embodied within the experimental results.

5.3.1 Assessment of Rod-to-Rod Radiation Implicit in the RLBLOCA Methodology

As discussed above, the FLECHT-SEASET and THTF tests were selected to assess and determine the S-RELAP5 code heat transfer bias and uncertainty. Uniform radial power distribution was used in these test bundles. Therefore, the rod-to-rod temperature variation in the rods away from the vessel wall is caused primarily by the variation in the sub-channel fluid conditions. In the real operating fuel bundle, on the other hand, there can be 5 to 10 percent rod-to-rod power variation. In addition, the methodology includes a provision to apply the uncertainty measurement to the hot pin. Table 5-1 provides the hot pin measurement uncertainty and a representative local pin peaking factor for several plants. These factors, however, relate the pin to the assembly average. To more properly assess the conditions under which rod-to-rod radiation heat transfer occurs, a more local peaking assessment is required. Therefore, the plant rod-to-rod radiation assessments herein set the average pin power for those pins surrounding the hot pin at 96 percent of that of the peak pin. For pins further removed the average power is set to 94 percent.

Table 5-1: Typical Measurement Uncertainties and Local Peaking Factors

Plant	$F_{\Delta H}$ Measurement Uncertainty (percent)	Local Pin Peaking Factor (-)
1	4.0	1.068
2	4.0	1.050
3	6.0	1.149
4	4.0	1.113
5	4.25	1.135
6	4.0	1.058

5.3.2 Quantification of the Impact of Thermal Radiation using R2RRAD Code

The R2RRAD radiative heat transfer model was developed by Los Alamos National Laboratory (LANL) to be incorporated in the BWR version of the TRAC code. The theoretical basis for this code is given in References 8 and 11 and is similar to that developed in the HUXY rod heatup code (Reference 10, Section 2.1.2) used by AREVA for BWR LOCA applications. The version of R2RRAD used herein was obtained from the NRC to examine the rod-to-rod radiation characteristics of a 5x5 rod segment of the 161 rod FLECHT-SEASET bundle. The output provided by the R2RRAD code includes an estimate of the net radiation heat transfer from each rod in the defined array. The code allows the input of different temperatures for each rod as well as for a boundary surrounding the pin array. No geometry differences between pin locations are allowed. Even though this limitation affects the view factor calculations for guide tubes, R2RRAD is a reasonable tool to estimate rod-to-rod radiation heat transfer.

The FLECHT-SEASET test series was intended to simulate a 17x17 fuel assembly and there is a close similarity, Table 5-2, between the test bundle and a modern 17x17 assembly.

Table 5-2: FLECHT-SEASET & 17x17 FA Geometry Parameters

Design Parameter	FLECHT-SEASET	17x17 Fuel Assembly
Rod Pitch (in)	0.496	0.496
Fuel Rod Diameter (in)	0.374	0.374
Guide Tube Diameter (in)	0.474	0.482

Five FLECHT-SEASET tests (Reference 6) were selected for evaluation and comparison with expected plant behavior. Table 5-3 characterizes the results of each test. The 5x5 selected rod array comprises the hot rod, 4 guide tubes and 20 near adjacent rods. The simulated hot rod is rod 7J in the tests.

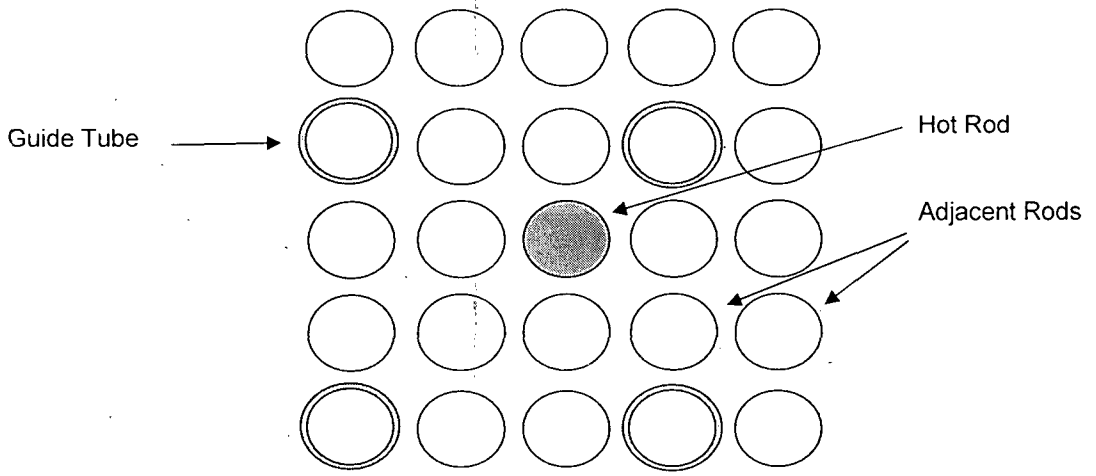

Figure 5-1: R2RRAD 5x5 Rod Segment

Two sets of runs were made simulating each of the five experiments and one set of cases was run to simulate the RLBLOCA evaluation of a limiting fuel assembly in an operating plant. For the simulation of Tests 31805, 31504, 31021, and 30817, the thimble tube (guide tube) temperatures were set to the measured values. For Test 34420, the thimble tube temperature was set equal to the measured vapor temperature. For the first experimental simulation set, the temperature of all 21 rods and the exterior boundary was set to the measured PCT of the simulated test. For the second experimental set, the hot rod temperature was set to the PCT value and the remaining 20 rods and the boundary were set to a temperature 25 °F cooler providing a reasonable measure of the variation in surrounding temperatures. To estimate the rod-to-rod radiation in a real fuel assembly at LOCA conditions and compare it to the experimental results, each of the above cases was rerun with the hot rod PCT set to the experimental result and the remaining rods conservatively set to temperatures expected within the bundle. The guide tubes (thimble tubes) were removed for conservatism and because peak rod powers frequently occur at fuel assembly corners away from either guide tubes or instrument tubes. In line with the

discussion in Section 5.3.1, the surrounding 24 rods were set to a temperature estimated for rods of 4 percent lower power. The boundary temperature was estimated based an average power 6 percent below the hot rod power. For both of these, the temperature estimates were achieved using a ratio of pin power to the difference in temperature between the saturation temperature and the PCT.

$$T_{24\ rods} = 0.96 \cdot (PCT - T_{sat}) + T_{sat} \quad \text{and}$$
$$T_{rurrounding\ region} = 0.94 \cdot (PCT - T_{sat}) + T_{sat}.$$

T_{sat} was taken as 270 F.

Figure 5-2 shows the hot rod thermal radiation heat transfer for the two FLECHT-SEASET sets and for the plant set. The figure shows that for PCTs greater than about 1700 °F, the hot rod thermal radiation in the plant cases exceeds that of the same component within the experiments.

Table 5-3: FLECHT-SEASET Test Parameters

Test	Rod 7J PCT at 6-ft (°F)	PCT Time (s)	htc at PCTtime (Btu/hr-ft^2-°F)	Steam Temperature -at 7l (6-ft) (°F)	Thimble Temperature at 6-ft (°F)
34420	2205	34	10	1850	1850*
31805	2150	110	10	1800	1800
31504	2033	100	10	1750	1750
31021	1684	29	9	1400	1350
30817	1440	70	13	900	750
		* set to steam temp			

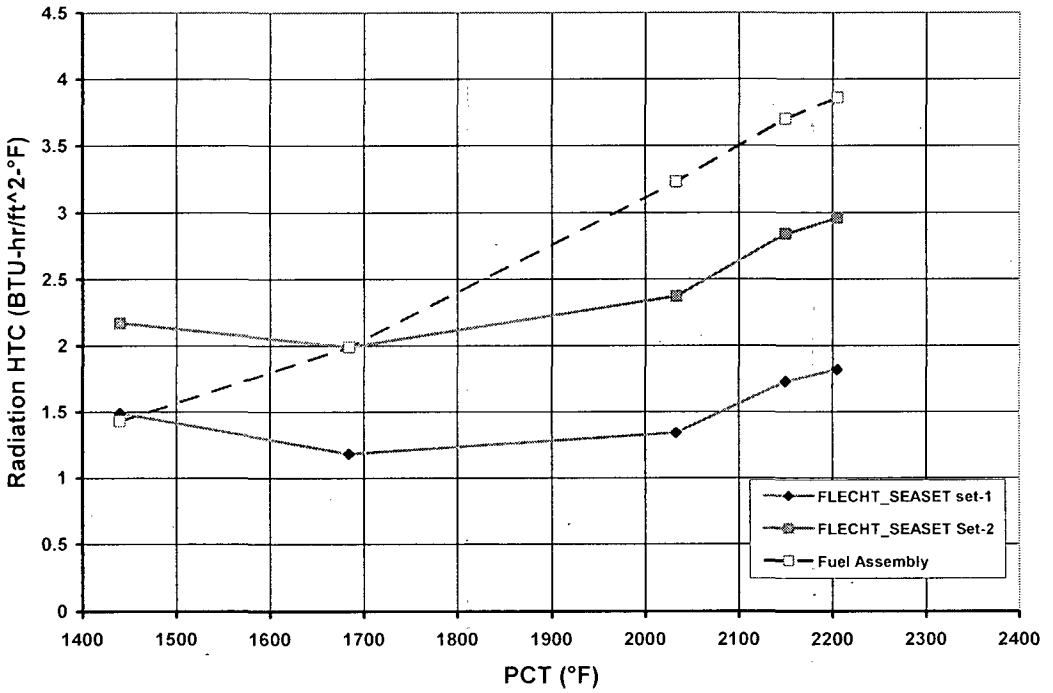

Figure 5-2: Rod Thermal Radiation in FLECHT-SEASET Bundle and in a 17x17 FA

5.3.3 Rod-to-Rod Radiation Summary

The AREVA Realistic large break LOCA (RLBLOCA) Revision 0 evaluation model (EM) does not include a rod-to-rod radiation model. Rather the convective heat transfer mechanisms are benchmarked and biased to reproduce the results of experiments that do involve rod-to-rod radiation. This approach subsumes rod-to-rod radiation under the convective heat transfer terms. The assessment of this approach was originally presented as a generic sensitivity study to demonstrate that the approach was reasonable for light water reactors of the US fleet. In fact, for the conditions of the study, the study showed that rod-to-rod radiation heat transfer expected from an explicit modeling of rod-to-rod radiation in the plant would be substantially higher than that present in the experiments to which the Revision 0 reflood heat transfer model benchmarked. The conclusion drawn was not intended to be a specific application for Harris, but rather to make that case that the Revision 0 approach was reasonable and likely somewhat conservative relative to explicit radiation modeling.

An important factor in the study was the local peaking difference between the hot rod and the surrounding 24 rods. Based on pin assessments for a relatively flat core (plant 6 in Table 5-1), this was set at 4 percent. Further, the calculation conservatively assumed no credit for the assignment of power uncertainty to the hot pin. The relative expectation for the near region local peaking for Harris can be obtained by comparing the local peaking times the assigned uncertainty for plant 6 (provided in Table 5-1) to the same product for Harris. The $F_{\Delta H}$ uncertainty applied for Harris is 4 percent. Consistent with

the information provided in Table 5-1, the limiting case fresh UO_2 radial local peaking is 1.051. This gives a combined value of 1.09 percent compared to the 1.10 for plant 6. It is, therefore, reasonable to expect a slightly reduced hot rod offset for Harris but not so much as to jeopardize the conclusion that the Revision 0 reflood heat transfer approach is reasonable to conservative. Table 3-5 provides results for the limiting PCT case.

The following table summarizes the PCT for all hot rods and average rods at the time of PCT.

Table 5-4: PCT for Fresh and Once-burned Hot Rods and Average Rods

No-LOOP Limiting Case #5 PCT (°F)					
	UO_2	2% Gad	4% Gad	6% Gad	8% Gad
Fresh	1919	1917	1915	1913	1910
Once-burned	1890	1860	1856	1849	1841
Hot Assembly		Surrounding 6 Assemblies		Average Core	Peripheral Core
1866		1322		1236	732

In summary, the conservatism of the heat transfer modeling established by benchmark can be reasonably extended to plant applications, and the plant local peaking provides a physical reason why rod-to-rod radiation should be more substantial within a plant environment than in the test environment. Therefore, the lack of an explicit rod-to-rod radiation model, in the version of S-RELAP5 applied for realistic LOCA calculations, does not invalidate the conclusion that the cladding temperature and local cladding oxidation have been demonstrated to meet the criteria of 10 CFR 50.46 with a high level of probability.

5.4 Film Boiling Heat Transfer Limit

Question: *In the Harris Nuclear Plant calculations, is the Forslund-Rohsenow model contribution to the heat transfer coefficient limited to less than or equal to 15 percent when the void fraction is greater than or equal to 0.9?*

Response: Yes, the version of S-RELAP5 employed for the HNP Unit 1 RLBLOCA analysis limits the contribution of the Forslund-Rohsenow model to no more than 15 percent of the total heat transfer at and above a void fraction of 0.9. Because the limit is applied at a void fraction of 0.9, the contribution of Forslund-Rohsenow within the 0.7 to 0.9 interpolation range is limited to 15 percent or less. This is a change to the approved RLBLOCA EM (Reference 1). This feature is carried forward into the UAPR09 version of S-RELAP5.

5.5 Downcomer Boiling

Question: *If the PCT is greater than 1800°F or the containment pressure is less than 30 psia, has the HNP Unit 1 downcomer model been rebenchmarked by performing sensitivity studies, assuming adequate downcomer noding in the water volume, vessel wall and other heat structures?*

Response: The downcomer model for HNP Unit 1 has been established generically as adequate for the computation of downcomer phenomena including the prediction of potential local boiling effects. The model was benchmarked against the UPTF tests and the LOFT facility in the RLBLOCA methodology, Revision 0 (Reference 1). Further, AREVA addressed the effects of boiling in the downcomer in a letter, from James Malay to U.S. NRC, April 4, 2003. The letter cites the lack of direct experimental evidence but contains sensitivity studies on high and low pressure containments, the impact of additional azimuthal noding within the downcomer, and the influence of flow loss coefficients. Of these, the study on azimuthal noding is most germane to this question; indicating that additional azimuthal nodalization allows higher liquid buildup in portions of the downcomer away from the broken cold leg and increases the liquid driving head. Additionally, AREVA has conducted downcomer axial noding and wall heat release studies. Each of these studies supports the Revision 0 methodology and is documented later in this section.

This question is primarily concerned with the phenomena of downcomer boiling and the extension of the Revision 0 methodology and sensitivity studies to plants with low containment pressures and high cladding temperatures. Boiling, wherever it occurs, is a phenomenon that codes like S-RELAP5 have been developed to predict. Downcomer boiling is the result of the release of energy stored in vessel metal mass. Within S-RELAP5, downcomer boiling is simulated in the nucleate boiling regime with the Chen correlation. This modeling has been validated through the prediction of several assessments on boiling phenomenon provided in the S-RELAP5 Code Verification and Validation document (Reference 12).

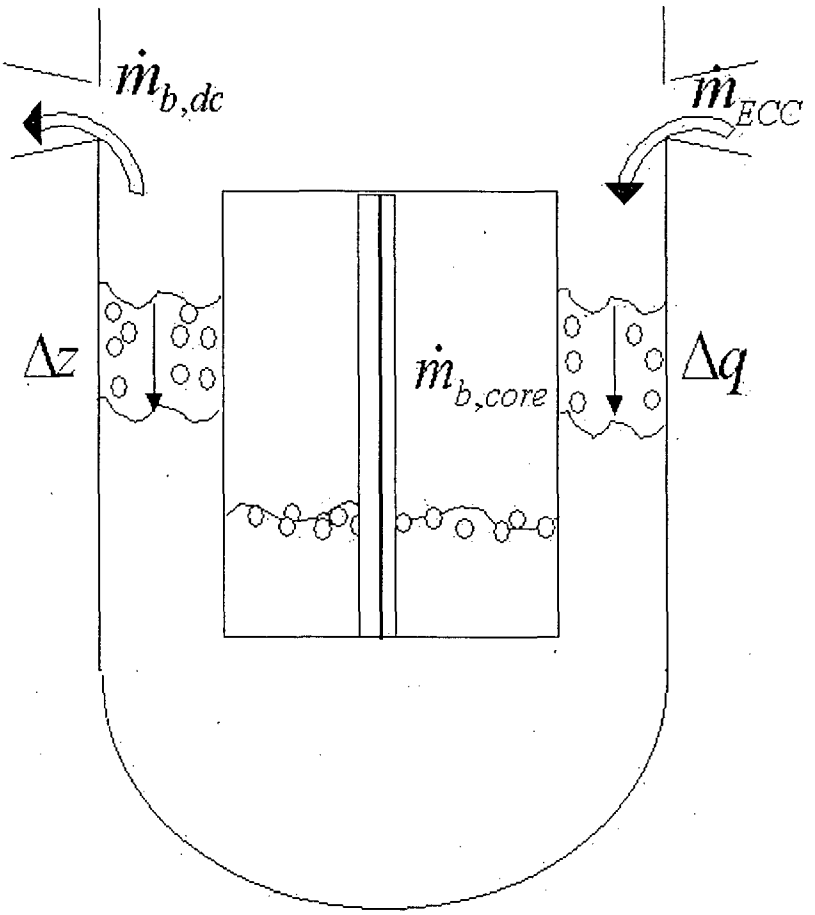

Figure 5-3: Reactor Vessel Downcomer Boiling Diagram

Hot downcomer walls penalize PCT by two mechanisms: by reducing subcooling of coolant entering the core and through the reduction in downcomer hydraulic head which is the driving force for core reflood. Although boiling in the downcomer occurs during blowdown, the biggest potential for impact on clad temperatures is during late reflood following the end of accumulator injection. At this time, there is a large step reduction in coolant flow from the ECC systems. As a result, coolant entering the downcomer may be less subcooled. When the downcomer coolant approaches saturation, boiling on the walls initiates, reducing the downcomer hydraulic static level.

With the reduction of the downcomer level, the core inlet flow rate is reduced which, depending on the existing core inventory, may result in a cladding temperature excursion or a slowing of the core cooldown rate.

While downcomer boiling may impact clad temperatures, it is somewhat of a self-limiting process. If cladding temperatures increase, less energy is transferred in the core boiling process and the loop steam flows are reduced. This reduces the required driving head to support continued core reflood and reduces the steam available to heat the ECCS water within the cold legs resulting in greater subcooling of the water entering the downcomer.

The impact of downcomer boiling is primarily dependent on the wall heat release rate and on the ability to slip steam up the downcomer and out of the break. The higher the downcomer wall heat release, the more steam is generated within the downcomer and the larger the impact on core reflooding. Similarly, the quicker the passage of steam up the downcomer, the less resident volume within the downcomer is occupied by steam and the lower the impact on the downcomer average density. Therefore, the ability to properly simulate downcomer boiling depends on both the heat release (boiling) model and on the ability to track steam rising through the downcomer. Consideration of both of these is provided in the following text. The heat release modeling in S-RELAP5 is validated by a sensitivity study on wall mesh point spacing and through benchmarking against a closed form solution. Steam tracking is validated through both an axial and an azimuthal fluid control volume sensitivity study done at low pressures. The results indicate that the modeling accuracy within the RLBLOCA methodology is sufficient to resolve the effects of downcomer boiling and that, to the extent that boiling occurs; the methodology properly resolves the impact on the cladding temperature and cladding oxidation rates.

5.5.1 Wall Heat Release Rate

The downcomer wall heat release rate during reflood is conduction limited and depends on the vessel wall mesh spacing used in the S-RELAP5 model. The following two approaches are used to evaluate the adequacy of the downcomer vessel wall mesh spacing used in the S-RELAP5 model.

5.5.1.1 Exact Solution

In this benchmark, the downcomer wall is considered as a semi-infinite plate. Because the benchmark uses a closed form solution to verify the wall mesh spacing used in S-RELAP5, it is assumed that the material has constant thermal properties, is initially at temperature T_i, and, at time zero, has one surface, the surface simulating contact with the downcomer fluid, set to a constant temperature, T_o, representing the fluid temperature. Section 4.3 of Reference 9 gives the exact solution for the temperature profile as a function of time as

$$(T(x,t) - T_o) / (T_i - T_o) = \text{erf}\{x / (2 \cdot (\alpha t)^{0.5})\}, \qquad (1)$$

where, α is the thermal diffusivity of the material given by

$\alpha = k/(\rho Cp)$,
k = thermal conductivity,
ρ = density,
Cp = specific heat, and
erf{} is the Gauss error function (given in Table A-1 of Reference 9).

The conditions of the benchmark are T_i = 500 °F and T_o = 300 °F. The mesh spacing in S-RELAP5 is the same as that used for the downcomer vessel wall in the RLBLOCA model. Figure 5-4 shows the temperature distributions in the metal at 0.0, 100 and 300 seconds as calculated by using Equation 1 and S-RELAP5, respectively. The solutions are identical confirming the adequacy of the mesh spacing used in the downcomer wall.

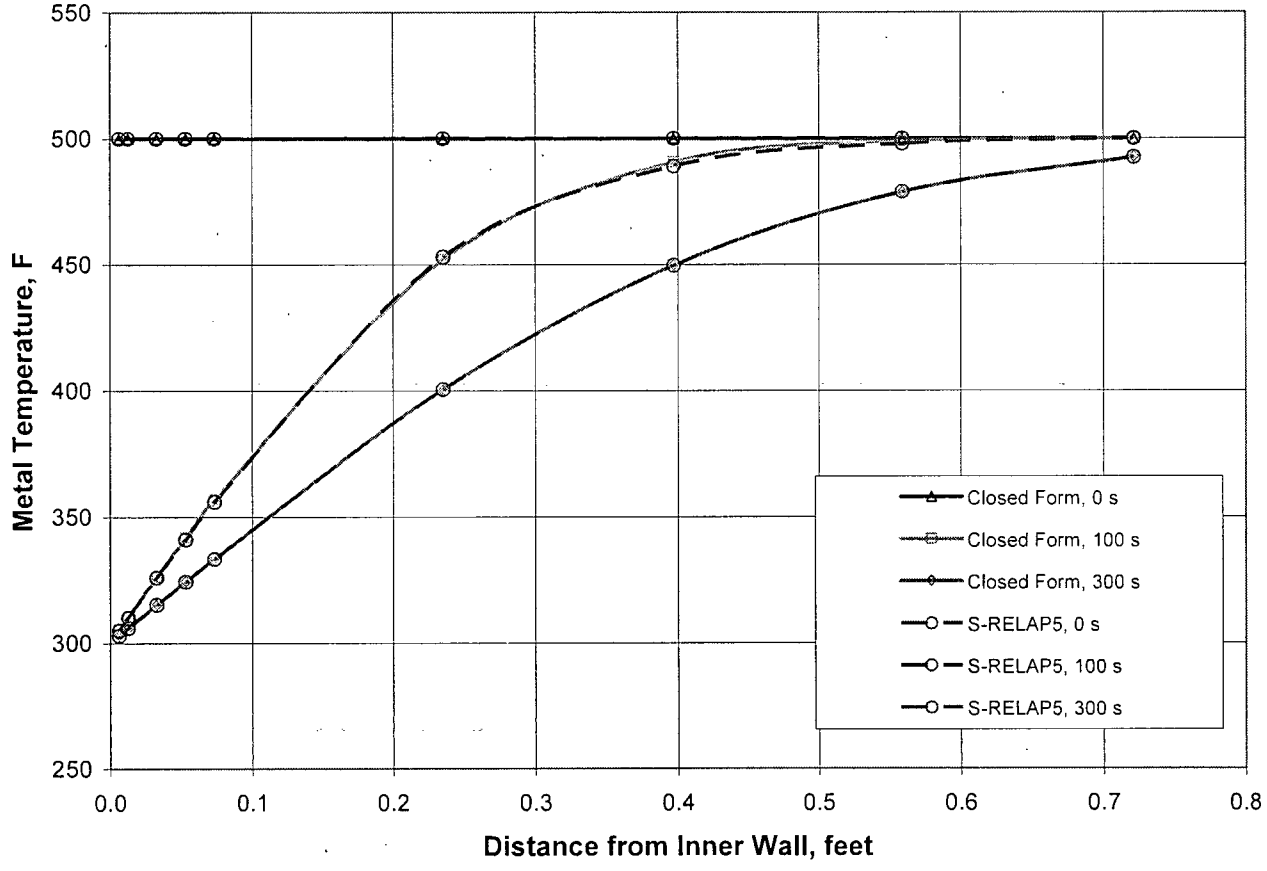

Figure 5-4: S-RELAP5 versus Closed Form Solution

5.5.1.2 Plant Model Sensitivity Study

As additional verification, a typical 4-loop plant case was used to evaluate the adequacy of the mesh spacing within the downcomer wall heat structure. Each mesh interval in the base case downcomer vessel wall was divided into two equal intervals. Thus, a new input model was created by increasing the number of mesh intervals from 9 to 18. The following four figures show the total downcomer metal heat release rate, PCT independent of elevation, downcomer liquid level, and the core liquid level, respectively, for the base case and the modified case. These results confirm the conclusion from the exact solution study that the mesh spacing used in the plant model for the downcomer vessel wall is adequate.

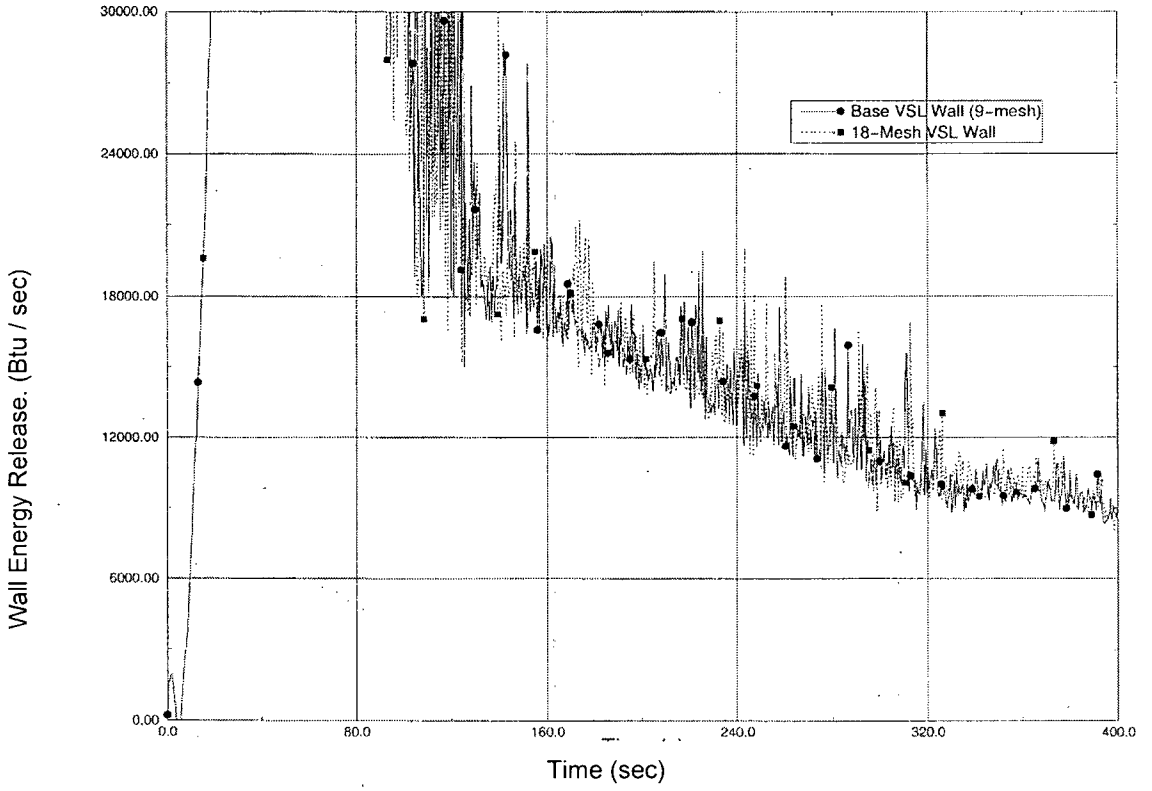

Figure 5-5: Downcomer Wall Heat Release – Wall Mesh Point Sensitivity

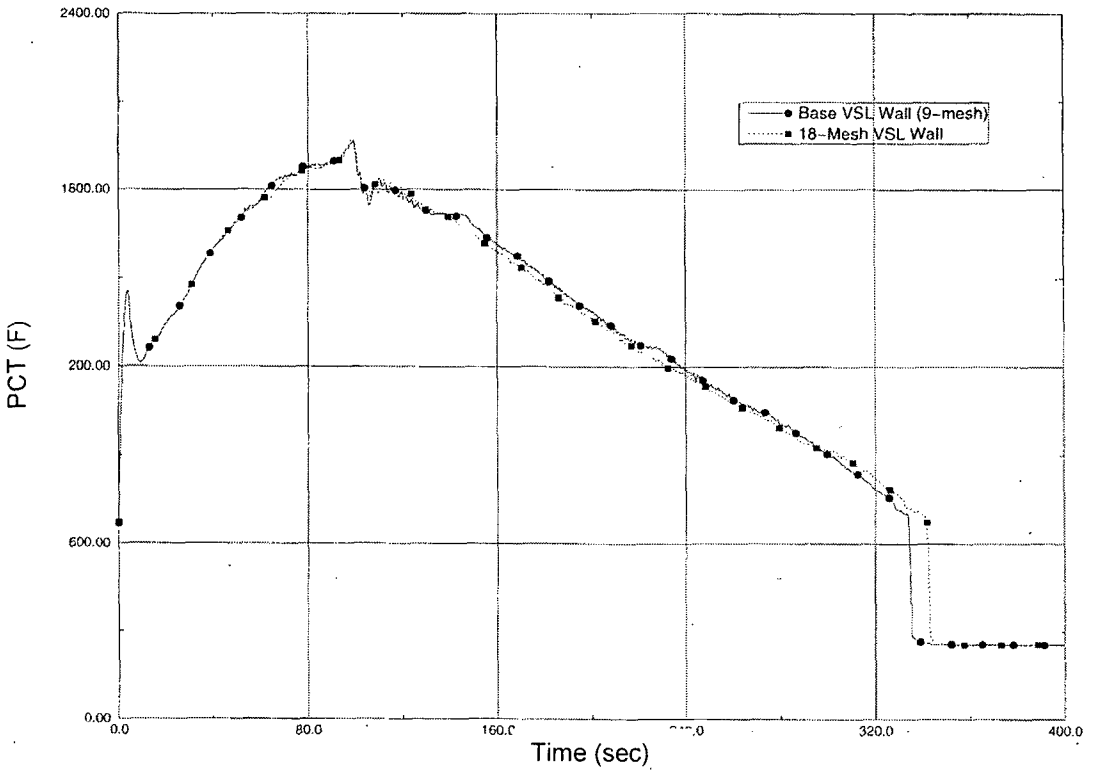

Figure 5-6: PCT Independent of Elevation – Wall Mesh Point Sensitivity

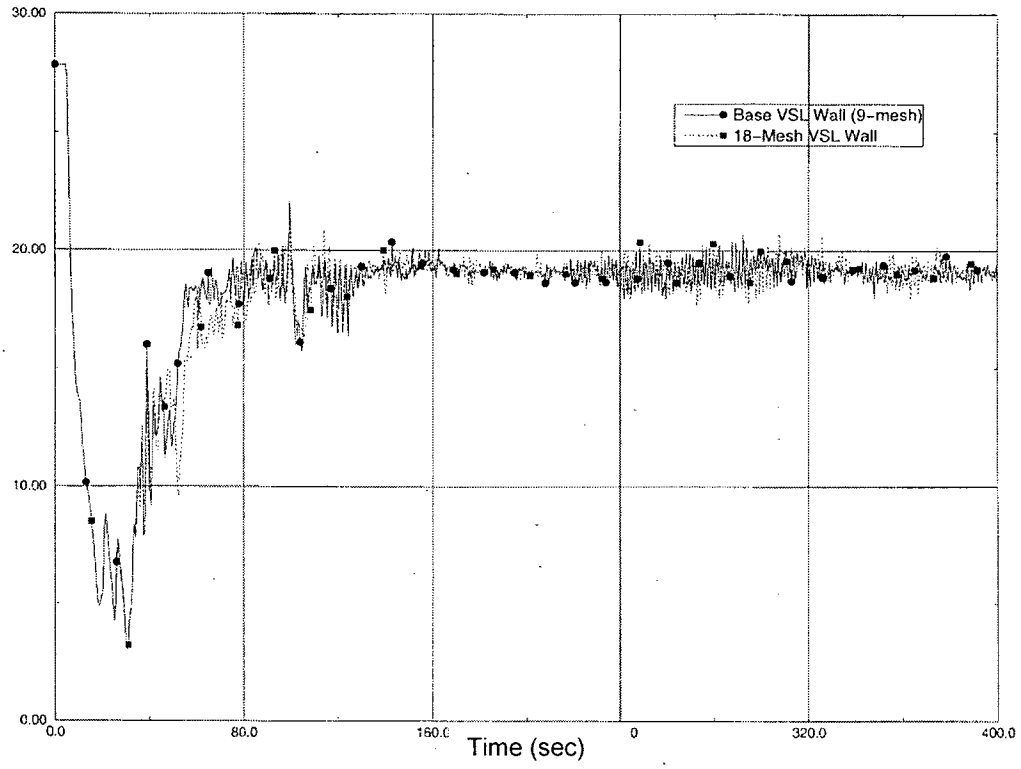

Figure 5-7: Downcomer Liquid Level – Wall Mesh Point Sensitivity

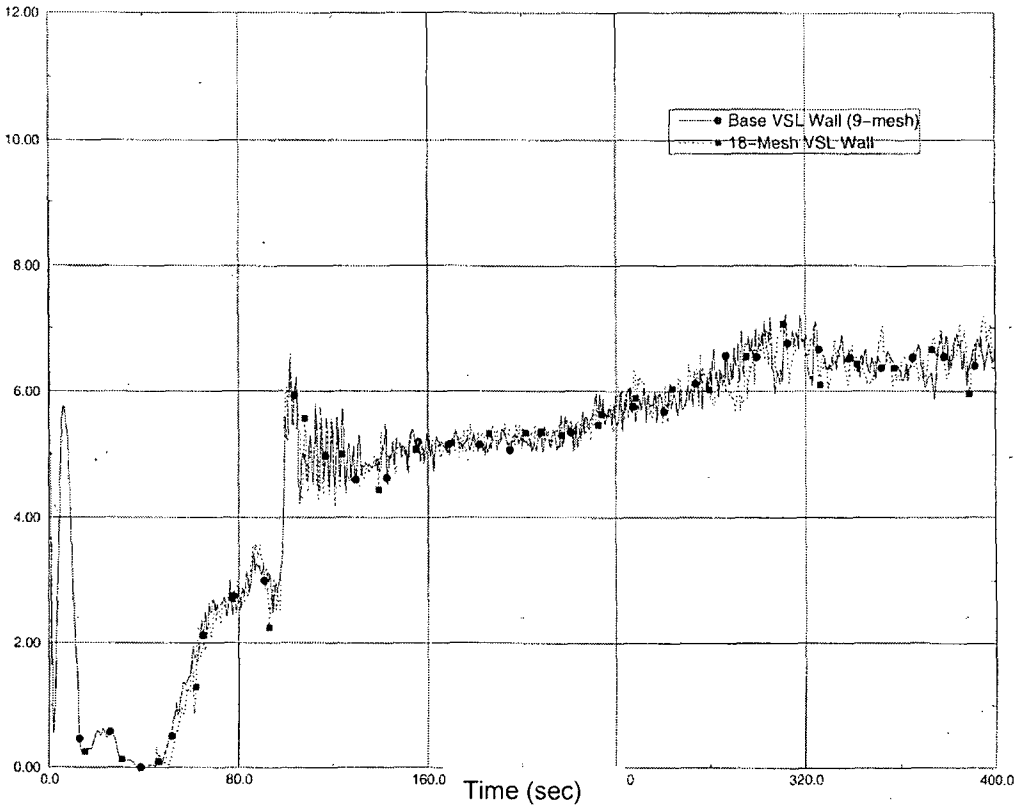

Figure 5-8: Core Liquid Level – Wall Mesh Point Sensitivity

5.5.2 Downcomer Fluid Distribution

To justify the adequacy of the downcomer nodalization in calculating the fluid distribution in the downcomer, two studies varying separately the axial and the azimuthal resolution with which the downcomer is modeled have been conducted.

5.5.2.1 Azimuthal Nodalization

In a letter to the NRC dated April, 2003 (Reference 1), AREVA documented several studies on downcomer boiling. Of significance here is the study on further azimuthal break up of the downcomer noding. The study, based on a 3-loop plant with a containment pressure of approximately 30 psia during reflood, consisted of several calculations examining the affects on clad temperature and other parameters.

The base model, with 6 axial by 3 azimuthal regions, was expanded to 6 axial by 9 azimuthal regions (Figure 5-9). The base calculation simulated the limiting PCT calculation given in the EMF-2103 three-loop sample problem. This case was then repeated with the revised 6 x 9 downcomer noding.

The change resulted in an alteration of the blowdown evolution of the transient with little evidence of any affect during reflood. To isolate any possible reflood impact that might have an influence on downcomer boiling, the case was repeated with a slightly adjusted vessel-side break flow. Again, little evidence of impact on the reflood portion of the transient was observed.

The study concluded that blowdown or near blowdown events could be impacted by refining the azimuthal resolution in the downcomer but that reflood would not be impacted. Although the study was performed for a somewhat elevated system pressure, the flow regimes within the downcomer will not differ for pressures as low as atmospheric. Thus, the azimuthal downcomer modeling employed for the RLBLOCA methodology is reasonably converged in its ability to represent downcomer boiling phenomena.

Base model

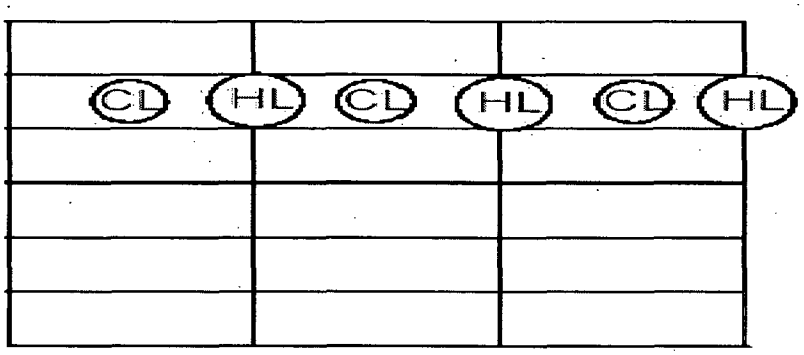

Revised 9 Region Model

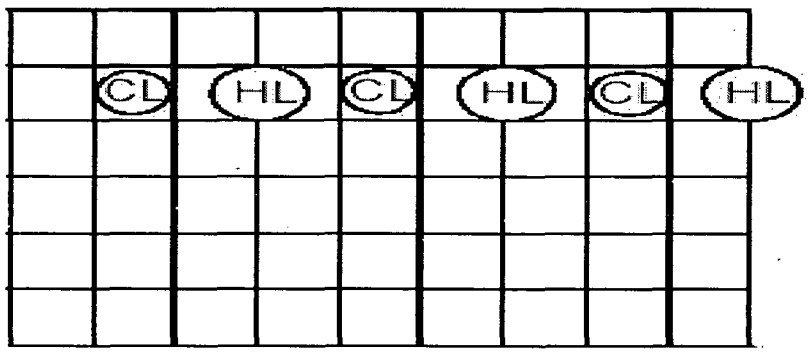

Figure 5-9: Azimuthal Noding

5.5.2.2 Axial Nodalization

The RLBLOCA methodology divides the downcomer into six nodes axially. In both 3-loop and 4-loop models, the downcomer segment at the active core elevation is represented by two equal length nodes. For most operating plants, the active core length is 12 feet and the downcomer segments at the active core elevation are each 6-feet high. (For a 14 foot core, these nodes would be 7-feet high.) The model for the sensitivity study presented here comprises a 4-loop plant with an ice condenser containment and a 12 foot core. For the study, the two nodes spanning the active core height are divided in half, revising the model to include eight axial nodes. Further, the refined noding is located within the potential boiling region of the downcomer where, if there is an axial resolution influence, the sensitivity to that impact would be greatest.

The results show that the axial noding used in the base methodology is sufficient for plants experiencing the very low system pressures characteristic of ice condenser containments. Figure 5-10 provides the containment back pressure for the base modeling. Figures 5-11 through 5-14 show the total downcomer metal heat release rate, PCT independent of elevation, downcomer liquid level, and the core liquid level, respectively, for the base case and the modified case.

The results demonstrate that the axial resolution provided in the base case, 6 axial downcomer node divisions with 2 divisions spanning the core active region, are sufficient to accurately resolve void distributions within the downcomer. Thus, this modeling is sufficient for the prediction of downcomer driving head and the resolution of downcomer boiling effects.

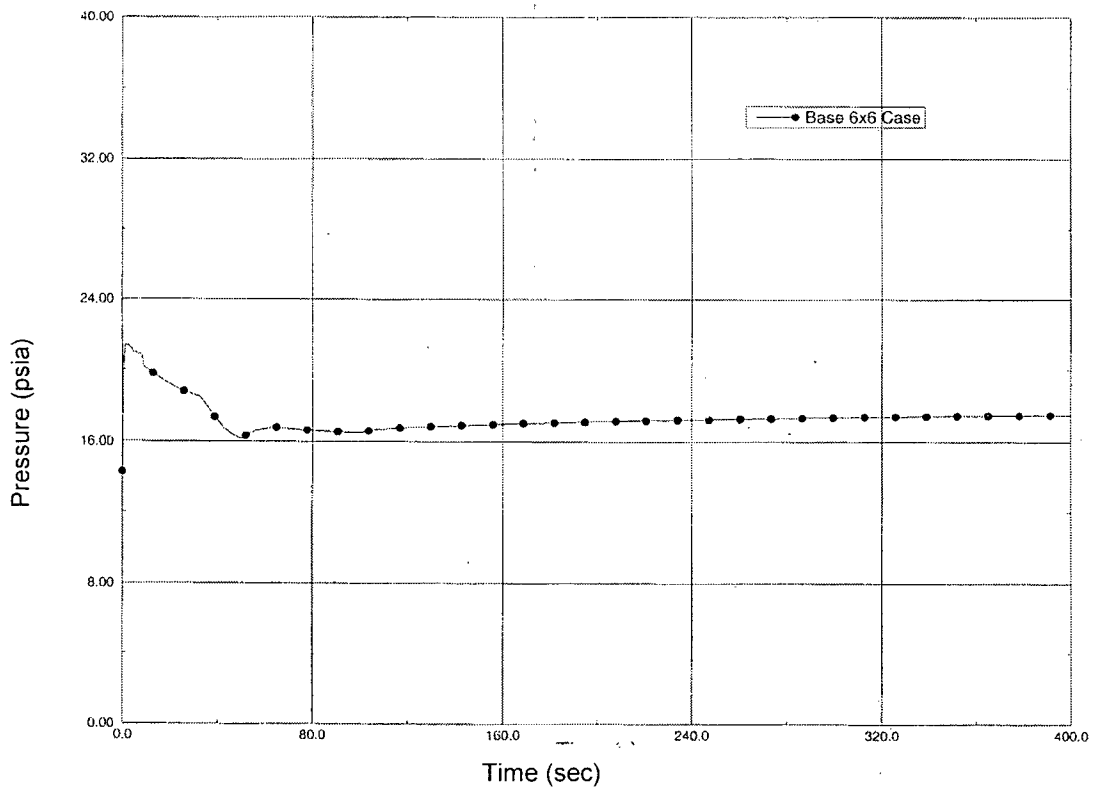

Figure 5-10: Lower Compartment Pressure versus Time

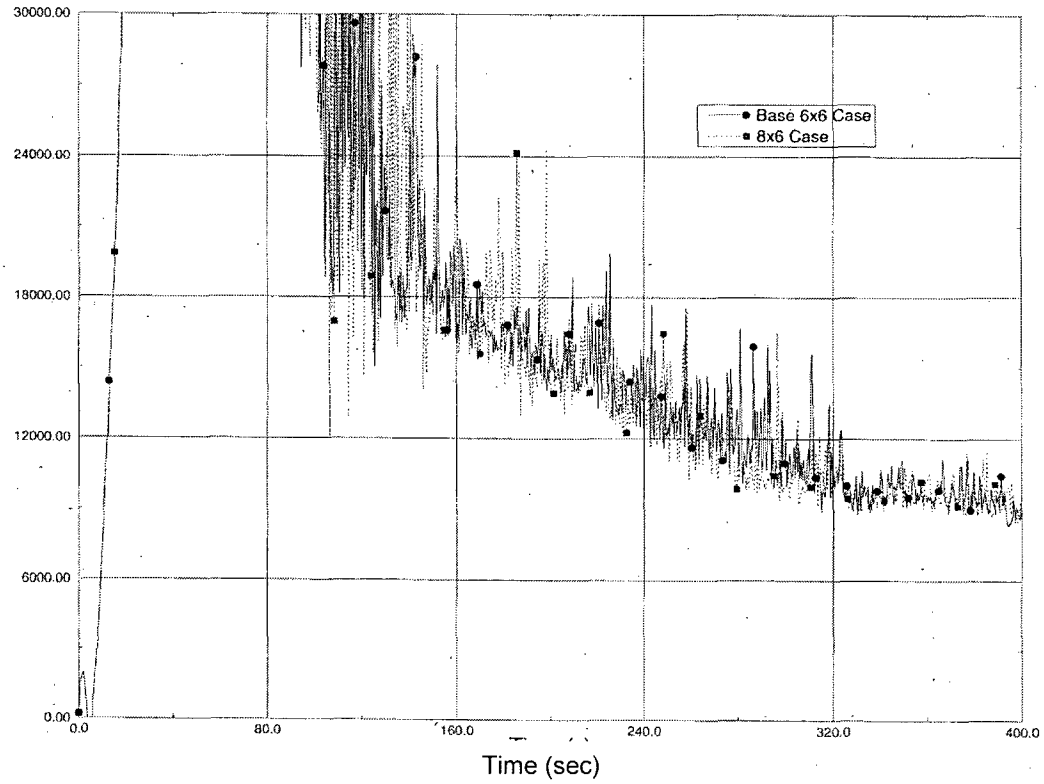

Figure 5-11: Downcomer Wall Heat Release – Axial Noding Sensitivity Study

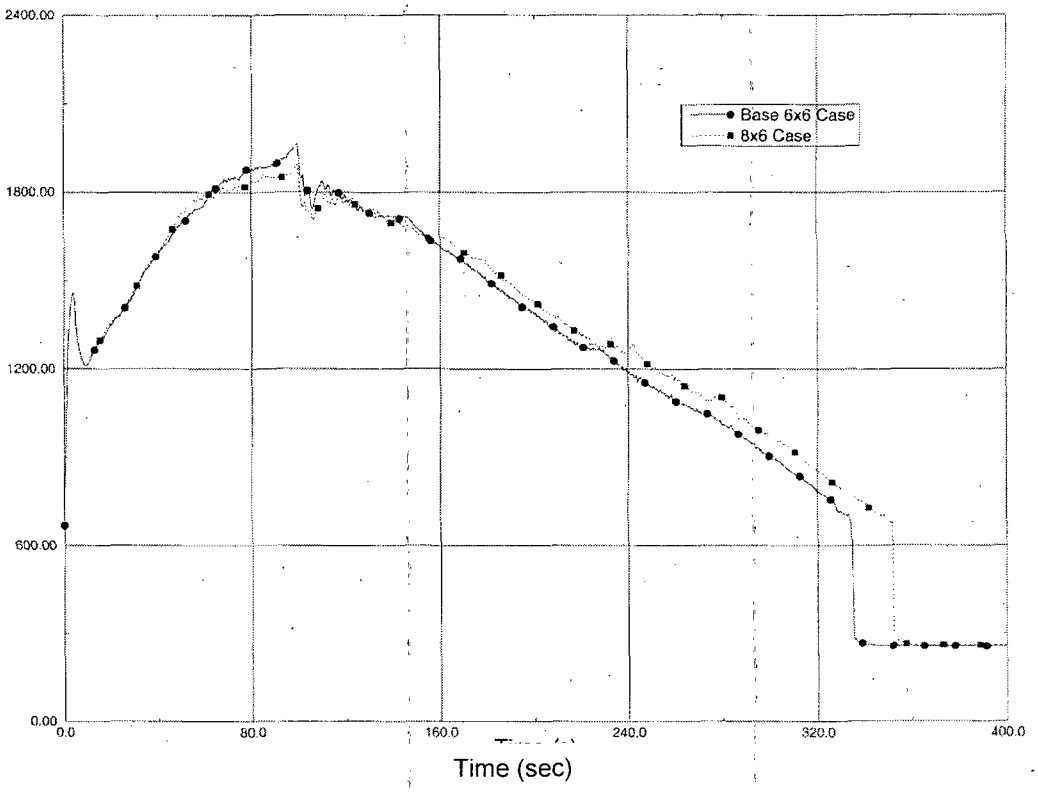

Figure 5-12: PCT Independent of Elevation – Axial Noding Sensitivity Study

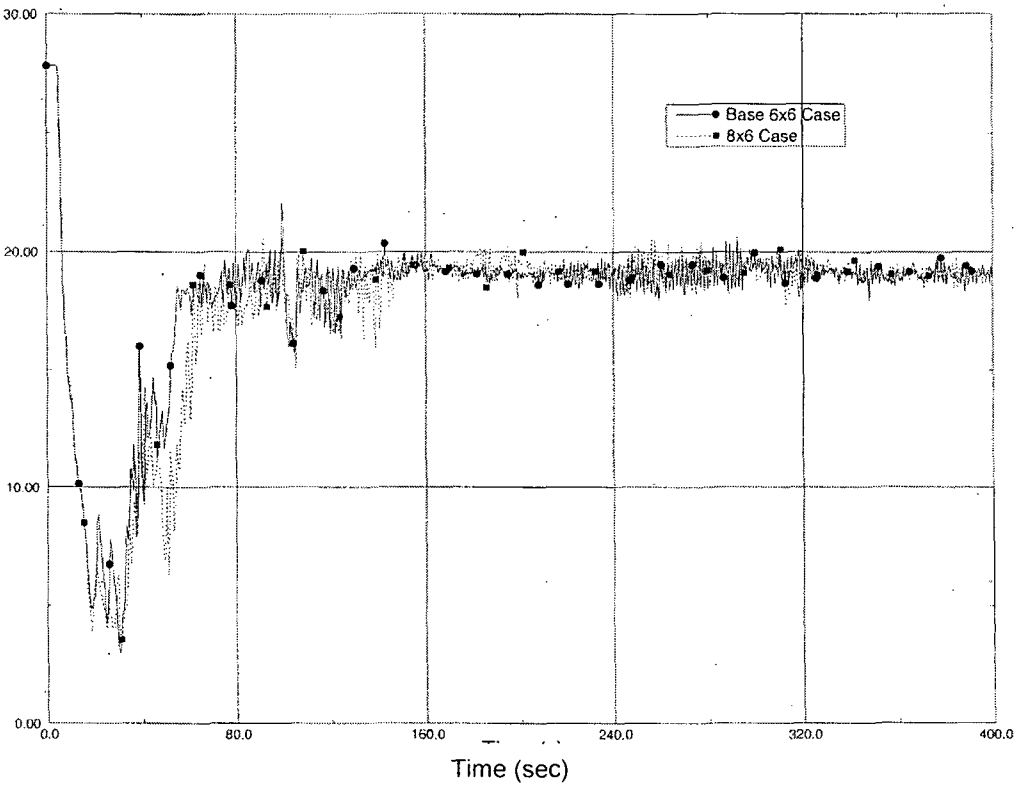

Figure 5-13: Downcomer Liquid Level – Axial Noding Sensitivity Study

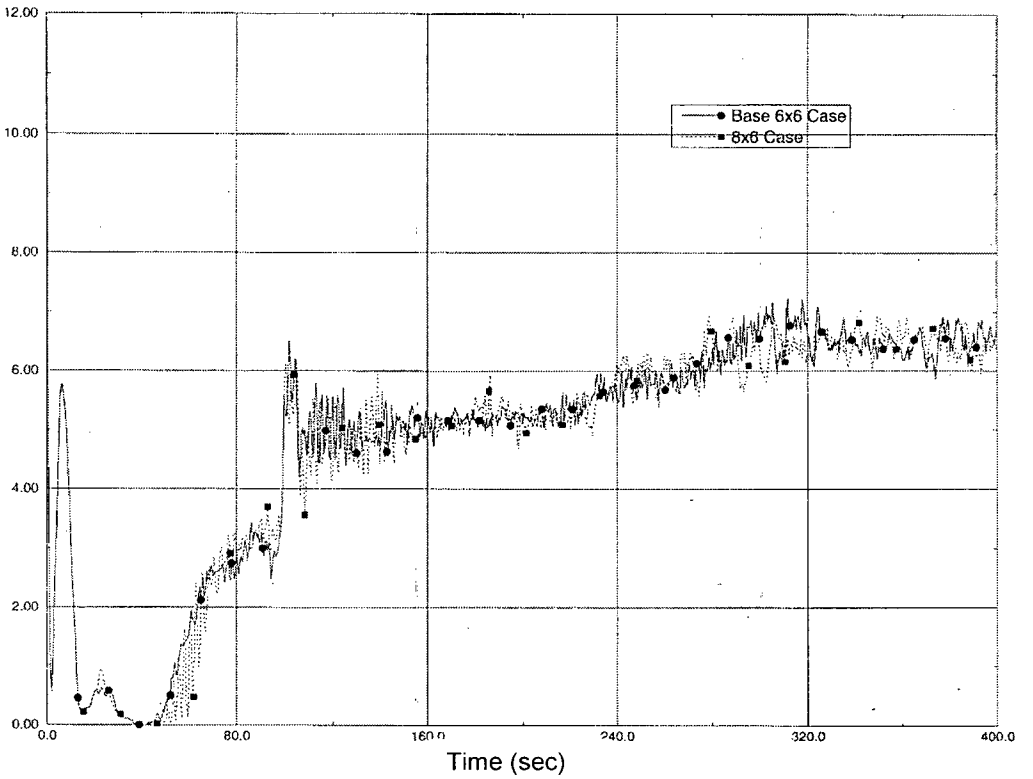

Figure 5-14: Core Liquid Level – Axial Noding Sensitivity Study

5.5.3 Downcomer Boiling Conclusions

To further justify the ability of the RLBLOCA methodology to predict the potential for and impact of downcomer boiling, studies were performed on the downcomer wall heat release modeling within the methodology and on the ability of S-RELAP5 to predict the migration of steam through the downcomer. Both azimuthal and axial noding sensitivity studies were performed. The axial noding study was based on an ice condenser plant that is near atmospheric pressure during reflood. These studies demonstrate that S-RELAP5 delivers energy to the downcomer liquid volumes at an appropriate rate and that the downcomer noding detail is sufficient to track the distribution of any steam formed. Thus, the required methodology for the prediction of downcomer boiling at system pressures approximating those achieved in plants with pressures as low as ice condenser containments has been demonstrated.

5.6 Break Size

Question: *Were all break sizes assumed greater than or equal to 1.0 ft^2?*

Response: Yes.

The NRC has requested that the break spectrum for the realistic LOCA evaluations be limited to accidents that evolve through a range of phenomena similar to those encountered for the larger break area accidents. This is a change to the approved RLBLOCA EM (Reference 1). The larger break area LOCAs are typically characterized by the occurrence of dispersed flow film boiling at the hot spot, which sets them apart from smaller break LOCAs. This occurs generally in the vicinity of 0.2 DEGB (double-ended guillotine break) size (i.e., 0.2 times the total flow area of the pipe on both sides of the break). However, this transitional break size varies from plant to plant and is verified only after the break spectrum has been executed. AREVA NP has sought to develop sufficient criteria for defining the minimum large break flow area prior to performing the break spectrum. The purpose for doing so is to assure a valid break spectrum is performed.

5.6.1 Break/Transient Phenomena

In determining the AREVA NP criteria, the characteristics of larger break area LOCAs are examined. These LOCA characteristics involve a rapid and chaotic depressurization of the reactor coolant system (RCS) during which the three historical approximate states of the system can be identified.

Blowdown The blowdown phase is defined as the time period from initiation of the break until flow from the accumulators begins. This definition is somewhat different from the traditional definition of blowdown which extends the blowdown until the RCS pressure approaches containment pressure. The blowdown phase typically lasts about 12 to 25 seconds, depending on the break size.

Refill is that period that starts with the end of blowdown, whichever definition is used, and ends when water is first forced upward into the core. During this phase the core experiences a near adiabatic heatup.

Reflood is that portion of the transient that starts with the end of refill, follows through the filling of the core with water and ends with the achievement of complete core quench.

Implicit in this break-down is that the core liquid inventory has been completely, or nearly so, expelled from the primary system leaving the core in a state of near core-wide dispersed flow film boiling and subsequent adiabatic heatup prior to the reflood phase. Although this break down served as the basis for the original deterministic LOCA evaluation approaches and is valid for most LOCAs that would classically be termed large breaks, as the break area decreases the depressurization rate decreases such that these three phases overlap substantially. During these smaller break events, the core liquid inventory is not reduced as much as that found in larger breaks. Also, the adiabatic core heatup is not as extensive as in the larger breaks which results in much lower cladding temperature excursions.

5.6.2 New Minimum Break Size Determination

No determination of the lower limit can be exact. The values of critical phenomena that control the evolution of a LOCA transient will overlap and interplay. This is especially true in a statistical evaluation where parameter values are varied randomly with a strong expectation that the variations will affect results. In selecting the lower area of the RLBLOCA break spectrum, AREVA sought to preserve the generality of a complete or nearly complete core dry out accompanied by a substantially reduced lower plenum liquid inventory. It was reasoned that such conditions would be unlikely if the break flow rate was reduced to less than the reactor coolant pump flow. That is, if the reactor coolant pumps are capable of forcing more coolant toward the reactor vessel than the break can extract from the reactor vessel, the downcomer and core must maintain some degree of positive flow (positive in the normal operations sense). The circumstance is, of course, transitory. Break flow is altered as the RCS blows down and the RC pump flow may decrease as the rotor and flywheel slow down if power is lost. However, if the core flow was reduced to zero or became negative immediately after the break initiation, then the event was quite likely to proceed with sufficient inertia to expel most of the reactor vessel liquid to the break. The criteria base, thus established, consists of comparing the break flow to the initial flow through all reactor coolant pumps and setting the minimum break area such that these flows match. This is done as follows:

$$W_{break} = A_{break} * G_{break} = N_{pump} * W_{RCP}.$$

This gives

$$A_{break} = (N_{pump} * W_{RCP})/G_{break}.$$

The break mass flux is determined from critical flow. Because the RCS pressure in the broken cold leg will decrease rapidly during the first few seconds of the transient, the critical mass flux is averaged between that appropriate for the initial operating conditions and that appropriate for the initial cold leg enthalpy and the saturation pressure of coolant at that enthalpy.

$$G_{break} = (G_{break}(P_0, H_{CL0}) + G_{break}(P_{CLsat}, H_{CL0}))/2.$$

The estimated minimum LBLOCA break area, A_{min}, is 1.07 ft^2 and the break area percentage, based on the full double-ended guillotine break total area, is 26 percent.

Table 5-4 provides a listing of the plant type, initial condition, and the fractional minimum RLBLOCA break area, for all the plant types presented as generic representations in the next section.

Table 5-5: Minimum Break Area for Large Break LOCA Spectrum

	Plant Description	System Pressure (psia)	Cold Leg Enthalpy (Btu/lbm)	Subcooled G_{break} (lbm/ft^2-s)	Saturated G_{break} (HEM) (lbm/ft^2-s)	No. of RCPs	RCP flow (lbm/s)	Spectrum Minimum Break Area (ft^2)	Spectrum Minimum Break Area (DEGB)
A	3-Loop W Design	2250	555.0	23190	5700	3	31417	2.18	0.26
B	3-Loop W Design	2249.7	544.5	23880	5450	3	28124	1.92	0.23
C	3-Loop W Design	2250	550.0	23540	5580	3	29743	2.04	0.25
D	2x4 CE Design	2100	538.8	22860	5310	4	21522	1.53	0.24
E	2x4 CE Design	2055	535.8	22630	5230	4	37049	2.66	0.27
F	4-Loop W Design	2160	540.9	23290	5370	4	39500	2.76	0.33

The split versus double-ended break type is no longer related to break area. In concurrence with Regulatory Guide 1.157, both the split and the double-ended break will range in area between the minimum break area (A_{min}) and an area of twice the size of the broken pipe. The determination of break configuration, split versus double-ended, is made after the break area is selected based on a uniform probability for each occurrence.

5.6.3 Intermediate Break Size Disposition

With the revision of the smaller break area for the RLBLOCA analysis, the break range for small breaks and large breaks are no longer contiguous. Typically the lower end of the large break spectrum occurs at between 0.2 to 0.3 times the total area of a 100 percent double-ended guillotine break (DEGB) and the upper end of the small break spectrum occurs at approximately 0.05 times the area of a 100 percent DEGB. This leaves a range of breaks that are not specifically analyzed during a LOCA licensing analysis. The premise for allowing this gap is that these breaks do not comprise accidents that develop high cladding temperature and thus do not comprise accidents that critically challenge the emergency core cooling systems (ECCS). Breaks within this range remain large enough to blowdown to low pressures. Resolution is provided by the large break ECC systems and the pressure-dependent injection limitations that determine critical small break performance are avoided. Further, these accidents develop relatively slowly, assuring maximum effectiveness of those ECC systems.

A variety of plant types for which analysis within the intermediate range have been completed were surveyed. Although statistical determinations are extracted from the consideration of breaks with areas above the intermediate range, the AREVA best-estimate methodology remains suitable to characterize the ECCS performance of breaks within the intermediate range. Table 5-4 provides a listing of the plant type, initial condition, and the fractional minimum RLBLOCA break area. Figures 5-15 through 5-20 provide the enlarged break spectrum results with the upper end of the small break spectrum and the lower end of the large break spectrum indicated by bars.

Table 5-6 provides differences between the true large break region and the intermediate break region (break areas between that of the largest SBLOCA and the smallest RLBLOCA). The minimum difference is 222 °F; however, this case is not representative of the general trend shown by the other comparisons. Considering this point as an outlier, the table shows the minimum difference between the highest intermediate break spectrum PCT and large break spectrum PCT, for the eight plants, as at least 463°F, and including this point would provide an average difference of 640°F for the CE 2x4 design plants and a maximum difference of 840°F for the 4-loop W plant design.

Thus, by both measures, the peak cladding temperatures within the intermediate break range will be several hundred degrees below those in the true large break range. Therefore, these breaks will not provide a limit or a critical measure of the ECCS performance. Given that the large break spectrum bounds the intermediate spectrum, the use of only the large break spectrum meets the requirements of 10CFR50.46 for breaks within the intermediate break LOCA spectrum, and the method demonstrates that the ECCS for a plant meets the criteria of 10CFR50.46 with high probability.

Table 5-6: Minimum PCT Temperature Difference – True Large and Intermediate Breaks

Plant Description	Generic Plant Label (Table 4-4)	Maximum PCT (°F) Intermediate Size Break	Maximum PCT (°F) Large Size Break	Delta PCT (°F)	Average Delta PCT (°F)
3-Loop W Design	A	1206[19]	1930	724	622
	B	1273	1951	678	
	C	1326	1789	463	
2x4 CE Design	D	984	1751	767	640
	E	1049	1740	691	
	F	791	1670	879	
	G	1464[20]	1686	222[20]	
4-Loop W Design	H	1127	1967	840	840

[19] The analysis for this W 3-Loop plant was performed with the Transition methodology and no break sizes fell into the intermediate break range. The PCT value of 1206 °F is the closest point to the maximum end of the intermediate break spectrum.

[20] The analysis for this 2x4 CE plant was performed with the Transition methodology and no break sizes fell into the intermediate break range. The PCT value of 1464 °F is the closest point to the maximum end of the intermediate break spectrum. From the trends of the other 2x4 CE analyses, breaks falling within the intermediate break spectrum would be significantly lower.

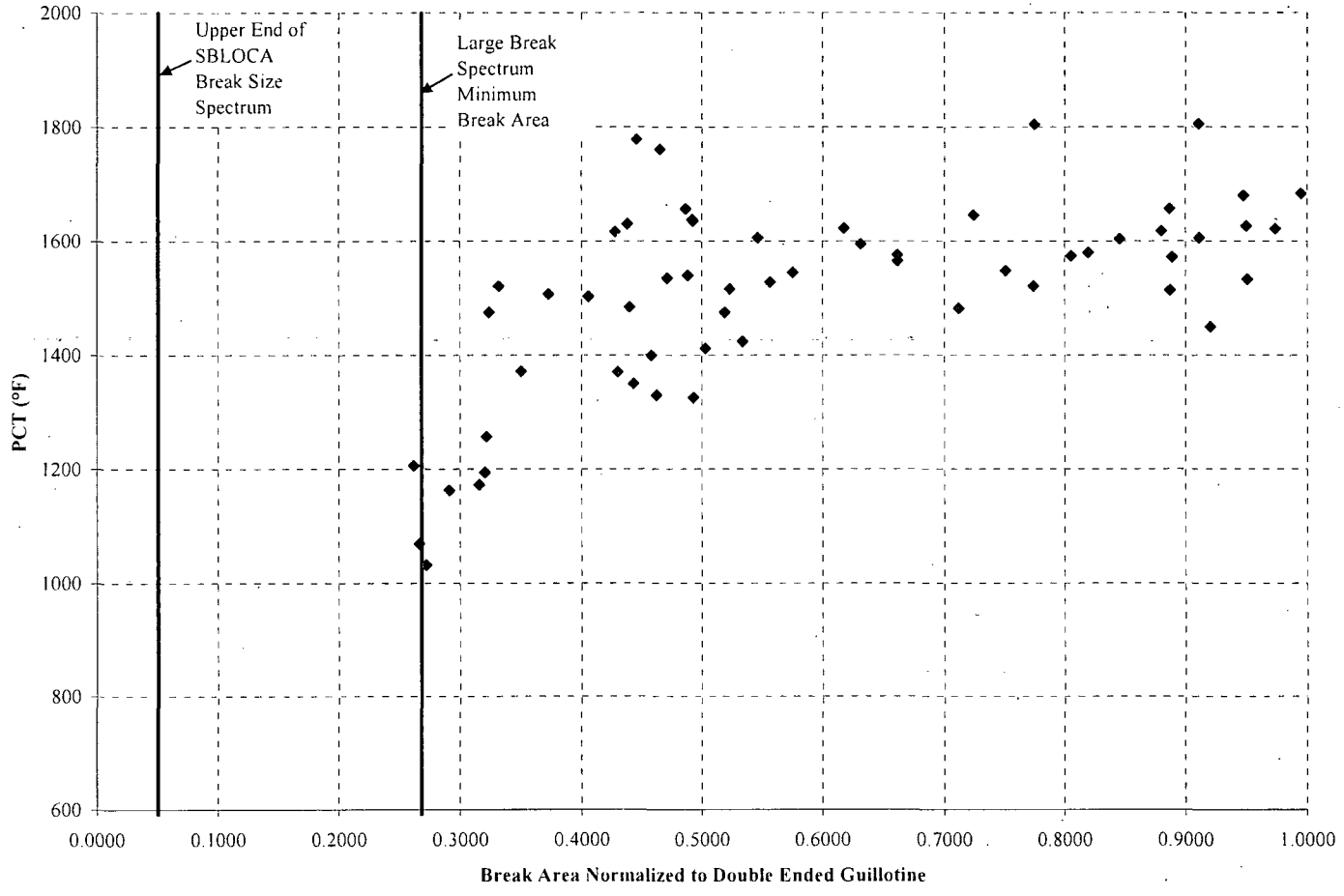

Figure 5-15: Plant A – Westinghouse 3-Loop Design

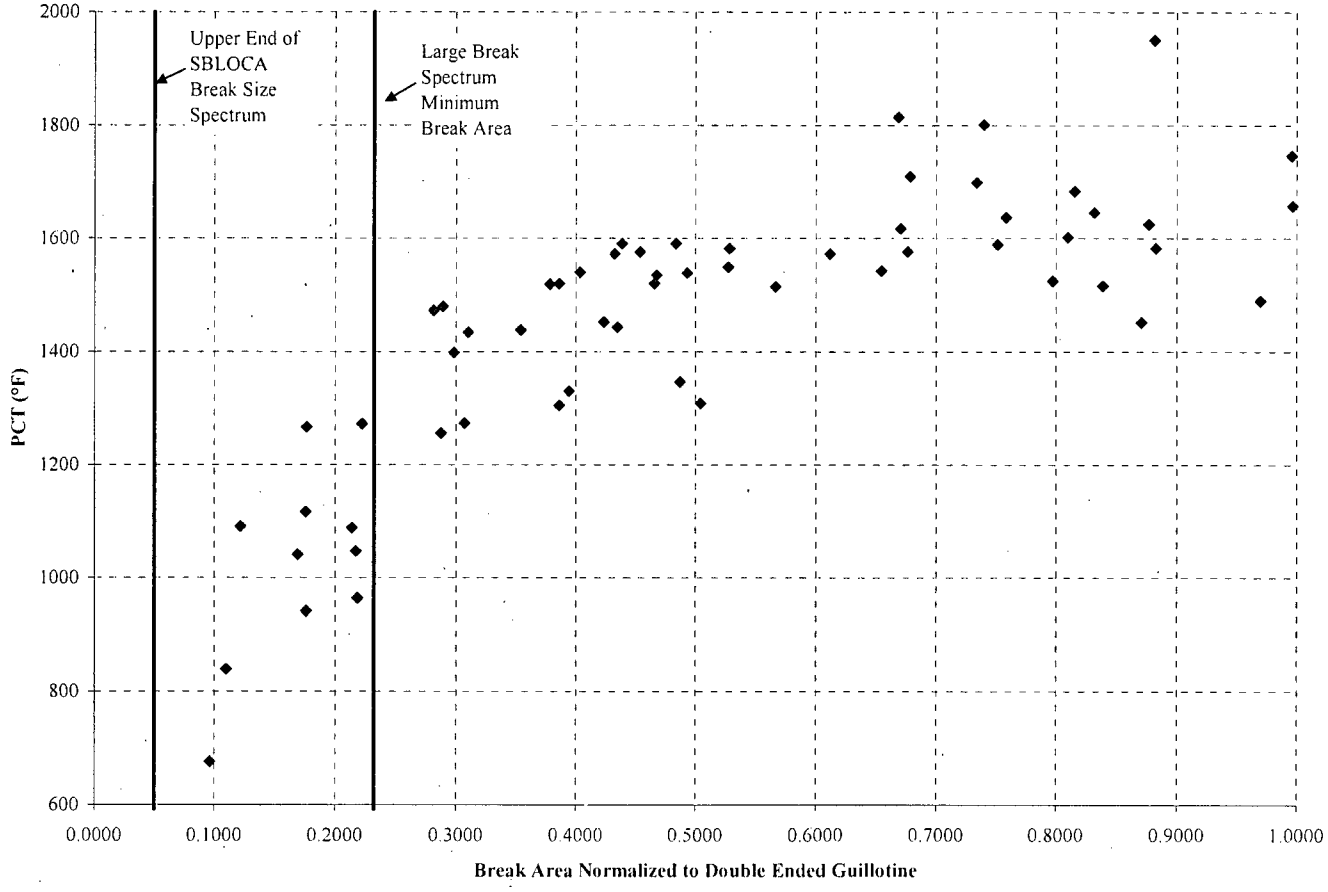

Figure 5-16: Plant B – Westinghouse 3-Loop Design

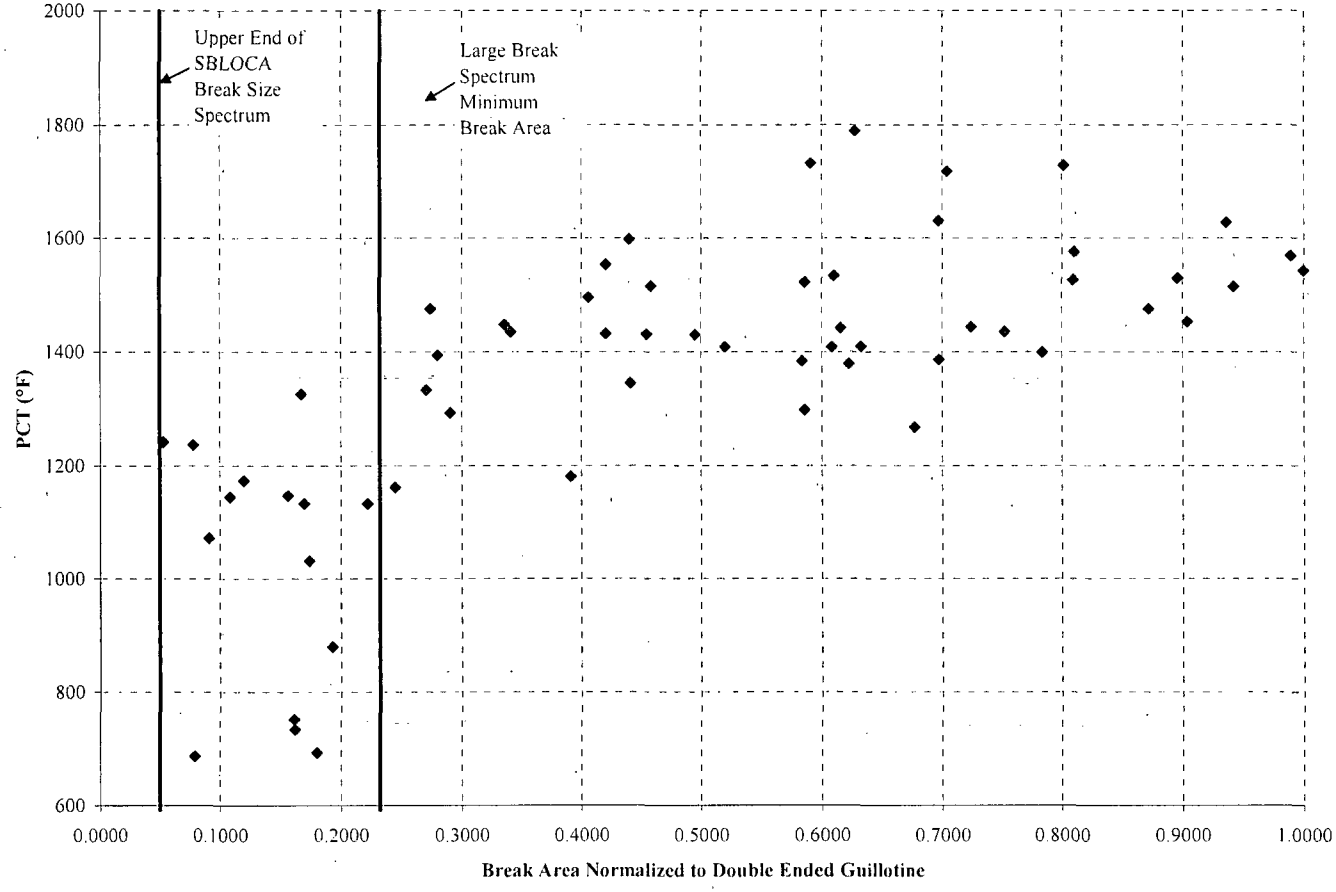

Figure 5-17: Plant C – Westinghouse 3-Loop Design

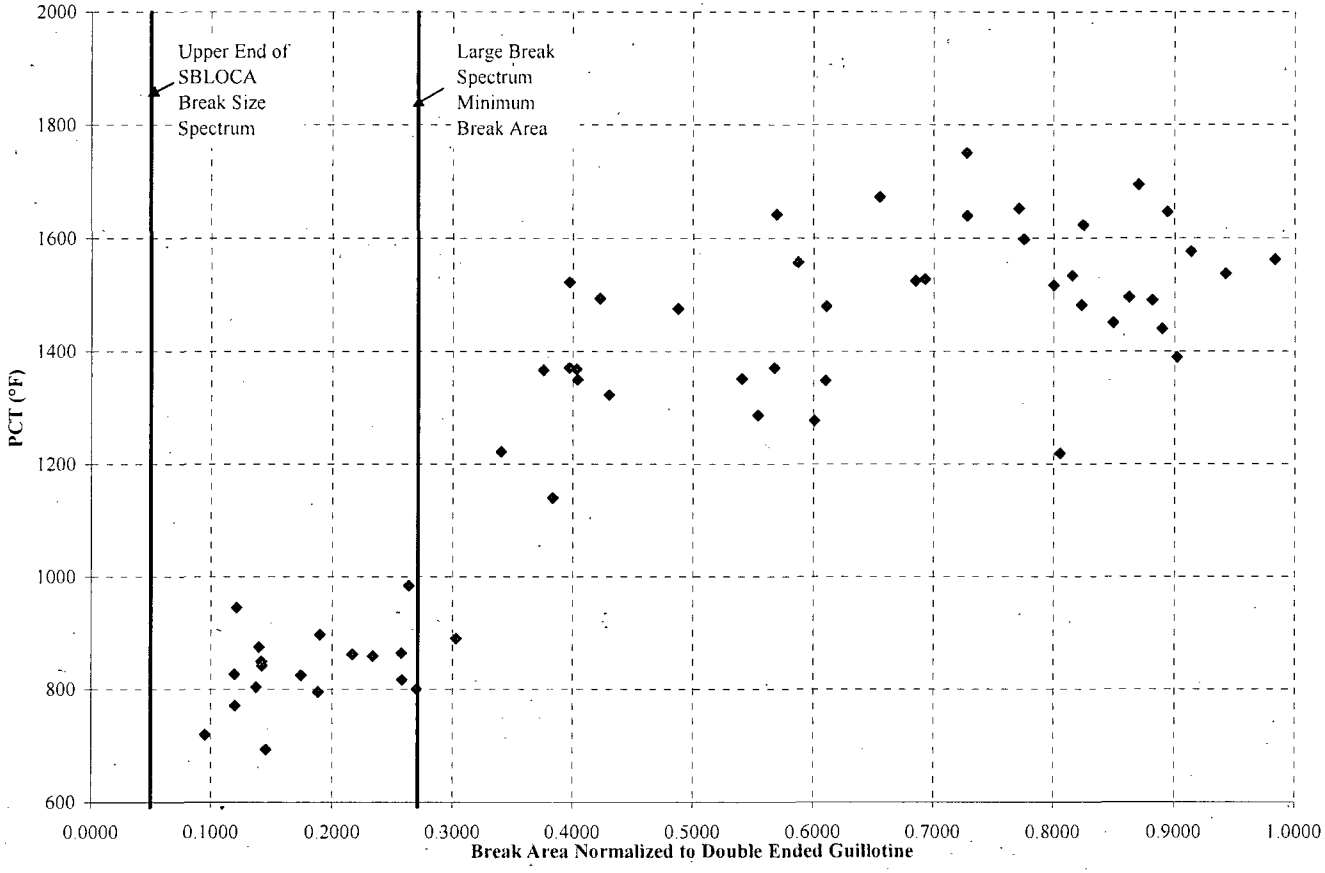

Figure 5-18: Plant D – Combustion Engineering 2x4 Design

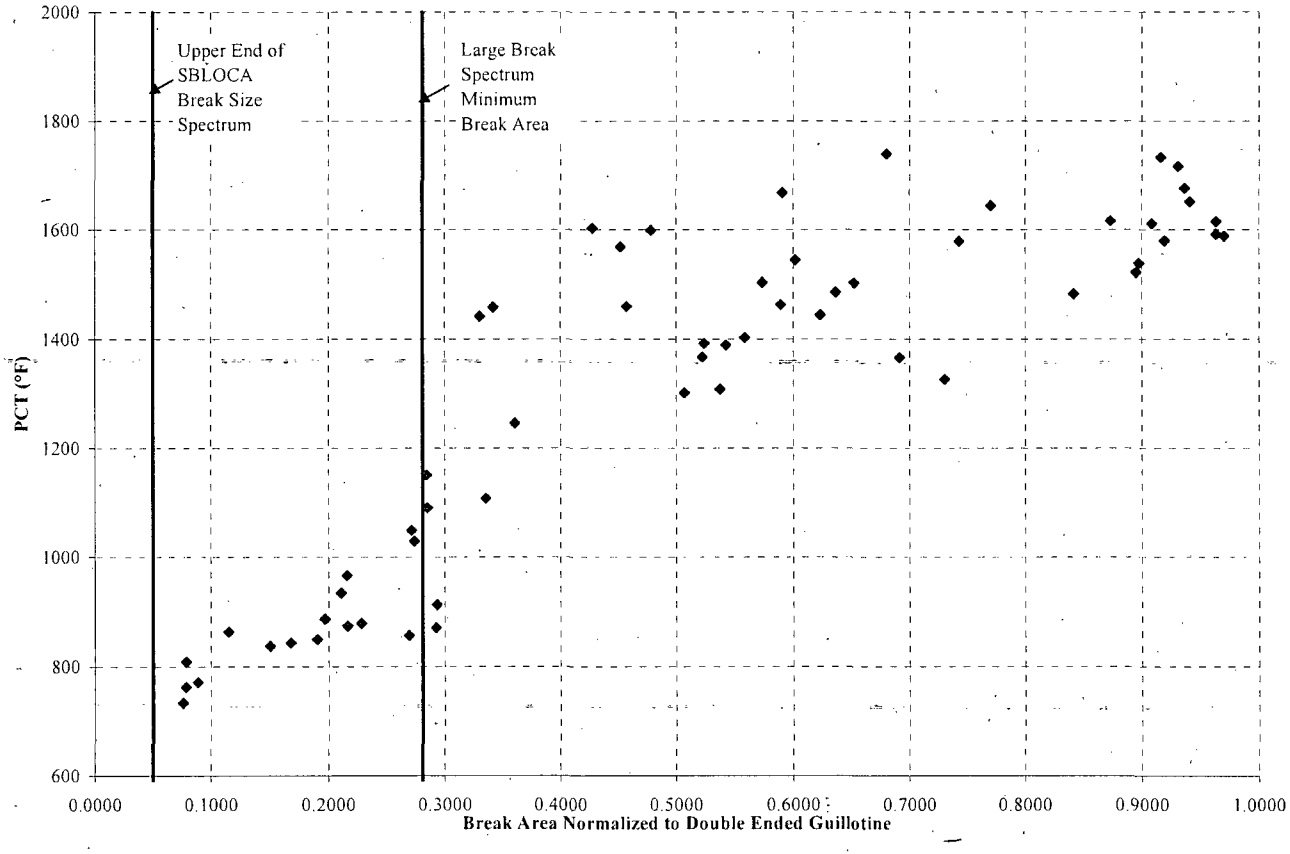

Figure 5-19: Plant E – Combustion Engineering 2x4 Design

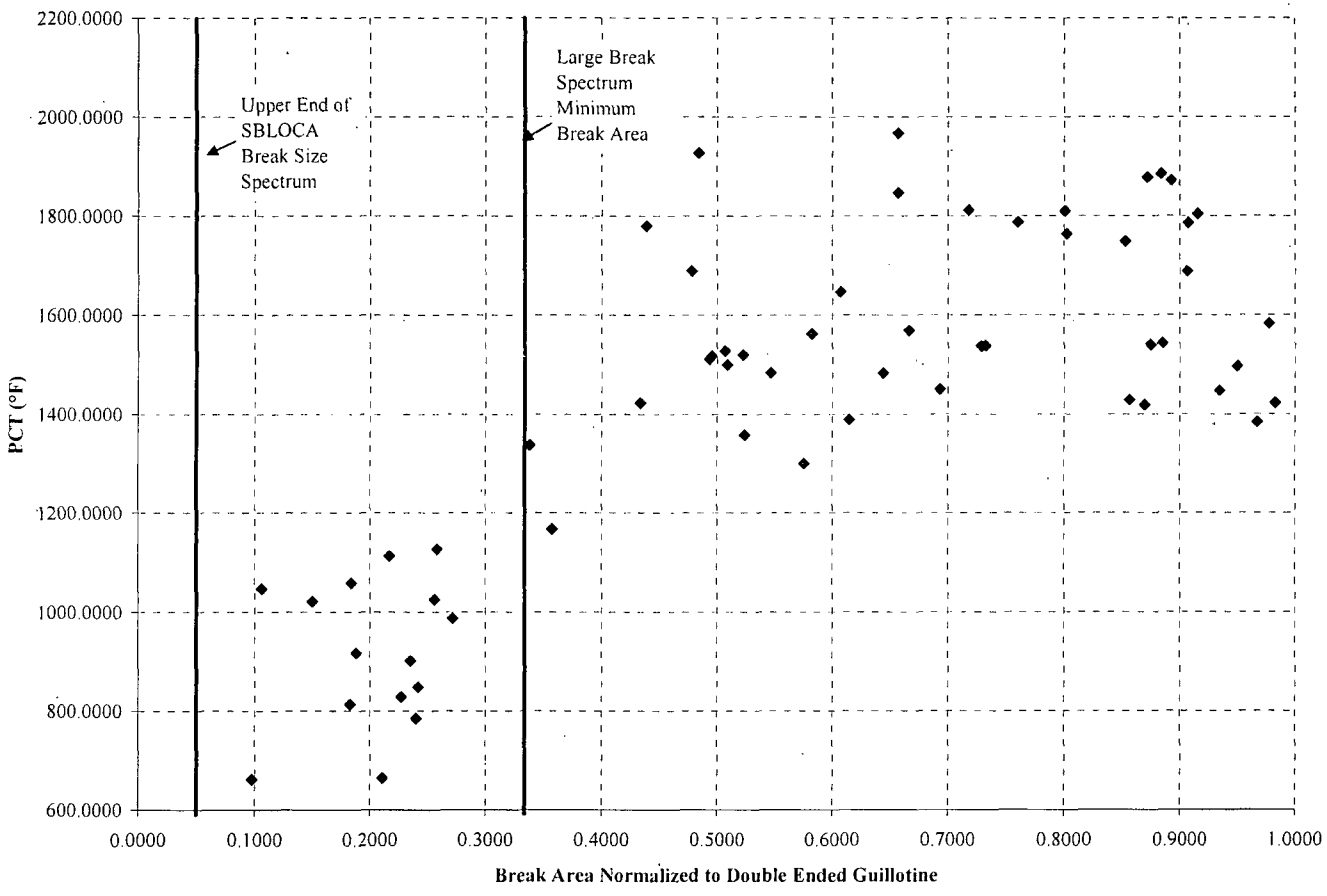

Figure 5-20: Westinghouse 4-Loop Design

5.7 Detailed Information for Containment Model (ICECON)

Question: *Verify that the ICECON model is that shown in Figure 5.1 of EMF-CC-39(P) Revision 2, "ICECON: A Computer Program Used to Calculate Containment Back Pressure for LOCA Analysis (Including Ice Condenser Plants)."*

The AREVA RLBLOCA Report shows that the containment parameters treated statistically are: (1) upper compartment containment volume, (2) upper compartment containment temperature, and (3) lower compartment containment temperature. ANP-2903(P) states that "in many instances" the guidance of NRC Branch Technical Position CSB 6-2 was used in determining the other containment parameters.

(a) How is the mixing of containment steam and ice melt modeled so as to minimize the containment pressure?

(b) Verify that all containment spray and fan coolers are assumed operating at maximum heat removal capacity.

(c) Describe how the limits on the volume of the upper containment were determined.

(d) How are the containment air return fans modeled and what is the effect of this modeling on the containment pressure?

(e) Describe how passive heat sink areas and heat capacities are modeled so as to minimize containment pressure.

Response: See Section 3.3 for discussion of questions (a) through (e). HNP Unit 1 is a dry atmospheric containment and items pertaining to ice condenser containments are not applicable to HNP. Containment initial conditions and cooling system information are provided in Table 3-8 and Heat Sinks are provided in Table 3-9. For HNP Unit 1, the scatter plots of PCT versus the sampled containment volumes is shown in Figure 3-11. PCT versus sampled accumulator temperature (containment temperature is coupled to accumulator temperature) is shown in Figure 5-21. Containment pressure as a function of time for limiting case is shown in Figure 3-22.

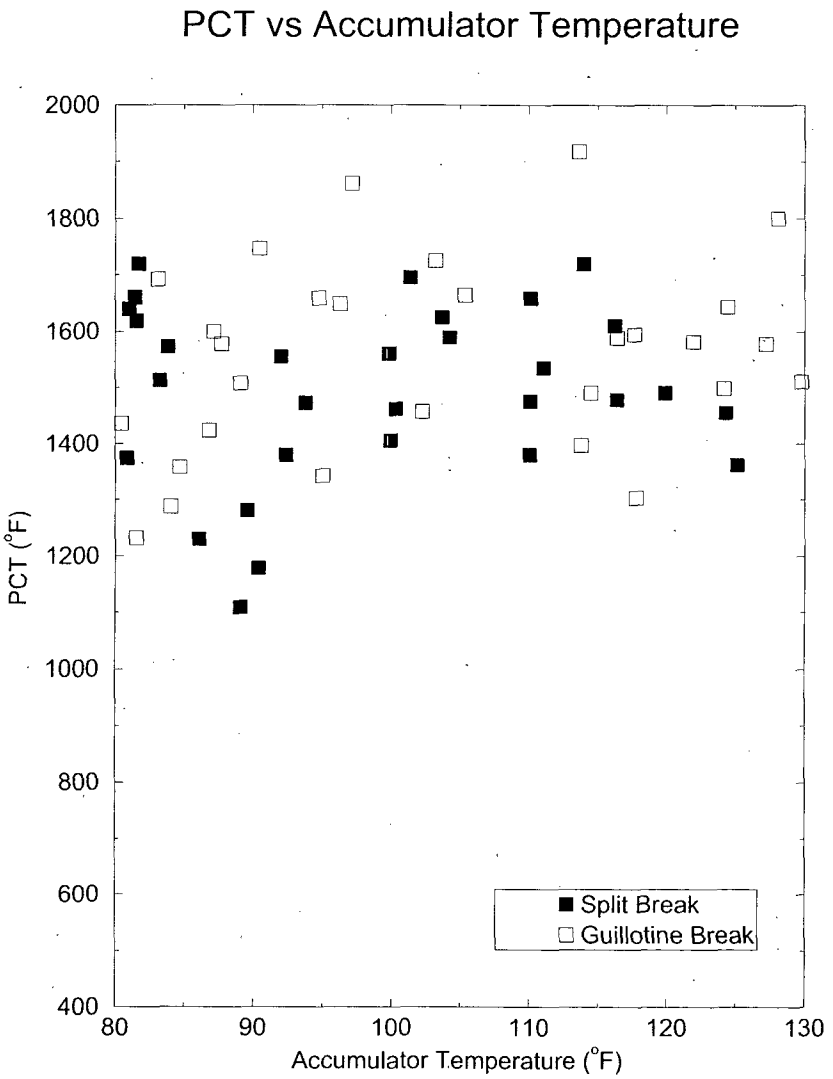

Figure 5-21: PCT versus Initial Containment Temperature

5.8 Cross-References to North Anna

Question: *In order to conduct its review of the Harris application of AREVA's realistic LBLOCA methods in an efficient manner, the NRC staff would like to make reference to the responses to NRC staff requests for additional information that were developed for the application of the AREVA methods to the North Anna Power Station, Units 1 and 2, and found acceptable during that review. The NRC Staff safety evaluation was issued on April 1, 2004 (Agency-wide Documentation and Management System (ADAMS) accession number ML040960040). The staff would like to make use of the information that was provided by the North Anna licensee that is not applicable only to North Anna or only to subatmospheric containments. This information is contained in letters to the NRC from the North Anna licensee dated September 26, 2003 (ADAMS accession number ML032790396) and November 10, 2003 (ADAMS accession number ML033240451). The specific responses that the staff would like to reference are:*

September 26, 2003 letter: NRC Question 1

NRC Question 2

NRC Question 4

NRC Question 6

November 10, 2003 letter: NRC Question 1

Please verify that the information in these letters is applicable to the AREVA model applied to Harris except for that information related specifically to North Anna and to sub-atmospheric containments.

Response: The responses provided to questions 1, 2, 4, and 6 are for the most part generic and related to the ability of ICECON to calculate containment pressures. Excepting as follows they are applicable to the HNP Unit 1 RLBLOCA submittal.

Question 1 – Completely Applicable

Question 2 – Completely Applicable

Question 4 – Completely Applicable (the reference to CSB 6-1 should now be to CSB Technical Position 6-2). The NRC altered the identification of this branch technical position in Revision 3 of NUREG-0800.

Question 6 - Completely applicable.

The supplemental request and response are applicable to HNP Unit 1.

5.9 GDC 35 – LOOP and No-LOOP Case Sets

Question: *10CFR50, Appendix A, GDC [General Design Criterion] 35 [Emergency core cooling] states that, "Suitable redundancy in components and features and suitable interconnections, leak detection, isolation, and containment capabilities shall be provided to assure that for onsite electric power system operation (assuming offsite electric power is not available) and for offsite electric power operation (assuming onsite power is not available) the system function can be accomplished, assuming a single failure."*

The Staff interpretation is that two cases (loss of offsite power with onsite power available, and loss of onsite power with offsite power available) must be run independently to satisfy GDC 35.

Each of these cases is separate from the other in that each case is represented by a different statistical response spectrum. To accomplish the task of identifying the worst case would require more runs. However, for LBLOCA analyses (only), the high likelihood of loss of onsite power being the most limiting is so small that only loss of offsite power cases need be run. (This is unless a particular plant design, e.g., CE [Combustion Engineering] plant design, is also vulnerable to a loss of onsite power, in which situation the NRC may require that both cases be analyzed separately. This would require more case runs to satisfy the statistical requirement than for just loss of offsite power.)

What is your basis for assuming a 50% probability of loss of offsite power? Your statistical runs need to assume that offsite power is lost (in an independent set of runs). If, as stated above, it has been determined that Palisades, being of CE design, is also vulnerable to a loss of onsite power, this also should be addressed (with an independent set of runs).

Response: In concurrence with the NRC's interpretation of GDC 35, a set of 59 cases each was run with a LOOP and No-LOOP assumption. The set of 59 cases that predicted the highest figure of merit, PCT, is reported in Section 2 and Section 3, herein. The results from both case sets are shown in Figure 3-23. This is a change to the approved RLBLOCA EM (Reference 1).

5.10 Progress Energy – AREVA Interface

Question: *Provide a statement confirming that Progress Energy and its LBLOCA analyses vendor have ongoing processes that assure that the input variables and ranges of parameters for the Harris LBLOCA analyses conservatively bound the values and ranges of those parameters for the as operated Harris plant. This statement addresses certain programmatic requirements of 10 CFR 50.46, Section (c).*

Response: Progress Energy and the LBLOCA Analysis Vendor have an ongoing process to ensure that all input variables and parameter ranges for the HNP Unit 1 realistic large break loss-of-coolant accident are verified as conservative with respect to plant operating and design conditions. In accordance with Progress Energy Quality Assurance program requirements, this process involves

1) Definition of the required input variables and parameter ranges by the Analysis Vendor

2) Compilation of the specific values from existing plant design input and output documents by Progress Energy and Vendor personnel in a formal analysis input summary document issued by the Analysis Vendor and

3) Formal review and approval of the input summary document by Progress Energy. Formal Progress Energy approval of the input document serves as the release for the Vendor to perform the analysis.

Continuing review of the input summary document is performed by Progress Energy as part of the plant design change process and cycle-specific core design process. Changes to the input summary required to support plant modifications or cycle-specific core alternations are formally communicated to the Analysis Vendor by Progress Energy. Revisions and updates to the analysis parameters are documented and approved in accordance with the process described above for the initial analysis.

6.0 RECENT NRC REQUEST FOR ADDITIONAL INFORMATION (RAI) AND AREVA RESPONSES

The NRC staff has found that strict adherence to currently referenced, or proposed for referencing AREVA methodologies are inconsistent with the NRC's requirements and review guidance without appropriate justification. This section addresses the NRC staff's concerns for the AREVA RLBLOCA methodology.

6.1 Thermal Conductivity Degradation

Question: *Please provide more information about the management of the fuel thermal conductivity degradation issue identified in NRC Information Notice 2009-23, "Nuclear Fuel Thermal Conductivity Degradation." Specifically:*

a. *"For each specific time in cycle, the fuel conditions are computed using RODEX3A prior to starting the S-RELAP5 portion of the analysis. A steady state condition for the given time in cycle using S-RELAP5 is established. A base fuel centerline temperature is established in this process. Then two-transformation adjustment to the base fuel centerline temperature is computed. The first transformation is a linear adjustment for an exposure of 10 MWd/MTU or higher. In the new process, a polynomial transformation is used in the first transformation instead of a linear transformation." Please clarify the following:*

   i. *Explain how the fuel pellet radial temperature profile is computed.*

   ii. *Explain which code is used to calculate this profile, both for initial conditions and through the postulated accident*

   iii. *Explain whether the polynomial transformation is applied merely to the centerline temperature, or to the entire pellet temperature*

b. *Provide additional information to describe the polynomial transformation. Summarize data used to develop the polynomial transformation and discuss consideration of applicable uncertainties.*

Response: The NRC concern covers a wide range of specific items but can be paraphrased as: "How does the AREVA RLBLOCA analysis for HNP Unit 1 provide a licensing basis for fuel throughout its operational life with particular attention to the phenomena of thermal conductivity degradation with burnup?" In response, the following explanation of the methodology employed for HNP Unit 1 is provided and followed by specific responses to each of the particular questions.

The AREVA transition package has been updated to specifically model both first and second cycle fuel rods. Third cycle fuel does not retain sufficient energy potential to achieve significant cladding temperatures nor cladding oxidation and is not included in the RLBLOCA individual pin calculations. The burnup for the individual first and second cycle rods analyzed is assigned according to the sampled time in cycle. The time in cycle is sampled once and is the same for both the fresh (first cycle) and

once-burnt (second cycle) fuel. Burnup for the fresh and once-burnt rods is different in accordance with the cycle management. Likewise, pin pressure and thermal conductivity differ.

In addition to the thermal conductivity and fuel temperatures adjustments for burnup, a burnup dependent reduction in allowed peaking is needed for the once-burnt fuel. For first cycle fuel, the RLBLOCA methodology increases the $F_{\Delta H}$ to the Technical Specification maximum (including uncertainty) for the first cycle hot rods in the model. Shortly into the cycle, once-burnt fuel that would be impossible to achieve. Figure 6-4 provides the bounding once-burnt fuel pins will be controlled as a function of burnup during the cycle. Figure 6-4 is bounding for the current fuel management process but is considered an input and may be modified as conditions require.

6.1.a.i The RODEX3 topical report, ANF-90-145(P)(A), Appendix B (Reference 29) details the calculation of the radial temperature distribution.

6.1.a.ii A portion of the RODEX3A fuel model was incorporated into the S-RELAP5 code to calculate fuel response for transient analyses. This coding, referred to as the S-RELAP5/RODEX3A model deals only with transient predictions and does not calculate the burnup response of the fuel. Instead, fuel conditions at the burnup of interest are transferred via a binary data file from RODEX3A to S-RELAP5/RODEX3A, establishing the initial state of the fuel prior to the transient. The data transferred from RODEX3A describes the fuel at zero power. A steady-state S-RELAP5/RODEX3A calculation is required to establish the fuel state at power. The transient fuel pellet radial temperature profile is computed by solving the conduction equation of S-RELAP5. Material properties are calculated in S-RELAP5/RODEX3A.

6.1.a.iii The adjustment is applied to the entire fuel pellet. The polynomial transformation provides a bias adjustment to the fuel centerline temperature. A sampled parameter provides a random assessment and adjustment of the centerline temperature uncertainty. These are combined and the total adjustment is achieved by iterating a multiplicative adjustment to the fuel thermal conductivity until the desired fuel centerline temperature is reached.

6.1.b Paraphrased concern: Provide information on the treatment of thermal conductivity degradation.

Thermal conductivity degradation impacts the ability to transfer energy from within the pellet to the pellet surface and consequently through the cladding to the coolant. Both the initial pellet temperature and the transient release of energy from the pellet are affected. The impact of thermal conductivity changes with burnup are treated by applying a bias. This bias and a measure of the uncertainty in the data were determined by benchmarking the fuel performance code, RODEX3A, to a set of data that extends past the licensed burnup. The bias adjusts the initial fuel temperature to the mean of the benchmark results. The sampled uncertainty is used to provide for the variance of the benchmarks.

The database for the benchmarks is that used to qualify and approve the RODEX4 code (Reference 13). The data from three experimental rods (cases 432R2, 432R6, and 597R8) were not used in the benchmarks. Test 597R8 was not appropriate for this application. Cases 432R2 and 432R6 are rod studies that are not configured appropriately for these types of comparisons. Essentially, these fuel rods are not representative of commercial PWR fuel. Part of the benchmark activity was to incorporate a fractional representation of difference between the RODEX3A calculated results and the data. The fractional adjustment provides a better adjustment over a range of initial temperatures. Therefore, for each benchmark case the $T_{fraction}$ was determined.

$$T_{fraction} = \frac{T_{rodex3A} - T_{data}}{T_{rodex3A}},$$

where:

$T_{fraction}$ = Delta fractional temperature of computed to data (K),

$T_{rodex3A}$ = Temperature computed by RODEX3A (K) and

T_{data} = Temperature from the RODEX4 database (K).

Figure 6-1 shows the RODEX3A benchmark results along with a polynomial fitted to the results using the least squares method. The negative of this polynomial is the bias which is added to RODEX3A predictions to achieve agreement with the data. Figure 6-2 shows the results of applying this bias in comparison to the results of applying the original RLBLOCA methodology Revision 0 bias. It is evident from Figure 6-2 that the bias makes the adjustment for burnup effects in accordance with the data.

The application of the bias within the methodology proceeds as follows: The burnup for the case hot rods, fresh and once burned, is determined by sampling the time in cycle and a RODEX3A calculation of the initial fuel centerline temperature performed. From the fit in Figure 6-1 an adjusted temperature is determined as per the equation below.

[ ]

where:

T_{new} = New fuel centerline temperature (K),

B = Burnup (Gwd/MtU or Mwd/KgU) and

$T_{original}$ = Base fuel centerline temperature (K).

Figure 6-3 provides the bias adjustment $T_{new}/T_{original}$, as function of burnup, using the above polynomial curve fit.

The uncertainty is determined from a Gaussian distribution charaterized by a [ ] standard deviation and added to T_{new}. The fuel temperature is then repeated with a multiplier, fuel K, on the code calculated fuel thermal conductivity. The fuel centerline temperature is compared to 'T_{new} + uncertainty' and the calculation is repeated with an adjusted fuel K as necessary. The process is continued until the calculated centerline fuel temperature matches 'T_{new} + uncertainty'. Since the process applies an adjustment to the fuel thermal conductivity, the temperature throughout the pellet is adjusted appropriately. The final multiplier is applied to the thermal conductivity throughout the transient.

Because the data fitting covers the complete range of applicable burnup it is applied as such and the zero bias offset used in Revision 0 for the first 10 GWd/mtU burnup is eliminated.

Follow-on Question:

Question: *The issue described in IN 2009-23 invalidates AREVA's generic disposition for analyzing fresh fuel only, which is based on sensitivity studies indicating that mid-second-cycle fuel had a PCT of 80°F lower than the limiting PCT. This work needs to be repeated accounting for fuel thermal conductivity degradation. Please provide several cases run at various times-in-life for once-burnt fuel, with information similar to the above list provided; burnup for the limiting rod is only necessary for the most limiting second-cycle case analyzed.*

For the PCT-limiting RLBLOCA case, please provide:

a. *Corrected and uncorrected radial temperature profile of the hot rod at the time and location of peak cladding temperature.*

b. *Temperature vs. time for the limiting PCT case at the limiting location, including the fuel centerline, fuel average, and clad surface temperatures. Indicate the end of blowdown, start of refill, and start of reflood on this graph.*

c. *Burnup for the limiting rod.*

Response: Figure 6-5 shows the corrected and uncorrected radial temperature profile for the limiting PCT case hot rod at the initiation of the transient. Because the uncorrected radial profile is never used or recorded in the methodology, it cannot be provided. However, the uncorrected centerline temperature is available and shown on Figure 6-5. As the pellet power is not adjusted the radial temperature profile must follow the corrected profile closely and the two must converge at the surface of the pellet. Figure 6-6 shows the centerline, surface, and average fuel temperatures of the fresh UO_2 rod at the PCT elevation for the limiting PCT case. In this case, all of the fresh rods have higher PCTs than the once-burnt rods. The most limiting once-burnt rod is the UO_2 rod. With a cycle burnup of approximately 8302 EFPH, the fresh UO_2 rod has a burnup of 18.8 GWd/MTU while the once-burnt UO_2 rod has a burnup of 39.7 GWd/MTU. A plot comparing the PCT of the fresh and once-burnt UO_2 rods for this case is shown in Figure 6-7.

Figure 6-1: Fractional Fuel Centerline Temperature Delta Between RODEX3A and Data

Figure 6-2: Fuel Centerline Temperature Delta of RODEX3A Calculations to Data (Original and Using the New Correlation)

Figure 6-3: Correction Factor (as applied for temperatures in Kelvin)

Figure 6-4: Once Burnt Fuel Power Ratios (2nd Cycle)

Figure 6-5: Radial Temperature Profile for Hot Rod

Figure 6-6: Temperature versus Time for Fuel Centerline, Clad Surface, and Fuel Average

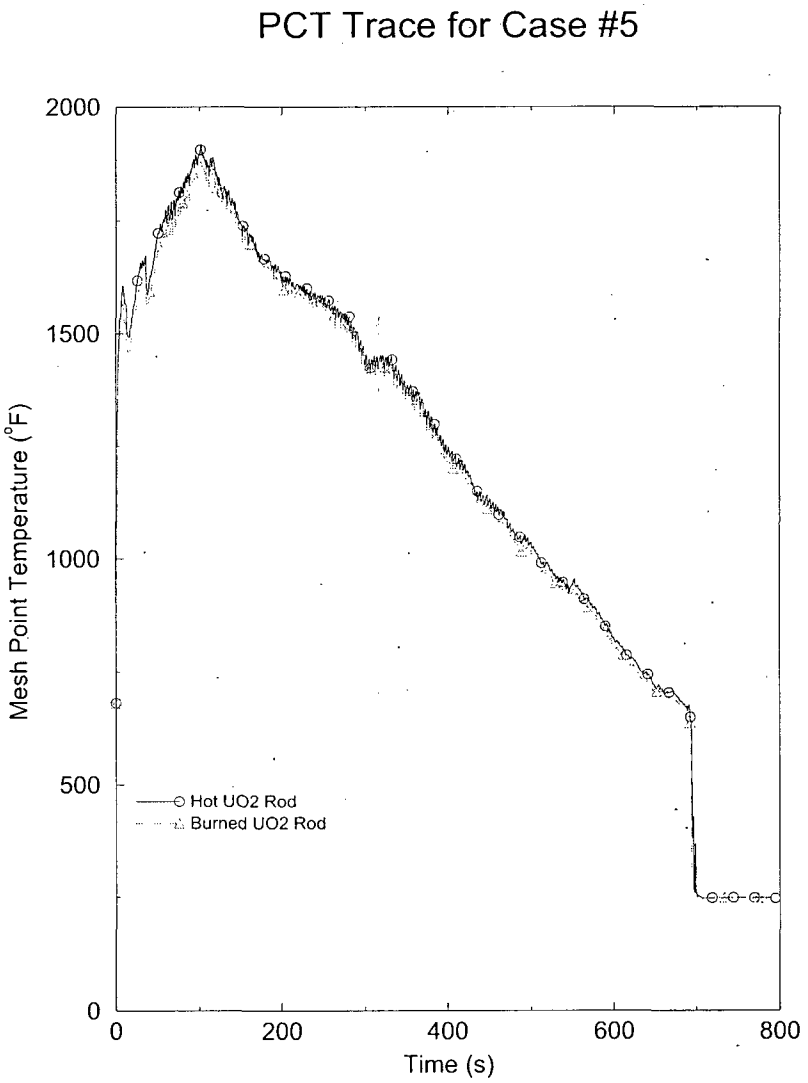

Figure 6-7: Fresh and Once-Burned UO_2 Rod PCT Trace

6.2 Limiting Condition – Single Failure

Question: *The current licensing basis, deterministic loss of coolant accident (LOCA) analysis concluded that the limiting condition did not involve a worst-case single failure, but rather that it depended on injected coolant delivered in such a condition that the resultant containment environment contributed to the limiting peak cladding temperature (PCT). Please provide information describing how this potentially limiting scenario was evaluated using the proposed best-estimate methodology.*

Response: The proposed licensing basis for HNP Unit 1 is AREVA's NRC-approved RLBLOCA evaluation model and the worst single failure considered is loss of diesel with fully functional containment sprays. The EM also conservatively prescribes:

(1) The use of full containment sprays without a time delay at the minimum technical specification temperature;
(2) Pumped ECCS injection at the maximum technical specification temperature; and
(3) Sampling of the containment volume (indirectly sampling containment pressure) from its nominal volume to its empty volume.

Studies, comparing several failure assumptions, including a no-failure assumption (see EMF-2103(P)(A) Revision 0, RAI response Numbers 26 and 111) validate that the ECCS and containment modeling of the AREVA methodology trends to the conservative. The containment pressure response is indirectly ranged by sampling the containment volume. The possible containment volume range to be sampled from was 2.266E+6 to 2.61E+6 ft^3 for HNP Unit 1. Figure 3-11 shows that there is little sensitivity between containment volume (indirectly pressure) and PCT for a statistical application. Thus, the methodology is responsive to the goal of a realistic evaluation, yet slightly conservative.

6.3 Compliance with GDC 35

Question: *Please provide additional information summarizing the single-failure evaluation performed to establish compliance with General Design Criterion (GDC) 35 requirements. Identify which single failures were considered, discuss whether each failure was evaluated or explicitly analyzed, and for those failures which were explicitly analyzed, explain whether they were analyzed in a reference case or explicitly as a part of the statistical methodology. Also discuss the basis for the single failure evaluation. For example, were single failures considered as a matter of experience with Harris specifically, or with a generic Westinghouse nuclear steam supply system design?*

Response: Section 5.9 discusses GDC 35. The single failure prescribed by EMF-2103(P)(A) (AREVA's RLBLOCA EM) is a loss of one train of ECCS (See response to RAI Number 6.8).

AREVA satisfies the GDC-35 criteria by running one set of 59 cases with offsite power available and one set of 59 cases with no offsite power available. The sampling seeds are held constant between

these two case sets, with the only difference being the offsite power assumption. The case set that produces the most limiting PCT is reported, for HNP Unit 1, this was offsite power available. Figure 3-23 in this document displays the results from the two case sets.

6.4 Core Liquid Levels

Question: *Section 3.3 states, "the RLBLOCA transients are of sufficiently short duration that the switchover to sump cooling water (i.e., RAS) for ECCS pumped injection need not be considered." Is the SRELAP-5 model of the limiting case capable of generating credible results after 350s? If so, please provide results for a period of the transient sufficient to demonstrate that the core collapsed liquid levels are stable or increasing.*

Response: Not applicable to the HNP Unit 1 analysis; Figure 3-21 clearly shows a steady level increase from 200 seconds through transient termination.

6.5 Pressurizer Level

Question: *Please provide information to enable comparison between Technical Specifications (TS) requirements and analytic input parameters for Pressurizer Level.*

Response: Technical Specification LCO 3.4.3 states "The pressurizer shall be OPERABLE with a water level of less than or equal to 92% of indicated span."

The sampled range for the liquid level in the pressurizer was centered on the nominal 60-percent span with a Gaussian distribution applied having a standard deviation of 7.4-percent and the distribution was cut-off at 92-percent of span on the high side. The Technical Specification for Harris is bounded.

6.6 Containment Temperature / RWST Temperature

Question: a.) *Please provide discussion to confirm that the assumed containment temperature is an acceptable minimum without a TS requirement.*

b.) The TS minimum for the refueling water storage tank (RWST) temperature is 40°F. Previous, deterministic analyses demonstrated that minimum safety injection temperatures resulted in a limiting PCT. In light of this information, please explain why a minimum RWST temperature case was not evaluated, or if a minimum RWST temperature case was evaluated, please summarize the evaluation and discuss its conclusions.

Response:

a.) Technical Specification 3.6/LCO 3.6.1.5 states "Primary containment average air temperature shall not exceed 120°F. The sampled range for the containment temperature was 80 to 130°F. The Technical Specification for Harris is bounded.

b.) The RWST borated water temperature Technical Specifications requirement for Harris is ≥ 40°F and ≤ 125°F (TS 3.1.2.6/b.3 and b.4). The NRC-approved RLBLOCA EM, EMF 2103(P)(A), prescribes use of the maximum temperature for the ECCS pumped injection and use of the minimum temperature for containment sprays. The temperatures for the Harris analysis are 125 °F for pumped injection and 40 °F for the containment sprays.

6.7 Accumulator Level

Question: *Please provide information to facilitate comparison between the assumed accumulator liquid volume expressed in cubic feet, and the TS-controlled volume, given in percent indicated level.*

Response: The correspondence between accumulator volume and % indicated volume is given in Table 6-1.

Table 6-1: Accumulator Level

Item	Value (% indicated)	Volume (ft^3)
Maximum TS SI Accumulator level	96	1029.4
Minimum TS SI Accumulator level	66	994.6

6.8 Limiting Single Failure and Containment and Maximum ECCS Spillage

Question:

a. *The staff also needs to understand how the limiting single failure for the W NSSS was determined, since the basis for the RAI response defers to NRC-approved methodology. Poring through EMF-2103, the staff only located sensitivity results on 3-loop W systems. In some cases, the limiting failure would be a single LPSI and in others it was a diesel. The staff could not locate a clear, generic disposition for the single failure at any place in EMF-2103.*

b. *What was done under the auspices of EMF-2103 development to ensure that the containment analysis produced a sufficiently conservative prediction that a no failure, max SI spillage case, for a W NSSS, is bounded by the chosen single failure? The staff will need to see that work.*

Response:

The definition for loss of a diesel scenario by itself would mean that in addition to loss of one LHSI and one HHSI pump, one train of containment spray would not be available. The current method models all containment pressure-reducing systems as fully functional. Containment fans start at time zero and containment sprays have a 0 second delay (Table 3-8).

The response to RAI #111 for EMF-2103 (Reference 14, Attachment 1 page 185 – 189) was based on sensitivities to 3-loop W plants. The Base Case, which produced the most limiting results, is described in the RAI #111 response as the loss of one diesel with full containment spray. Figure 6-8 (recreated from RAI #111, Figure 111.2) shows that for the sample plant analysis, W 3-loop, the base case, AREVA ECCS failure assumptions, is 35 °F higher in PCT than a fully consistent loss of diesel and over 170 °F greater than the loss of one LHSI case.

Figure 6-8: Clad Temperature Response from Single Failure Study

A sensitivity study of the HNP Unit 1 limiting case for offsite power available (NO-LOOP) (Case 5) and the limiting case for no offsite power available (LOOP) (Case 2) from the HTP Evaluation Model (HTP EM) documented herein. The sensitivity was conducted with "maximum" ECCS flow conditions to demonstrate that the minimum ECCS single failure assumption is conservatively bounding.

The loss of offsite power (LOOP) case (2) for the max ECCS configuration had a PCT value of 1718°F compared to HTP EM LOOP with minimum ECCS, which had a PCT of 1829°F. The no loss of offsite power (NO-LOOP) case (5) for the max ECCS configuration had a PCT value of 1693°F compared to HTP EM NO-LOOP case with minimum ECCS, which had a PCT of 1919°F. This demonstrates that the AREVA single failure assumption produces conservative results. Figure 6-9 through Figure 6-12 show the respective PCT trace, containment and system pressure, ECCS injection rates, and downcomer level for both the HTP EM (limiting No LOOP Case) and the max ECCS sensitivity.

Figure 6-10 demonstrates that the maximum ECCS flow does not have a significant impact on the containment pressure up to about 50 seconds (approximately the time that the accumulator empties); the max ECCS containment pressure overlaps the HTP EM containment pressure for the majority of the transient. Figure 6-12 gives the downcomer level for both the HTP EM and the max ECCS case. It can be seen that the downcomer level in the max ECCS case is higher than the HTP EM, consequently providing more driving head for the reflood of the core. The higher driving head in the max ECCS case is enough to compensate for small differences in containment pressure (Figure 6-10) resulting in a faster post peak cooldown.

The AREVA RLBLOCA application, despite the loss of diesel assumption, models both trains of containment pressure-reducing systems and conservatively assumes them to be fully functional. The HTP EM conservatively assumes an on-time start and normal lineups of the containment spray and fan coolers to conservatively reduce containment pressure and increase break flow. The results of the study demonstrate that the HTP EM ECCS configuration is PCT-limiting and oxidation-limiting.

Figure 6-9: Comparison of PCT Independence of Elevation for Max ECCS and Min ECCS

Figure 6-10: Comparison of Containment and System Pressure for Max ECCS and Min ECCS

Figure 6-11: Comparison of ECCS Flows for Max ECCS and Min ECCS

Figure 6-12: Downcomer Level

6.9 Clad Swelling and Rupture

Question: *The following questions are based on a July 14, 2009, letter from Gardner, AREVA NP, to the USNRC, re: Informational Transmittal Regarding Requested White Papers on the Treatment of Exposure Dependent Fuel Thermal Conductivity Degradation in Legacy Fuel Performance Codes and Methods.*

a. *AREVA postulates that clad swelling and rupture produces a benefit to PCT, and because of this, the realistic large break loss of coolant accident (RLBLOCA) model does not include a clad swelling and rupture model. Does this conjecture include consideration of test data, which has shown that following fuel rupture, the ballooned region fills with fuel fragments? What analytic studies support this conclusion? How are they applicable to Harris? Please also address the potential for co-planar blockage with the fuel relocation evaluation.*

b. *Since blowdown ruptures can occur at end of life conditions, show that blowdown ruptures do not occur at the end of life for the postulated Harris large break LOCA.*

Response:

[

]

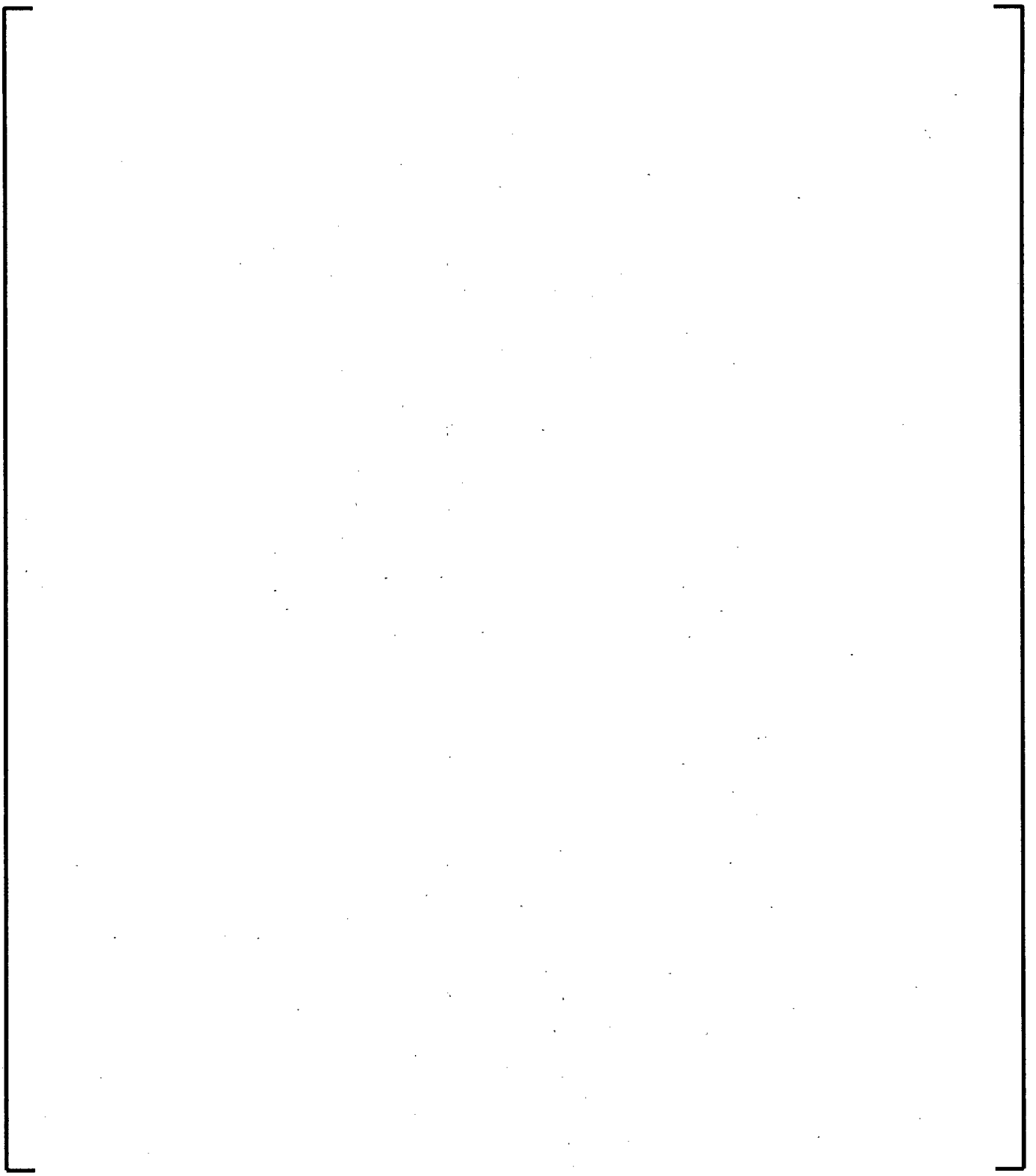

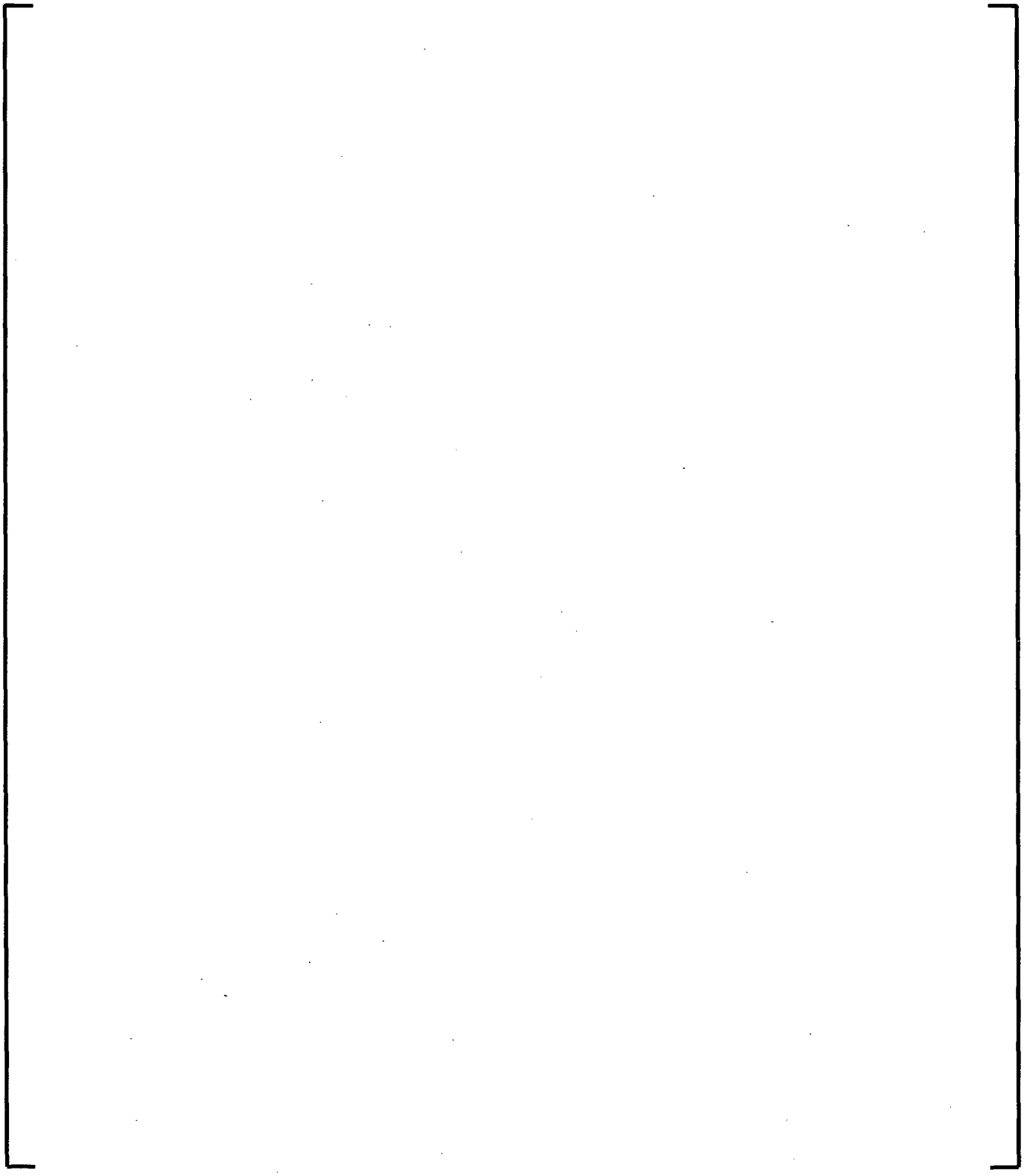

Table 6-2: Region Description of Swelling, Rupture, and Fuel Relocation Model

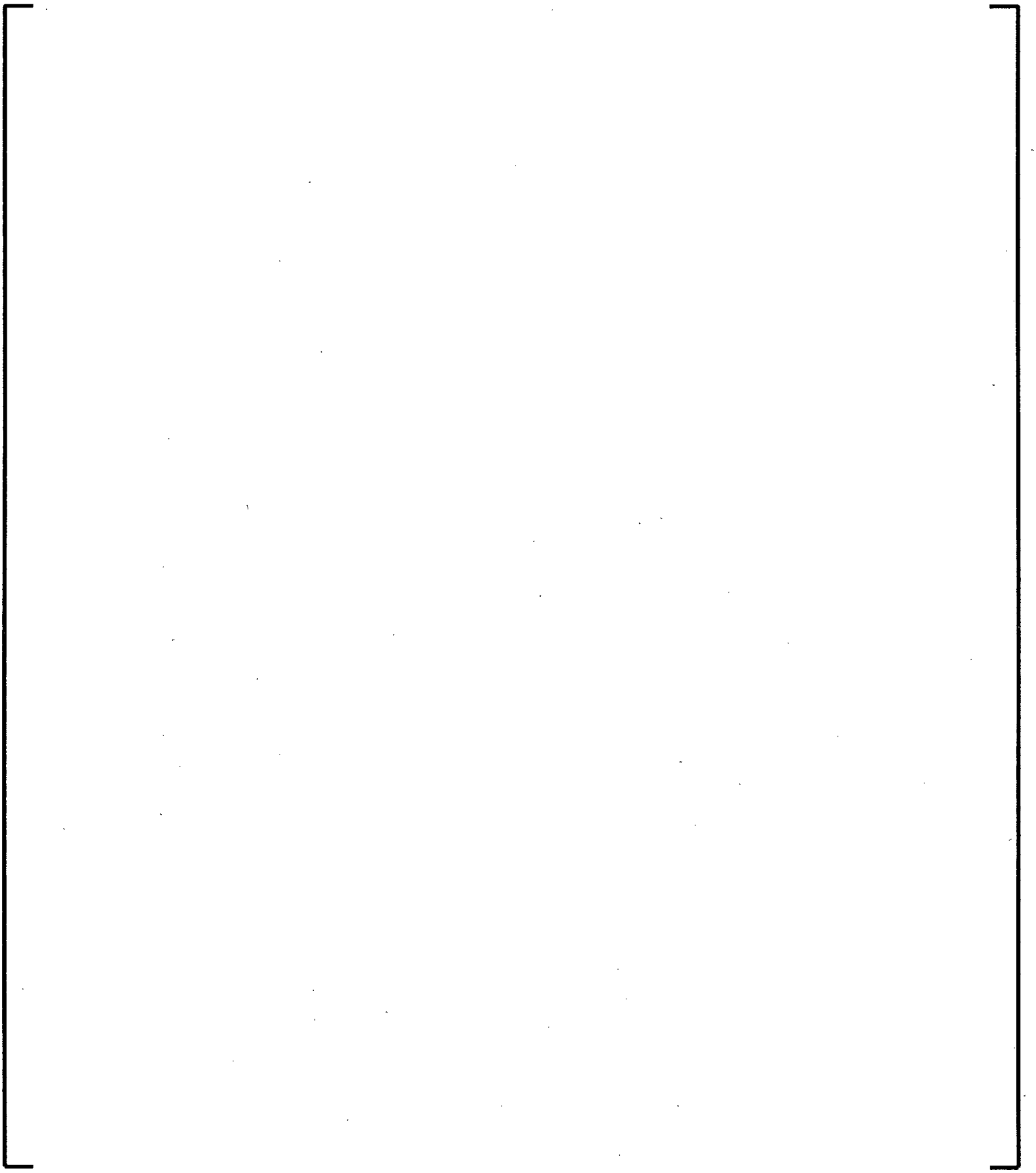

Figure 6-13: Rupture Phenomena

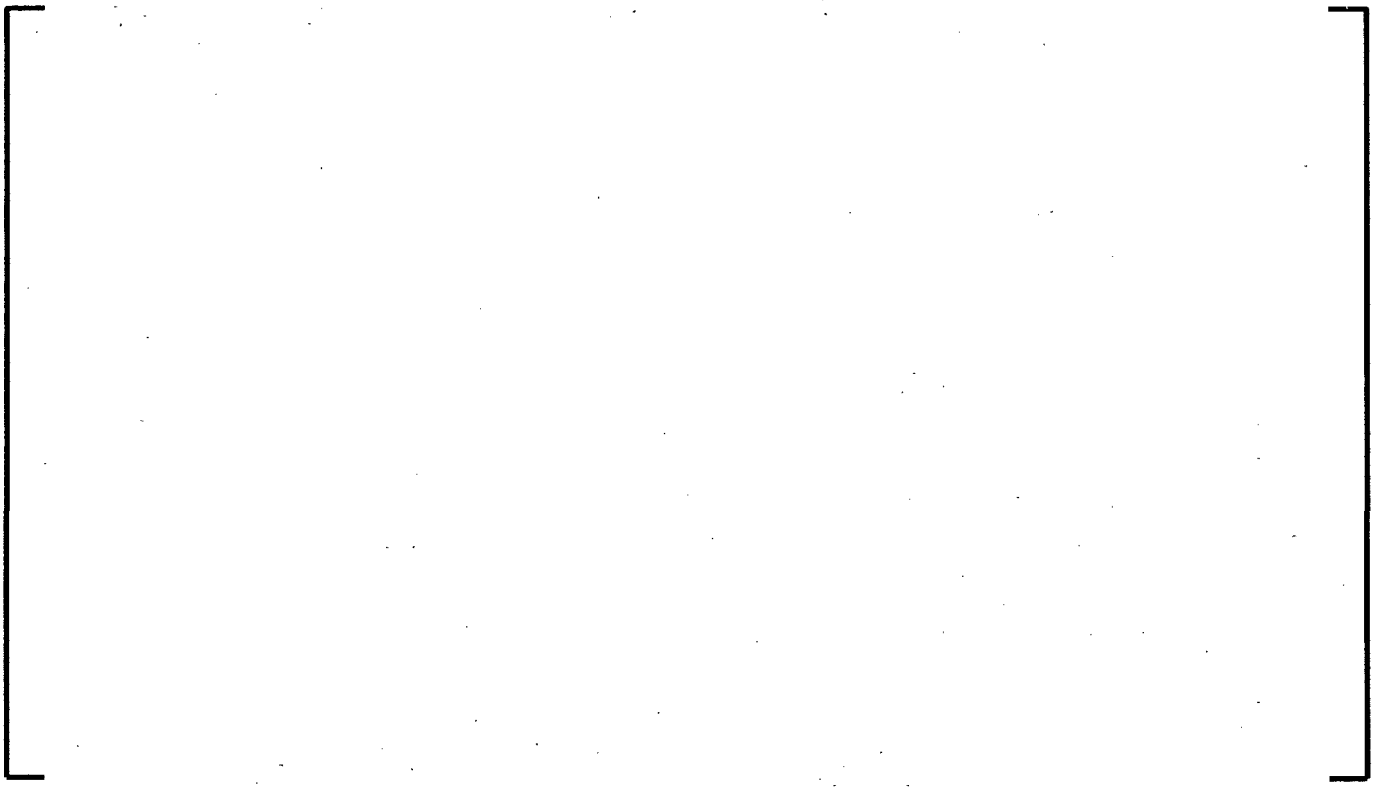

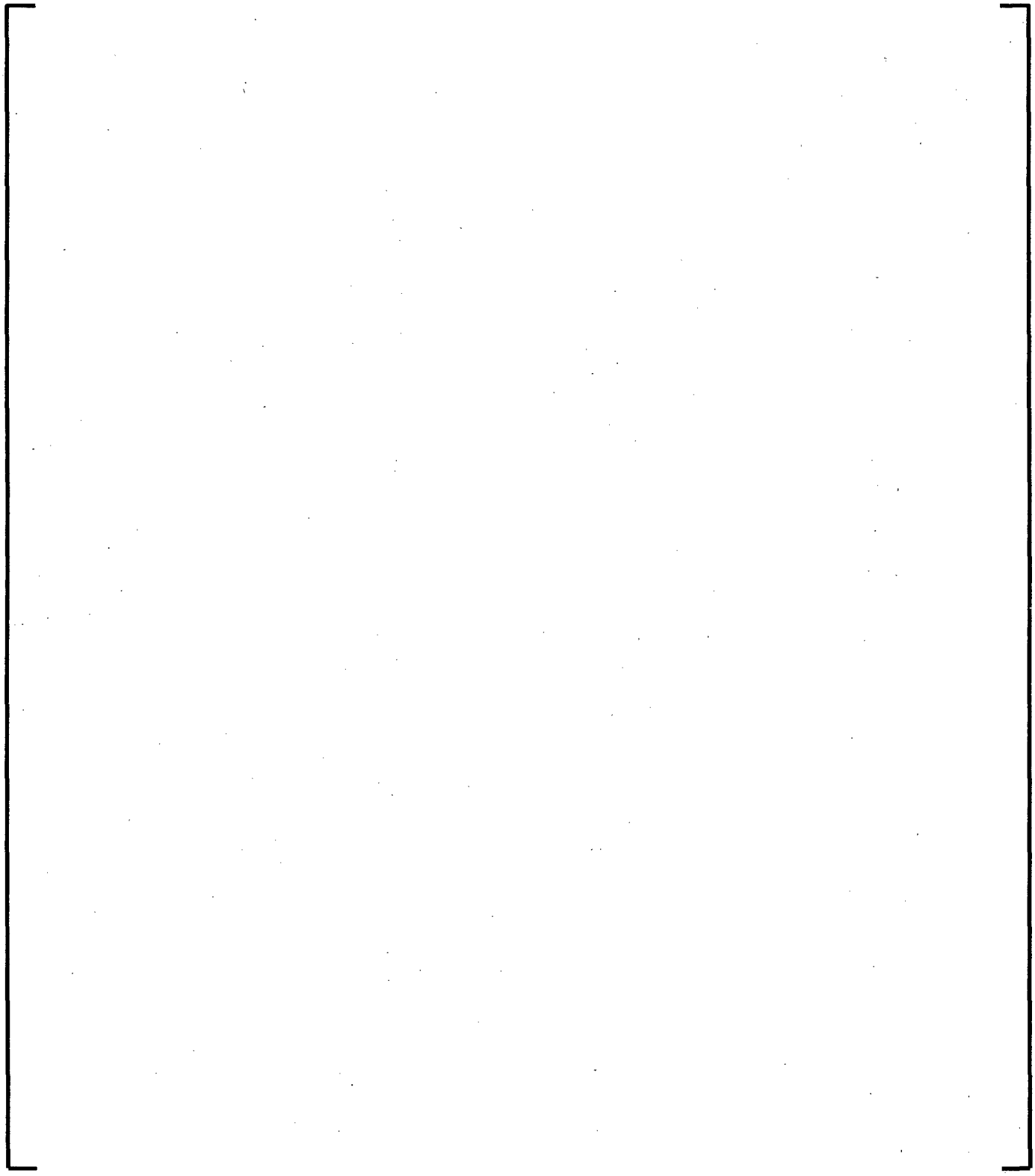

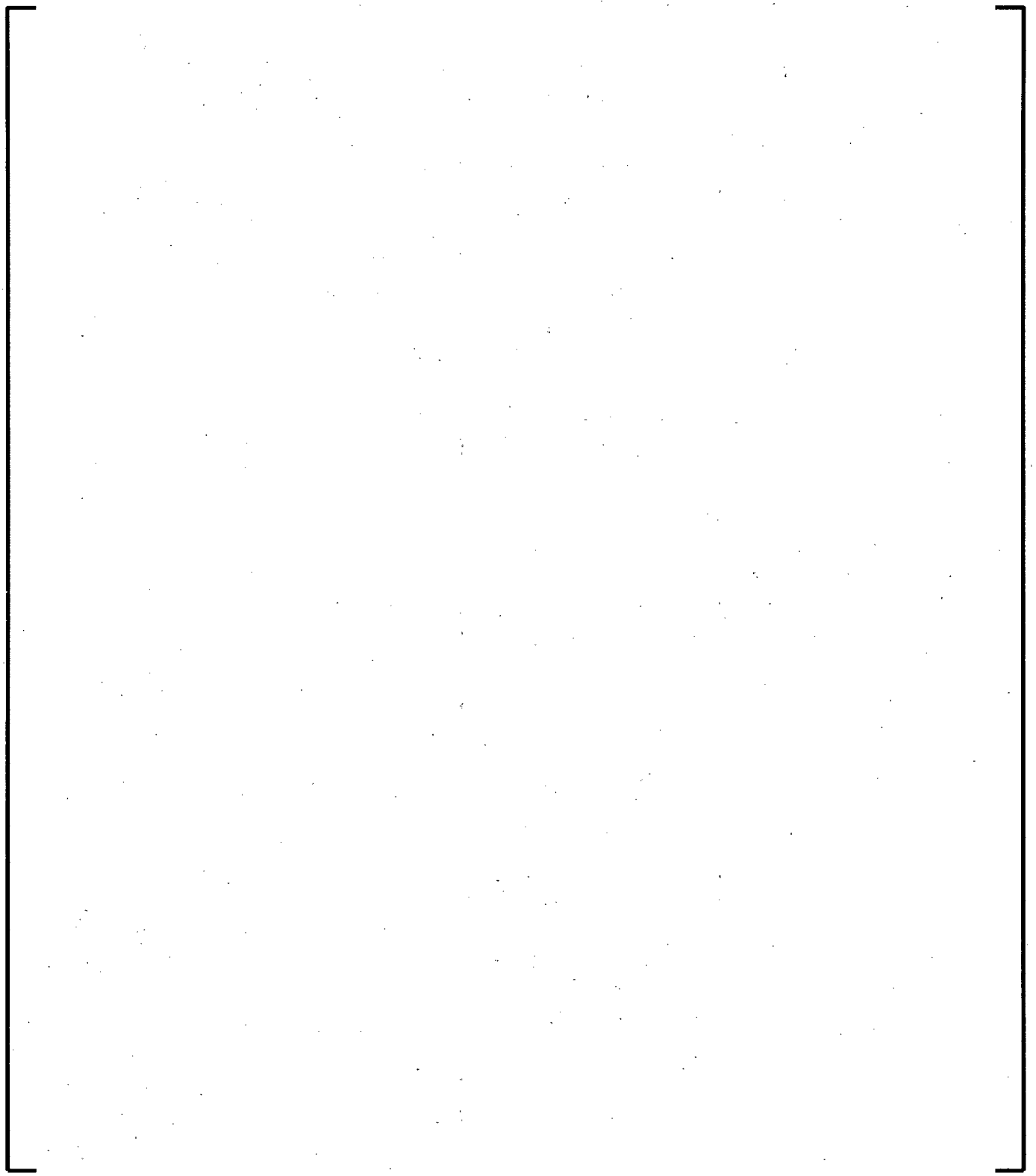

[

]

Figure 6-14: FLECHT-SEASET Test 61607 Benchmark

Figure 6-15: REBEKA-6 Test Benchmark Rod Surface Temperatures

Figure 6-16: REBEKA-6 Test Benchmark Position of CHF Elevation

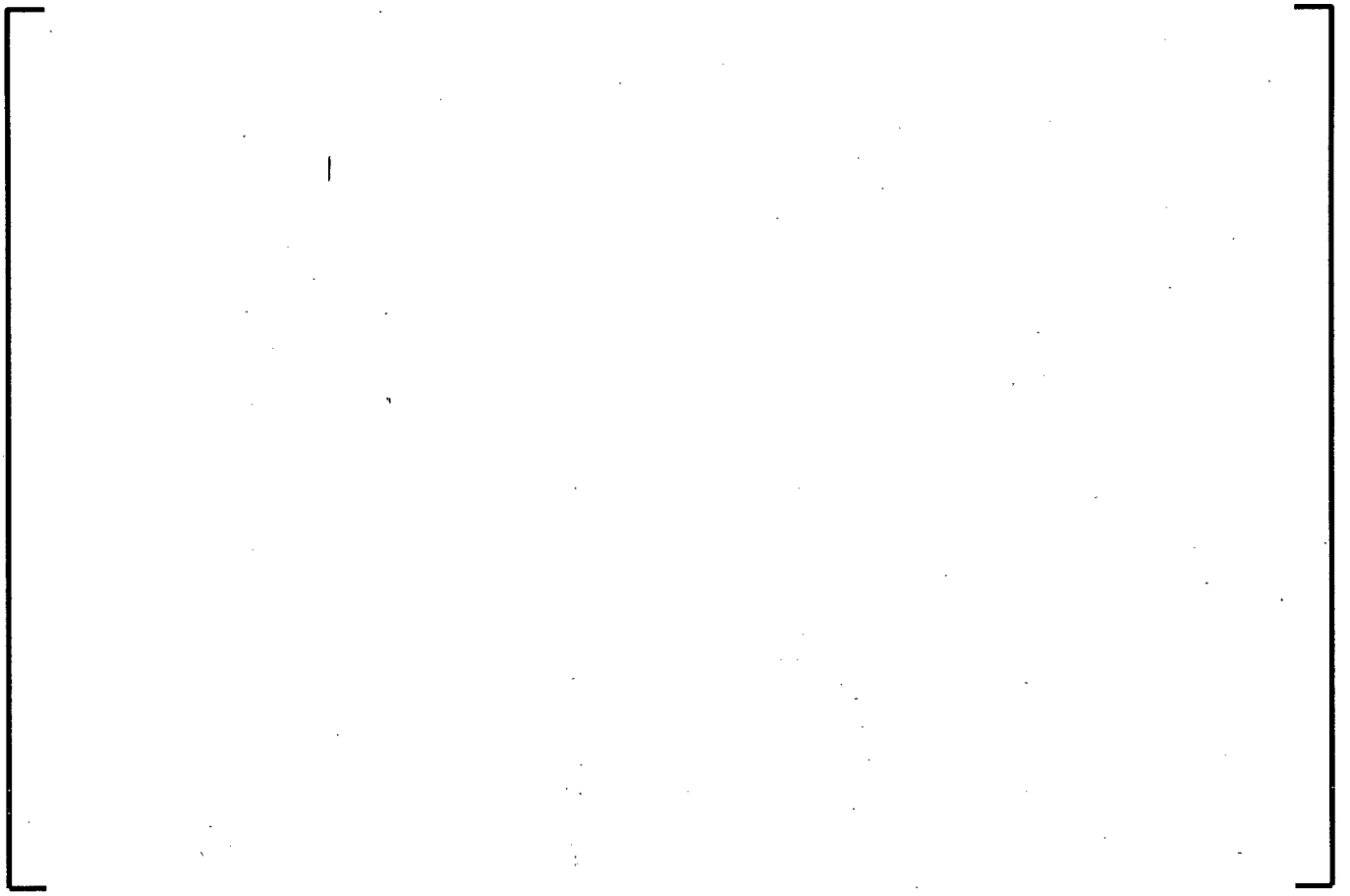

Figure 6-17: Comparison of HNP RLBLOCA Case Set PCTs with and without Swelling, Rupture and Fuel Relocation Model Activated

[ ]

6.10 Single Sided Oxidation Model

Question: *Provide information to illustrate the conservative nature of the single-side only oxidation model and its application to the Harris RLBLOCA analysis.*

Response: AREVA's NRC-approved RLBLOCA EM uses the maximum un-ruptured cladding oxidation as representative or bounding of the oxidation that would have been computed at a rupture location. The position is supported by three aspects of the performed oxidation calculation.

- The cladding is initialized with no initial corrosion layer. Because the oxidation rate is inversely proportional to the oxidation layer present, the use of clean cladding at the start of the accident leads to substantially higher reaction rates. For corrosions in the range of the first cycle of M5 cladding, the difference in rate is a minimum of a 50-percent increase and increases during the cycle. The increase applies to both exterior and post-rupture interior oxidation.

- The cladding temperature even in the presence of fuel relocation is reduced for the ruptured region of the cladding. In the KfK experiments (page 210 of NRC:02:062 Attachment 1 to Reference 14 and included in Reference 15) the temperature drop at rupture was between 50 and 75 K. Since the oxidation rate is exponentially proportional to the cladding temperature, a drop of 50 to 75 K for HNP Unit 1 provides an oxidation rate reduction of 50-percent or more.

- For ruptured cladding either the cladding interior oxidation rate is reduced by attached pellet fragments, moderate to highly burned fuel, or the cladding temperature decrease at rupture is much more than the 50 to 75 K explained in Item 2. In either case, an additional mechanism exists to reduce the local oxidation at the rupture location.

In conclusion, insights into the EM oxidation process and those that will evolve after rupture clearly identify differences that will reduce the oxidation at the rupture location to less than that which the EM calculates at un-ruptured locations. Thus, the RLBLOCA Revision 0 EM approach to reporting local transient oxidation is clearly appropriate to demonstrate compliance with the local oxidation criterion of 10CFR50.46, when combined with the pre-transient oxidation.

The initial corrosion layer was calculated to be 0.9464-percent for the Fresh UO_2 rod (at 18.8 GWd/MTU) and 1.6825-percent for the once-burned UO_2 rod (at 39.7 GWd/MTU) with M5 cladding. The initial corrosion layer for the once-burned UO_2 rod with Zr-4 cladding was calculated to be 3.4447-percent (at 39.7 GWd/MTU). The initial corrosion layer was added to the transient calculated value and the total is in Table 3-5.

6.11 Decay Heat Uncertainty Assumption

Question: *Provide additional information to justify the use of the selected analytic treatment for decay heat uncertainty in the RLBLOCA model.*

a. *The NRC needs to understand the sensitivity that PCT has with respect to the decay heat uncertainty, please re-execute the limiting case with a 1.03 decay heat multiplier and report the results.*

b. *The NRC requests to provide the following parameters for the limiting LBLOCA with the 1.03 multiplier on the decay heat curve: core power, RCS pressure, hot assembly inlet mass flow rate, hot assembly outlet mass flow rate, break flow rate (pump side and vessel side), ECC injection mass flow rate, PCT , hot spot vapor temperature, hot spot heat transfer coefficient (total), downcomer liquid level, core liquid level and containment pressure.*

Response: The RLBLOCA EM decay heat calculations are based on the 1979 ANSI/ANS standard (Reference 19). The standard is applicable to light water reactors containing low enriched uranium as the initial fissile material; all plants, to which the RLBLOCA EM is applicable, including Harris, are such plants. The selected approach to simulate fission product decay assures a representative yet conservative treatment. The EM fission product decay heat uncertainty and the basis for the conservatism of the approach are outlined in the remainder of the response.

Non-Sampling Approach to Decay Heat

The RLBLOCA methodology proposed herein utilizes the U235 decay curve from the 1979 ANSI/ANS standard for fully saturated decay chains as the decay for all fission products. The fully saturated chains result from an assumption of infinite operation. The total energy per fission is assumed to be 200 MeV (Reference 19). No bias or uncertainty is assigned to the fission product decay heat. Differing from the base EMF-2103 evaluation model approach, the uncertainty for the decay heat parameter is set to zero and no sampling is done on this parameter, resulting in the decay heat being used with a 1.0 multiplier. The decay heat in the analysis is always the 1979 ANS standard for decay heat from U235 with fully saturated decay chains, corresponding to infinite operation, assuming 200 MeV per fission.

Conservatism in the Approach

In the approach used, the total energy per fission is assumed to be 200 MeV whereas a more accurate value for U235 would be greater than 202 MeV per fission. This imparts a direct 1-percent conservatism.

During irradiation, plutonium accumulates such that the ratio of plutonium-to-uranium fission-energy production rate is substantial and increasing. Because the decay energy resulting from plutonium fissions is less than that from U235, the decay energy is reduced from U235 fully saturated decay chains as the fuel is burned. Thus, as burnup increases, the RLBLOCA decay heat modeling with

U235 only accrues conservatism. This conservatism applies to all regions of the core according to the mix of burnups represented within each region.

The fresh fuel, hot pin and hot assembly, begin operation with no plutonium. Therefore, the reduction in decay heat due to plutonium build-up is not applicable to the low burnup fuel in the initial period of the cycle. However, for fresh fuel, the concentrations of long decay term fission products will not have built up. The lack of long decay term sources comprises a reduction in decay heat rate of several percent over the first year of operation, making the infinite operation assumption conservative while the plutonium concentration is accumulating.

Calculations of these considerations based on the 1979 ANS standard have been performed to demonstrate the conservatism of the selected approach. Figure 6-18 and Figure 6-19 show the decay heat versus time for:

1) Infinite Operation of U235 (the AREVA decay heat model)

2) Finite Operation to 0.1 GWD/mtU of all fissionable isotopes with uncertainties added

3) Finite Operation to 1 GWD/mtU of all fissionable isotopes with uncertainties added

4) Finite Operation to 1 GWD/mtU of all fissionable isotopes without uncertainties

5) Finite Operation to 20 GWD/mtU of all fissionable isotopes with uncertainties added

6) Finite Operation to 40 GWD/mtU of all fissionable isotopes with uncertainties added

7) Finite Operation to 60 GWD/mtU of all fissionable isotopes with uncertainties added

In order to treat the Plutonium buildup effect conservatively, the finite operations curves are based on cycle management and enrichment assumptions that minimize the build up of Plutonium. No uncertainty is included in the infinite operation curve. The uncertainties incorporated in the other curves are 2 sigma values for the individual isotopes as published in the 1979 ANS standard. This provides greater than a 95/95 confidence in each of the decay heat contributions. The contributions are added linearly according to the individual isotopes fractional occurrence of fission.

Because of the range of the decay heat parameter, the early comparison of the relationships is difficult to ascertain. Clearly the U235 infinite operation curve is conservative for all times after a few seconds (~2 seconds). To better demonstrate the relationships, Figure 6-20 and Figure 6-21 provide the ratios of the finite operation curves to the infinite operation curves. The curvature of the plotted ratios during the first 2 to 3 seconds is due to the increased uncertainties during this time phase. The 1979 ANS standard is based on measured data and the difficulty of measuring decay heat within a few seconds of shutdown is reflected in these uncertainties. The highest combined finite operation decay heat curve with uncertainties exceeds the AREVA decay heat curve by only 2.5 percent at shutdown and falls below the AREVA curve in less than 2 seconds. Thus, there is only a 5 percent probability that the infinite operation curve of decay heat will be exceeded by up to 2.5 percent and that possibility exists

for the first 2 seconds of the transient. The potential accumulated under prediction is of short duration and of no consequence to the LOCA evaluation. The decay heat curve selected is suitable while somewhat conservative for the realistic evaluation of LOCA.

In conclusion, the choice of infinite operation with pure U235 fission product decay heat provides a base model that is conservative relative to the decay heat for finite operation. For RLBLOCA evaluation, the sampling of a decay heat multiplier has been removed such that the decay heat for all cases is 1.0 times the infinite operation U235 decay chain providing conservative treatment of the 1979 ANS standard with the assumption of 200 Mev/fission.

Figure 6-18: Decay Heat Comparisons, Infinite Operation U235, Finite Operation All Isotopes (0.1 - 10sec)

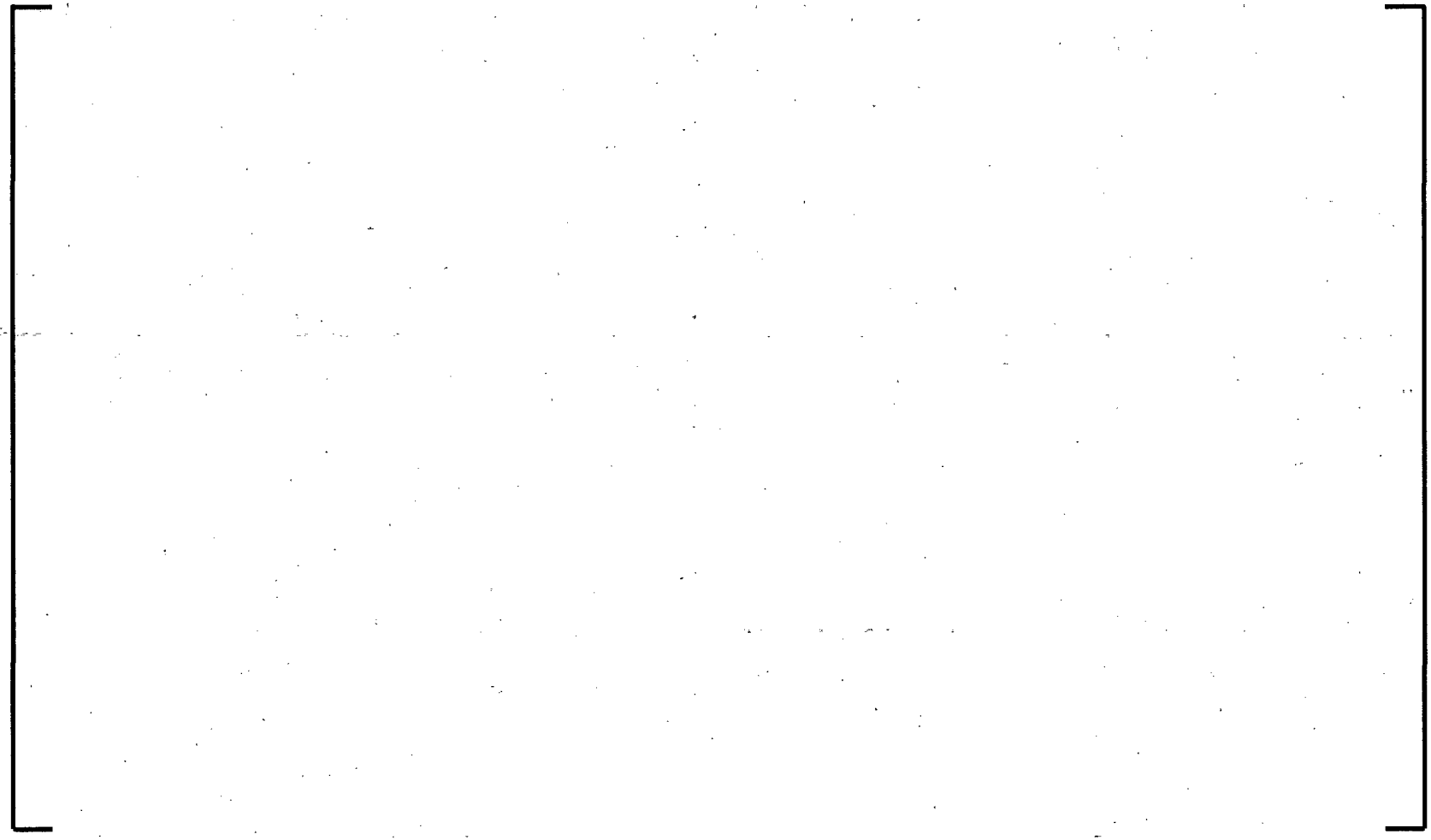

Figure 6-19: Decay Heat Comparisons, Infinite Operation U235, Finite Operation All Isotopes (10 - 1000sec)

Figure 6-20: Decay Heat Ratios, Finite Operation over Infinite Operation U235 All Isotopes (0 – 10 sec)

Figure 6-21: Decay Heat Ratios, Finite Operation over Infinite Operation U235 All Isotopes

7.0 REFERENCES

1: EMF-2103(P)(A) Revision 0, *Realistic Large Break LOCA Methodology*, Framatome ANP, Inc., April 2003.

2. Technical Program Group, *Quantifying Reactor Safety Margins*, NUREG/CR-5249, EGG-2552, October 1989.

3. Wheat, Larry L., "CONTEMPT-LT A Computer Program for Predicting Containment Pressure-Temperature Response to a Loss-Of-Coolant-Accident," Aerojet Nuclear Company, TID-4500, ANCR-1219, June 1975.

4. XN-CC-39 (A) Revision 1, "ICECON: A Computer Program to Calculate Containment Back Pressure for LOCA Analysis (Including Ice Condenser Plants)," Exxon Nuclear Company, October 1978.

5. U. S. Nuclear Regulatory Commission, NUREG-0800, Revision 3, Standard Review Plan, March 2007.

6. NUREG/CR-1532, EPRI NP-1459, WCAP-9699, "PWR FLECHT SEASET Unblocked Bundle, Forced and Gravity Reflood Task Data Report," June 1980.

7. G.P. Liley and L.E. Hochreiter, "Mixing of Emergency Core Cooling Water with Steam: 1/3 – Scale Test and Summary," EPRI Report EPRI-2, June 1975.

8. NUREG/CR-0994, "A Radiative Heat Transfer Model for the TRAC Code" November 1979.

9. J.P. Holman, Heat Transfer, 4th Edition, McGraw-Hill Book Company, 1976

10. EMF-CC-130, "HUXY: A Generalized Multirod Heatup Code for BWR Appendix K LOCA Analysis Theory Manual," Framatome ANP, May 2001.

11. D. A. Mandell, "Geometric View Factors for Radiative Heat Transfer within Boiling Water Reactor Fuel Bundles," Nucl. Tech., Vol. 52, March 1981.

12. EMF-2102(P)(A) Revision 0, *S-RELAP5: Code Verification and Validation*, Framatome ANP, Inc., August 2001.

13. EMF-2994(P) Rev. 4, "RODEX4: Thermal-Mechanical Fuel Rod Performance Code Theory Manual," December 2009.

14. AREVA Letter NRC:02:062, December 20, 2002, Responses to a Request for Additional Information on EMF-2103(P) Revision 0, "Realistic Large Break LOCA Methodology for Pressurized Water Reactors," (TAC No. MB2865).

15. P. Ihle, Heat Transfer in Rod Bundles with Severe Clad Deformations, KfK 3607 B, April 1984.

16. M.J. Loftus, et al., PWR FLECHT SEASET 163-Rod Bundle Flow Blockage : Task Data Report, No. 13, NUREG/CR-3314, October 1983.

17. NEA/CSNI/R(2004)19, *SEGFSM Topical Meeting on LOCA Fuel Issues*, Argonne National Laboratory, May 25-26 2004, Published by Organization for Economic Cooperation and Development Nuclear Energy Agency, Isy-les-Moulineaux, France, November 2004.

18. K. Wieher and U. Harten, Datenbericht REBEKA-6, KfK 3986, March 1986.

19. ANSI/ANS-5.1-1979, American National Standard for Decay Heat Power in Light Water Reactors, approved August 29, 1979.

20. Letter from J.C. Warner to U.S. Nuclear Regulatory Commission, "Shearon Harris, Unit 1, Request for Exemption in Accordance with 10 CFR 50.12 Regarding Use of M5 Alloy in Fuel Rod Cladding", Accession Number: ML110250473, Reference Number: HNP-10-125, dated 1/19/2011.

21. BAW-10166(P)(A) – Revision 5, BEACH – Best Estimate Analysis Core Heat Transfer, AREVA, Lynchburg, Virginia, November 2003.

22. BAW-10227(P)(A), Evaluation Of Advanced Cladding and Structural Material (M5) in PWR Reactor Fuel, AREVA, Lynchburg, Virginia, February 2000.

23. J. Chiou et. al., "Spacer Grid Heat Transfer Effects during Reflood," NUREG/CR-0043, US NRC 1982.

24. L.H.J. Watchers et. al., "The Heat Transfer from a Hot Wall to Impinging Water Drops in the Speroidal State," Chem. Eng. Sci., 21, pp. 1047-1056, 1966.

25. L.H. J. Watchers et. al., "The Heat Transfer from a Hot Wall Impinging Water Drops in the Speroidal State," Chem. Eng. Sci., 21, ppg. 1231-1238, 1966.

26. J. Sugimoto and Y. Murao, "Effect of Grid Spacers on Reflood Heat Transfer in PWR LOCA," J. of Nucl. Sci. Technol., pp. 102-114, February 1984.

27. NUREG/CR-4166, M.J. Loftus et. al., "Analysis of FLECHT-SEASET 163-Rod Blocked Bundle Data Using COBRA-TF," NRC/EPRI/Westinghouse Report No. 15, October 1985.

28. B.C. Oberlander, M. Espeland, and N.O. Solum, "PIE Results from High Burn-Up (92 MWd/Kg) PWR Segment After LOCA Testing in IFA 650-4," Paper 7 Session F2, Enlarged Halden Programme Group Meeting, Storefijell Hotel, Gol, Norway, March 2007.

29. ANF-90-145(P)(A), "RODEX3 Fuel Rod Thermal-Mechanical Response Evaluation Model," April 1996.

APPENDIX A: REVIEW OF IMPLICATION FROM RECENT SWELLING, RUPTURE, AND FUEL RELOCATION TESTING

Over the last several years there has been interest within the industry in the potential consequences of fragments of cracked fuel pellets falling into the ballooned region of a ruptured fuel rod. If this relocation were to occur, the rod power within the ballooned region may exceed that present prior to the balloon developing with the potential for increased cladding temperature. The phenomena have been investigated with both experimental and analytical studies. Some analyses have predicted cladding temperature increases of potential consequence. This appendix reviews the analytical and experimental efforts, with commentary, and concludes that an appropriate interpretation of the experimental results leads to the conclusion that fuel relocation does not increase cladding temperature.

In judging the veracity of opinion on the effect of fuel relocation, it is important to maintain a balance between the positive and negative aspects of clad swelling, rupture and fuel relocation. It is obvious, that any evaluation that attempts to quantify only the negative aspects will result in a prediction of cladding temperature increases. Such analyses have value but do not contribute to an in depth understanding of the phenomena and if not properly qualified lead to extreme conservatism in the perception of the phenomena. In what follows, the properties of post relocation heat load (power within the balloon region) and post rupture cooling phenomena are kept in balance so that a true perspective can be drawn as to consequence. The following largely follows the historical path of recent developments with excursions from the timeline as is necessary to support or clarify the arguments.

A.1 IRSN Presentation at Argonne in 2004

IRSN presented an analysis of fuel relocation at an OECD meeting at Argonne National Laboratory in 2004, Reference A-1. The analysis predicted cladding temperature increases of 110 to 160 C based on symmetric strain development and high packing fractions. No consideration of rupture induced cooling mechanisms was included. The heat load within the balloon was a 70 percent increase over the pre-rupture heat load. However, symmetric, circular expansion of the balloon is only possible for strains below about 35 percent, and had the influence of adjacent pins been considered in the calculation the heat load would have increased a more moderate 36 percent. This increase in heat load would have been approximately 20 percent less than the heat transfer area increase. Thus, including a more reasonable estimate of the heat load would likely have altered the result to show no cladding temperature increase even without consideration of the rupture induced cooling mechanisms of increased vapor turbulence and decreased vapor temperature due to droplet shattering on ruptured clad.

A.2 KfK FR2 Tests (Reference A-2)

One of the references for the IRSN study was the KfK FR2 Tests, Reference A-2. A total of 47 single rod tests were performed in the FR2 reactor using test rods with an active length of 0.5 m. The purpose of these tests was to study the rupture behavior and the resulting relocation of fuel fragments. These tests used rods with a burn-up range of 2.5 to 35 GWd/MtU. Figure A-1 shows the fuel mass per unit internal volume as a function of sample average strain away from the rupture location. The solid line on Figure A-1 represents the calculated mass per unit length when only the initial pellet mass is allowed to expand into the swelling. It should be noted that when the strain is less than 30 percent (e.g., tests other than E5) either the pellets in the low strain region did not crack and relocate or any relocation was outward rather than vertical.

The only fuel mass data at the rupture locations provided in Reference A-2 was for Test E5. The results for E5 indicate that at strains of 48.5% and 67.5%, as shown in Figure A-1, the corresponding fill ratios are 55.5% and 61.5%, respectively.

To study fuel relocation effects, Test E4 was conducted using added thermocouples near the top of the active fuel region, and a rod irradiated to 8 GWd/MtU. As shown in Figure A-2, there was a strong decrease in cladding temperature near the upper end of the sample, indicating a loss of fuel mass from the top of the fuel stack following clad rupture. The thermocouples below those at the top of the sample which indicate relocation and near the rupture location demonstrate common cladding temperature excursions. These results indicate that the mass moving down from the top region of the fuel rod may have been lost via the opening at the rupture location and that what mass accumulated in the balloon was not sufficient to overcome the cooling mechanisms present.

A.3 Halden Tests (Reference A-3)

To provide additional information on fuel relocation the OECD Halden Reactor project (HRP) conducted several LOCA series tests using a 0.5 meter single fuel rod enclosed in a cylindrical heater. The fourth test of the series, IFA-650.4 (Reference A-3) comprised a test rod with a burn-up of 92 GWd/mtU. Gamma scans indicate that nearly all of the pellet material above the ruptured balloon region relocated out of the test rod or into the balloon. This was confirmed by Post Irradiation Examination (PIE) of the sample. During the interim between the test and the availability of the PIE results, benchmarks of the tests were conducted based on available data. Because there are no thermocouples or other direct temperature measurements of the cladding made in the HALDEN apparatus, the Paul Scherrer Institute (PSI), Reference A-4, and the IRSN, Reference A-5, benchmarked the test by comparing to a thermocouple attached to the cylindrical heater that surrounds the sample. This thermocouple is mounted near the bottom of the ballooned region. PSI credited radiation from the sample rod to the heater cylinder to match the measured thermocouple temperature. This required an increase in heat load adjacent to the thermocouple comparable to that used in the 2004 IRSN calculation with the resultant conclusion that the packing fraction in the test was on the order of 60 to 70 percent. Even at

this heat load the calculated cladding temperature in the ballooned region remained below that which would have been calculated had swelling and rupture not occurred (curve D versus curve A in Figure A-6). Once the PIE examination was completed the packing factor was shown to be on the order of 50 percent. The thermocouple result can be explained by an alternate approach that incorporates the fuel particle distribution observed.

Reference A-6 performed a detailed PIE evaluation of IFA-650.4. Figure A-3, Figure A-4, and Figure A-5 show respectively the cross section view of the rod at upper edge of balloon zone (235mm down from the upper region of the test section), at maximum balloon position (255 mm down), and at a lower region in the balloon (275 mm down). The following observations can be made from these figures:

- At the maximum ballooned zone, Figure A-4, the clad swelling eliminated the gap between the fuel rod and the electrical tube heater, resulting in a blockage that caused substantial fuel fragments to accumulate in the gap between the rod and heater above the peak rupture zone, as shown in Figure A-3.
- The direct contact between the packed fuel fragments and heater must have resulted in direct heating of the heater.
- Visual observation of the packing factor near the rupture zone shows the factor is close to 50 percent.
- Due to rod bow, there is fuel rod contact with the heater at 275 mm. This is where the heater thermocouple temperature was measured. The azimuthal location of the thermocouple is not available.

Reference A-6 also states that the measured packing fraction inside the cladding at and above the middle of the rupture was indeed 50 to 53 percent and the particulate, inside and outside the rod is characterized as fragments of varied dimension between 0.05 mm to 6 mm. The small lower end of the fragment size range was possibly due to the high burn-up rim.

With the measured packing fraction at 275 mm of 38 percent, observable in Figure A-5 (also Figure 5 in Reference A-3), radiation from a higher power fuel segment is not a credible explanation for the heater thermocouple temperature. If fuel particle position assumptions were adjusted to match the test results and axial and azimuthal heat conduction within the heater modeled, the thermocouple temperature result can be explained.

In Reference A-3 NEA conducted a detailed evaluation of IFA-650.4 and made the following recommendation (Item 6 in Section 6 of Reference A-3).

> "Assume realistic filling ratios, e.g. as observed in IFA-650.4 where the product of lower fragment density and increased volume results in about the same power density as before ballooning and relocation"

The only qualification on this recommendation was in regard to the possibility that new tests may show different results. The recommendation is consistent with the PIE results and by extension concludes that the impact on the cladding temperature near the rupture zone is small.

In Section 3.3 (Reference A-3) related to relocation, NEA further states:

> "In summary the IFA-650 experiments are relevant for investigating some aspects of fuel relocation during LOCA. However, the results should not be extrapolated to other issues (such as the impact of the fuel relocation on peak cladding temperature)"

NEA also observed that the high burn-up fuel structure, which is characterized by high porosity and small grain size, represents more than 42 percent of the fuel volume of the IFA650.4 segment.

GRS in its benchmark calculation of IFA-650.4 using ATHLET-CD code (Section 8.3 of Reference A-7) considered the PIE results and assumed a fill factor of 0.0, which means that they assumed no fuel mass addition in the rupture zone. The assumption is roughly equivalent to the application of a packing fraction of 40 to 50 percent. With this assumption, GRS was able to calculate the heater temperature at 275 mm from the top of the active fuel (about 20 mm below the maximum blockage zone).

IFA 650.10 was conducted in May 2010 (Reference A-8) using a rod with a burn-up of 61 GWd/MtU. There was very little ballooning at the rupture location and as a result, the rupture opening was small and no fuel relocated. However, the preliminary PIE results, Figure A-7 (Reference A-8), show relatively large particle size and only a small fraction of pellet fragmentation to smaller particles. This result is consistent with the NEA expectations.

A.4 Argonne Tests

The NRC conducted swelling and rupture tests on BWR rods with burnups approaching 60 GWd/mtU in 2001, 2002, Reference A-9. The test samples were approximately 12 inches long and heated to rupture in a radiant furnace as opposed to internal nuclear heating. Sample temperature was controlled by adjusting the furnace output. Thus, temperature results are not useful in regards to fuel relocation effects. However, the tests did show cracking of the fuel pellet and relocation into the balloon. From Figure 12 of Reference A-9, the appearance of the rubble in the balloon is an approximate equivalent of that in the HALDEN 650.4 test. This supports the NEA recommendation that the heat load in the balloon region will approximate the heat load prior to swelling, rupture and relocation.

A.5 Studsvik Tests (Reference A-10)

The NRC is conducting a series of integral Loss-of-Coolant Accident (LOCA) tests at Studsvik on high burn-up, fueled rod segments for the purpose of determining the survivability of the balloon region during an accident. The rod segments were 300 mm in length and fabricated from two ZIRLO rods provided by Westinghouse and irradiated at North Anna Power Plant. The burn-up of the rod segments was ≈70 GWd/MtU.

In these tests, there was a significant amount of fuel loss through the rupture opening. Post test pictures show no fuel in the ballooned region. When or how the fuel was removed has not been determined. Images, Figure A-8, of the fragmented fuel indicate the rubble size was small but quantitative measurements have not yet been conducted. Thus the test shows relocation of some sort and may give particulate size information in the future.

A.6 Additional Tests

In 2005 IRSN (Reference A-11) and in 2009 NEA/OECD (Reference A-12) did reviews of various tests conducted to evaluate fuel behavior under LOCA conditions. The review included out-of-pile single rod and multi-rod test programs like REBEKA, ORNL, and JAERI and in-pile test programs like PBF-LOC, FR2, FLASH, NRU, PHEBUS, and HALDEN. The results of HALDEN and FR2 have been disused. The out-of-pile tests are not useful to evaluate the effect of fuel relocation, since most of these tests used electrically heated rods. No information regarding the detailed PIE examinations of the NRU and PHEBUS tests was provided and IRSN concluded that for the PBF-LOC tests fuel fragment movements occurred when the rods were transported from the test site to the measuring site (Section 4.1.1 in the IRSN report). Similar fuel fragment relocations also occurred in the FLASH tests (Section 4.1.5 in the IRSN report). Therefore, the fuel packing results reported for these tests, although sited in the 2004 IRSN analysis, should not be considered in evaluations of swelling, rupture, and fuel relocation

A.7 Conclusions

The analytical evaluations of swelling, rupture, and fuel relocation conducted in recent years have been inconsistent in approach and predicted inconsistent results. Those indicating significant increases in cladding temperature response have been inconsistent with available experimental evidence and have not incorporated cooling phenomena expected during an actual LOCA in a commercial power plant. The analyses which are consistent with experimental results show that the heat load at the balloon region is essentially the same as prior to rupture. The conclusion is thus, that the heat load at the balloon region is only slightly affected and that cooling mechanisms associated with swelling and rupture should produce some decrease in cladding temperature even with fuel relocation. For analytical purposes, it is noted that the heat load is a combination of cladding strain and particle packing factor. Thus, for the evaluations of swelling, rupture, and fuel relocation presented in the main body of this report, AREVA has selected to use the conservative circular strain development, of our deterministic LOCA models, in combination with the 50 percent packing fraction measured in the IFA 650.4 test.

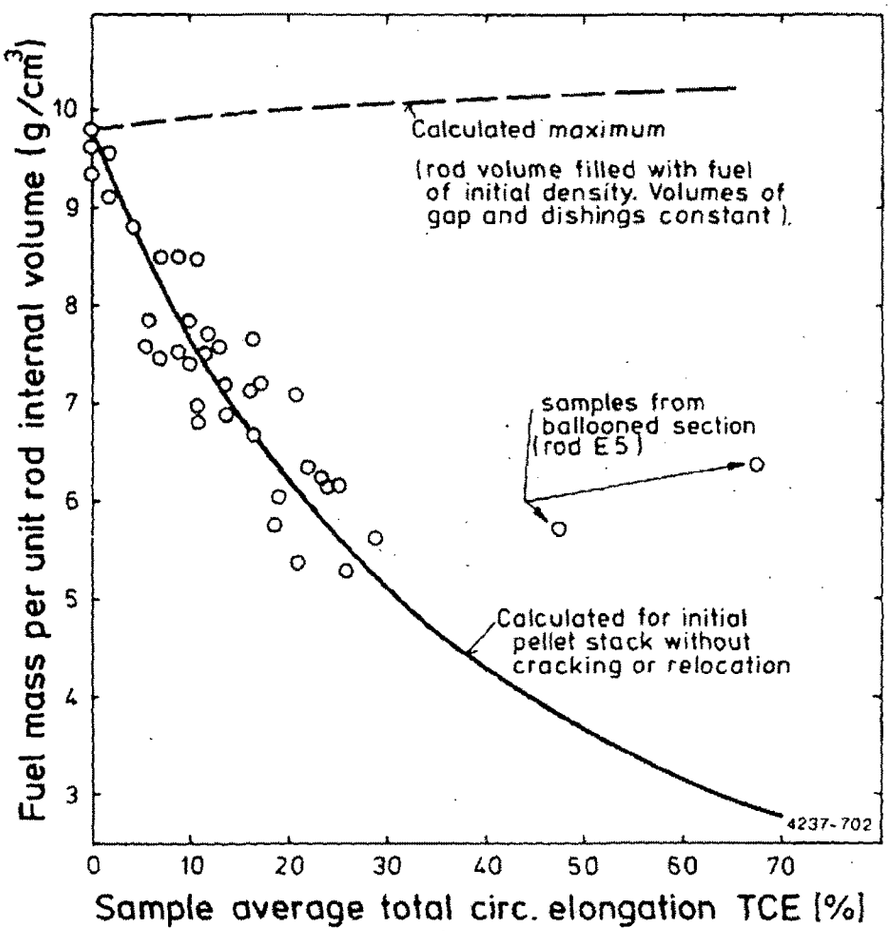

Figure A-1: KfK FR2, Test E5

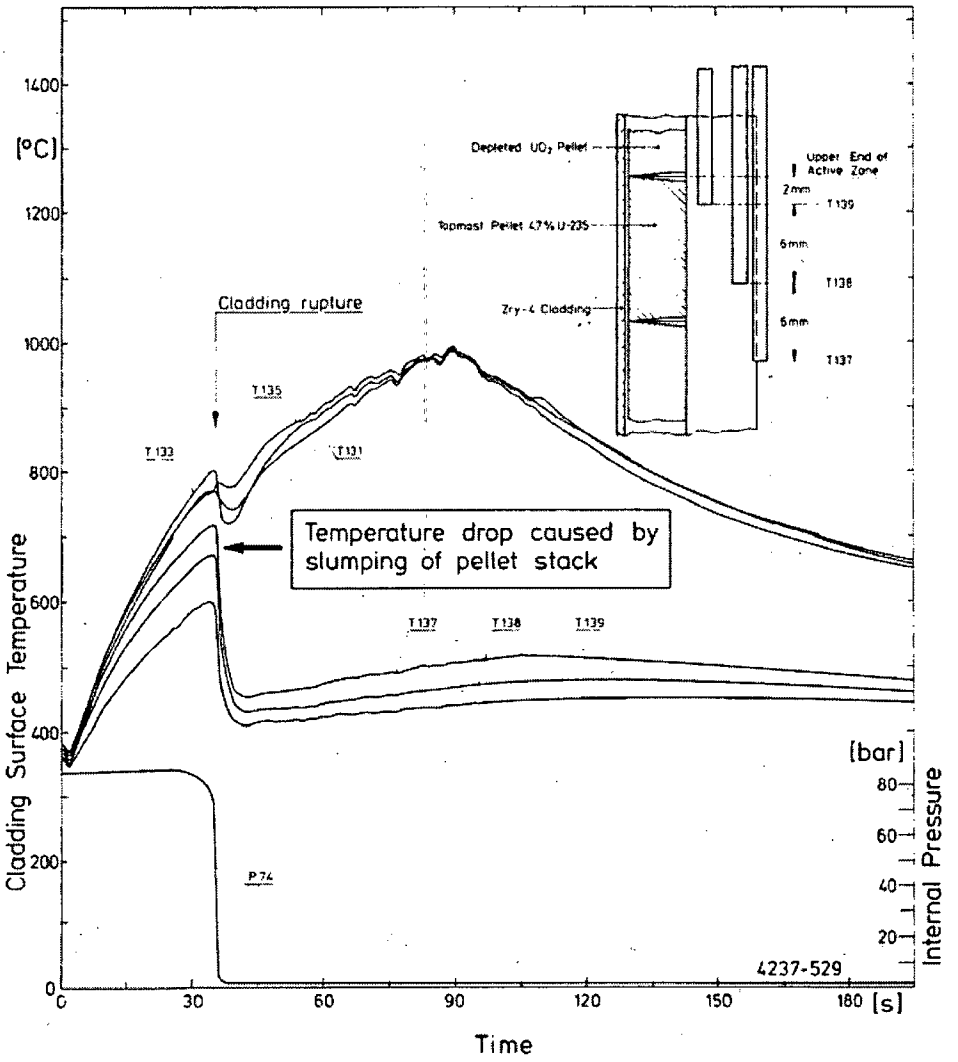

Figure A-2: KfK FR2, Test E4

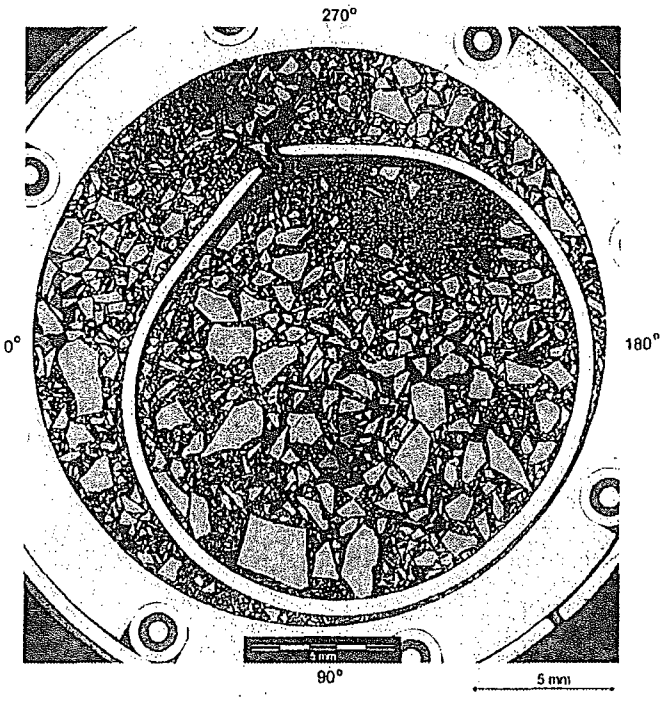

232mm, end of upper crack opening. Fuel is fragmented (fragment Ø≤2mm).

•Fuel particles were blown out when the rod burst.

•Fuel from upper part of the rod collapsed into the balloon

•Fuel particles / fragments are relocated outside between cladding and inner heater wall.

Figure A-3: Halden Test IFA-650.4, Rod Cross Section (235 mm)

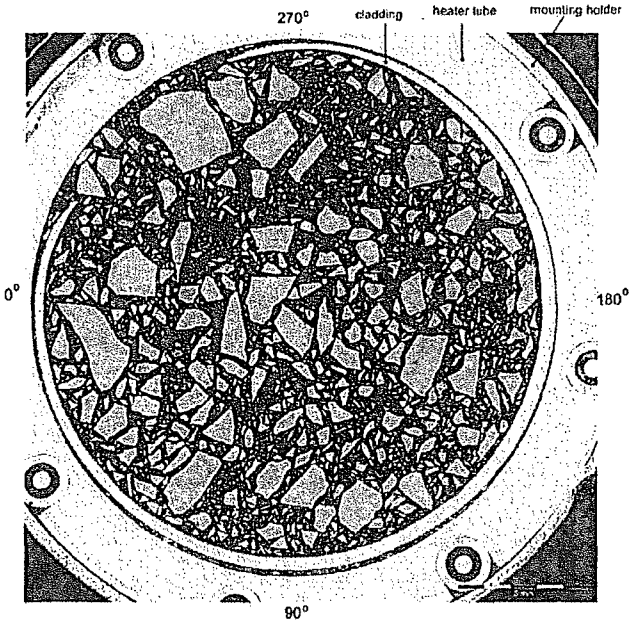

Macrograph showing the transverse cross section of IFA-650-4 at axial position 255.0 mm from upper end of fuel stack (Met5)

255mm Max ballooning. Clad and fuel fragments f free space inside the hea tube. Fuel was blown out when rod burst.

Figure A-4: Halden Test IFA-650.4, Rod Cross Section (255 mm)

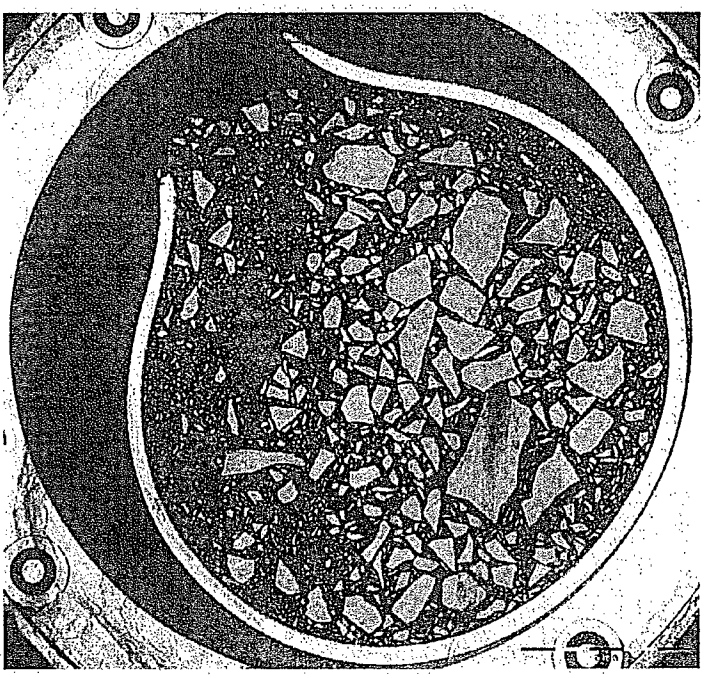

Met4, 275mm
Below max ballooning.
•The max ballooning hindered majored fuel particle/ fragment relocation from the upper to the lower part of the rod

Figure A-5: Halden Test IFA-650.4, Rod Cross Section (275 mm)

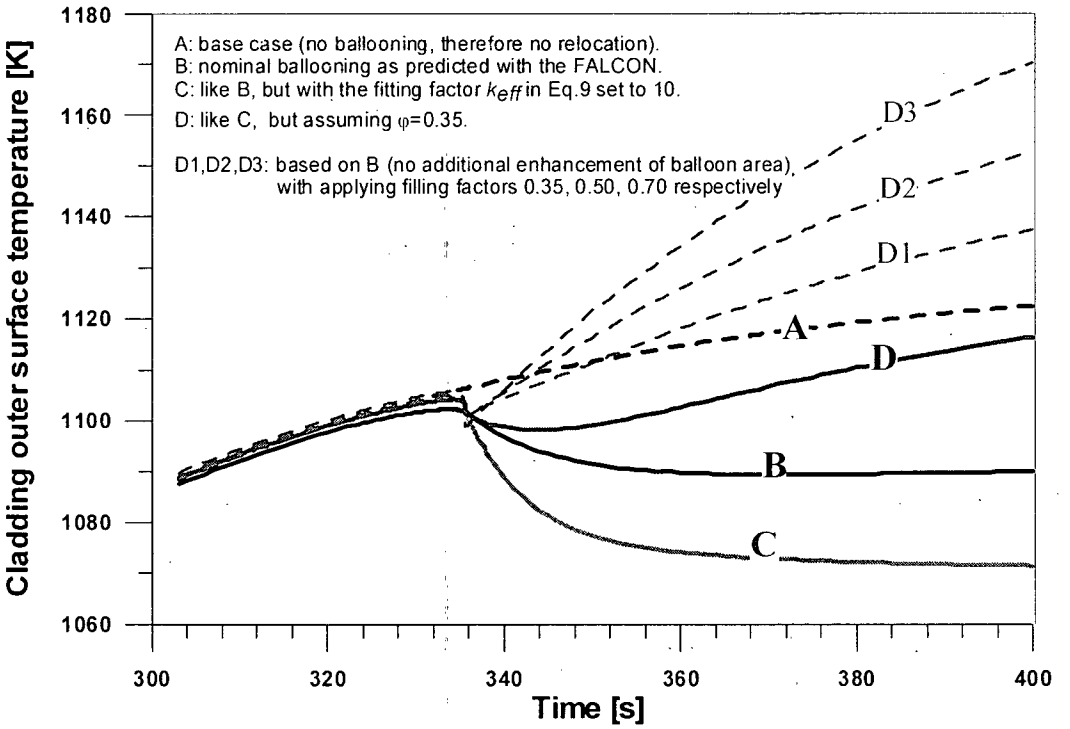

Figure A-6: Halden Test, Cladding Temperature versus Time

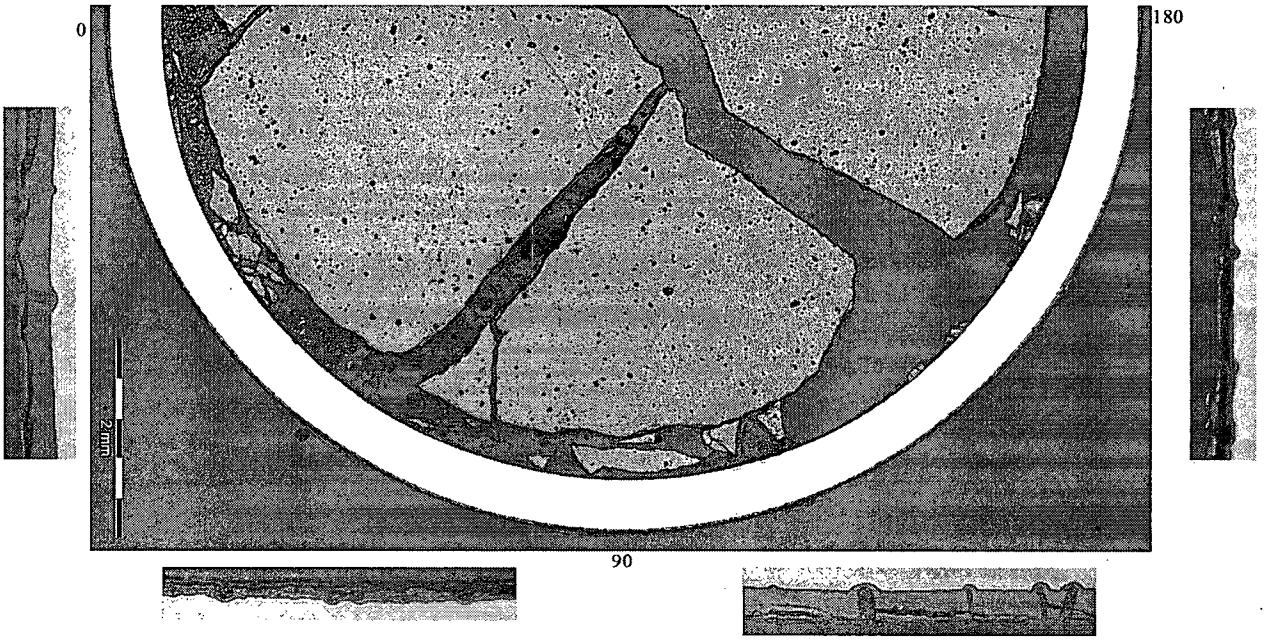

Figure A-7: Halden Test IFA-650.10, PIE Results

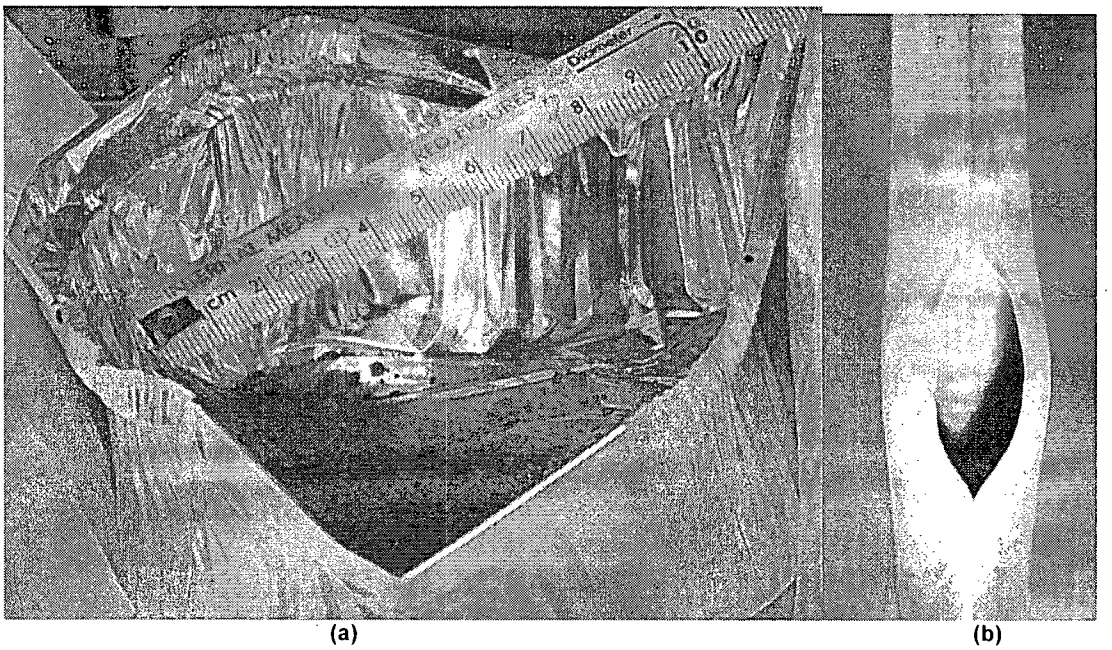

Figure A-8: NRC Test at Studsvik, Zirlo Rod at 70 GWd/MtU

APPENDIX A REFERENCES

A-1 V. Guillard et al., Use of CATHAR2 Reactor Calculations to Anticipate Research Needs, SEGFSM Topical Meeting on LOCA Fuel Issues, Argonne National Laboratory May 2004, NEA/CSNI/R(2004)19.

A-2 E.H Karb et al., LWR Fuel Rod Behavior in the FR2 In-pile Tests Simulating the Heatup Phase of a LOCA, Final Report", KfK 3346, March 1983.

A-3 "Safety Significance of the Halden IFA-650 LOCA Test Results, "NEA/CSNI/R(2010)5, November 15. 2010.

A-4 G. Khvostov, A. Romano, and M. A. Zimmermann, " Modeling the Effects of Axial fuel relocation in the IFA-650.4 LOCA Test," Paper:7, Session F4, , Presented at the Enlarged Halden Programme Group Meeting in Norway, March 2007.

A-5 C. Gandjean, "Calculation of the IFA-650.4 & 5 LOCA Tests", Paper:9, Session: F4 , Presented at the Enlarged Halden Programme Group Meeting in Norway, March 2007.

A-6 B. C. Oberlander, M. Espeland, and N.O. Solum, "PIE Results from High Burn-up (92 MWd/Kg) PWR segment After LOCA Testing in IFA 650-4, " Paper 7 Session F2, Presented at the Enlarged Halden Programme Group Meeting in Norway, March 2007.

A-7 "Benchmark Calculations on Halden IFA-650 LOCA Test Results, "NEA/CSNI/R(2010)6, November 15, 2010.

A-8 B. C. Oberlander and H.K. Jenssen, "LOCA IFA650.10: PIE of a PWR Rod with a Burn-up of 61 MWd/KgU after LOCA Testing in the HBWR", Slides presented in the HPG- Meeting, Budapest, Hungary, May 2011.

A-9 Y. Yan, R. V. Strain and M. C. Billone, LOCA Research Results for High-Burnup BWR Fuel, Proceeding of the 2002 Nuclear Safety Research Conference, U.S. NRC, NUREG/CP-0180, pp. 127-155 (2003).

A-10 M. Flanagan et al., Draft Abstract for Results of Integral, High-Burnup, Fueled LOCA Tests and Companion Testing with As-Fabricated and Pre-hydrided Cladding, NRC, Private Communication (email correspondence).

A-11 C. Grandjean, " A state-of the-art Review of Past Programs Devoted to fuel Behavior Under LOCA conditions, Part One: Clad Swelling and Rupture Assembly Flow Blockage", Technical Report SEMCA-2005-313, IRSN, December 2005.

A-12 "Nuclear Fuel Behavior in loss-of-Coolant Accident (LOCA) Conditions, State-of-the art Report,", ISBN 978-92-64-99091-3, OECD 2009, NEA No. 6846.